Energy Advances

ROYAL SOCIETY OF CHEMISTRY

REVIEW ARTICLE

View Article Online
View Journal | View Issue

Cite this: *Energy Adv.*, 2025, 4, 966

Advances in supported monometallic and bimetallic catalysts towards green aviation fuels: a review†

Nur Athirah Adzahar,[ab] G. AbdulKareem-Alsultan,[*ab] Hwei Voon Lee[c] and Y. H. Taufiq-Yap[*abde]

The worldwide energy crisis is triggered by the increasing exhaustion of fossil fuel supplies along with the population increase in developing nations. In addition, fossil fuels are not environmentally benign owing to their association with issues such as climate change, high toxicity, and non-biodegradability. Consequently, they are regarded as an unsustainable source of energy. Undoubtedly, green aviation fuels, also referred to as bio-jet fuels, are potential and sustainable long-term energy sources that can help decrease our reliance on fossil fuels, owing to the availability and renewability of their feedstocks. In contrast to biodiesel, which is produced through transesterification, green aviation fuel is produced *via* deoxygenation to eliminate oxygen and other impurities, resulting in a fuel that chemically mimics petroleum diesel. Thus, conventional homogeneous and heterogeneous catalytic systems for producing biodiesel from vegetable oil are no longer justifiable for the sustainable aviation fuel (SAF) industry in the foreseeable future. This is primarily due to the presence of oxygen-containing compounds in biodiesel (~10–12%), which increases its susceptibility to oxidation and degradation over time, resulting in the formation of gum, clogging of filters, and decreased fuel storage stability, all of which are crucial concerns for aviation. Furthermore, jet engines are engineered to operate on drop-in fuels that closely resemble hydrocarbon-based jet fuels without requiring modifications. This review provides a detailed and systematic procedure for converting non-edible oils such as palm kernel oil (PKO) into SAFs using bimetallic nickel–cobalt onto magnetite-supported catalysts. The enhanced catalytic system can effectively convert palm kernel oil with a high yield and selectivity towards kerosene for aviation sectors *via* deoxygenation reactions. The use of palm kernel oil as a raw material for SAF production will help address the problem of food security that arises from using food-grade oil for SAF production while decreasing the overall manufacturing expenses for green fuel production. This article aims to highlight the use of heterogeneous bimetallic acid/base catalysts for the production of SAFs from environmentally friendly and non-edible palm kernel oil. Future research should focus on optimizing bimetallic catalysts to improve the efficiency of sustainable aviation fuel (SAF) production from non-edible oils, with the aim of reducing energy consumption and minimizing environmental impact. Additionally, it is crucial to investigate alternative sustainable feedstocks and assess their scalability to ensure the widespread adoption of green fuels in the aviation sector, addressing food security and long-term energy needs. In conclusion, this study provides insights and potential advancements for the future.

Received 20th March 2025,
Accepted 25th June 2025

DOI: 10.1039/d5ya00078e

rsc.li/energy-advances

1. Introduction

The predominant fuel type for commercial and military aircraft is jet fuel, which is mostly produced *via* petroleum refining. The rapid increase in air passenger mobility has driven the global aviation sector to consume jet fuel at an unsustainable rate, resulting in a significant increase in greenhouse gas (GHG) emissions. The New York Times reported in September 2021

[a] *Catalysis Science and Technology Research Centre, Faculty of Science, Universiti Putra Malaysia, 43400 UPM Serdang, Selangor, Malaysia. E-mail: taufiq@upm.edu.my, kreem.alsultan@yahoo.com; Tel: +60182534058*
[b] *Department of Chemistry, Faculty of Science, Universiti Putra Malaysia, 43400 UPM Serdang, Selangor, Malaysia*
[c] *Nanotechnology and Catalysis Research Centre (NANOCAT), Universiti Malaya, 50603 Kuala Lumpur, Malaysia*
[d] *Biomass Valorization and Biomass Energy (BVBE), Catalysis Science and Technology Research Centre, Faculty of Science, Universiti Putra Malaysia, 43400 UPM Serdang, Selangor, Malaysia*
[e] *University International MAIWP, Taman Batu Muda, Batu Caves, 68100, Kuala Lumpur, Malaysia*
† Electronic supplementary information (ESI) available. See DOI: https://doi.org/10.1039/d5ya00078e

that Earth is currently hotter than it has been for at least 1000 years because CO_2-GHG gas concentrations have risen to nearly 900 million metric tons globally.[1–3] NASA claimed that in October 2021, CO_2 levels had already surpassed those in the mid-1700s (280 ppm) and were 416 parts per million (ppm).[4,5] The increase in CO_2 levels has thus resulted in frequent extreme weather conditions, the effects of which may result in global financial crises and loss of life. Consequently, an increasing number of climate-conscious experts have sparked the creation of a new generation of jet fuels made from renewable biomass. As a sustainable and clean-burning alternative to the commercial jet fuel, biodiesel is a liquid fuel made of mono-alkyl esters of fatty acids. Unfortunately, the higher oxygen content in biodiesel appears to cause thermal instability, low volatility, poor combustion quality, and a heightened soothing propensity to limit its direct use in engines.[6–9] Therefore, a different procedure that produces less-oxygenated molecules with a mimicked hydrocarbon structure within the jet range fuel (C_{10}–C_{16}) is necessary.[10]

Deoxygenation or hydrodeoxygenation reactions can be used to accomplish this. In contrast to deoxygenation, which involves the removal of oxygenated compounds in the form of CO_2/CO through direct C–O bond cleavage under H_2-free conditions, hydrodeoxygenation involves the addition of H_2 and removal of O_2 in the form of hydrocarbons and H_2O as a by-product.[11–13] In contrast to deoxygenation, which results in a fuel fraction with fewer carbon atoms than its fatty acids, hydrodeoxygenation yields a fuel fraction with a carbon length similar to that of its fatty acid.[6,11,14] Deoxygenation has received increasing attention due to H_2-free reaction method that can provide fuel fractions while hydrodeoxygenation is not economically viable.[15–17] Fatty acids appear to be a potential feedstock for producing bio-jet fuel *via* a deoxygenation reaction. Apart from fatty acids, triglycerides (TGs) are another major component of both plant and animal fats and oils. When triglycerides are hydrolysed, fatty acids are produced.[18] TGs and fatty acids can also be used as chemical intermediates to create alcohols, aldehydes, and alkenes, and using them as feedstocks for deoxygenation is advantageous.[19,20] The qualities of the fuel, such as viscosity, flash point, and cetane number, were improved by the presence of these intermediates. In addition to TGs and fatty acids, the deoxygenation procedure also demonstrated notable ability to remove the oxygen from lignin species from lignocellulosic biomass and enhance aromatic hydrocarbons.[21,22] The deoxygenation process was shown to be a very effective method for all feedstocks, with majority of the deoxygenated TGs or fatty acid products having a bright yellow colour.

The catalytic deoxygenation process has been studied extensively in the past by employing sulfided metals, such as ReNiMo, NiMo, CoMo, and NiW, as well as noble metals, such as Pt and Pd.[23–28] Although noble catalysts were found to be superior at deoxygenating feeds, they were unappealing owing to their high price and limited availability.[13,29–31] However, sulfided catalysts are an issue because they might cause sulfur to seep out and contaminate the final product.[32,33] Consequently, it is essential to develop catalysts that are both affordable and devoid of sulfur. It is interesting to note that because transition metal oxides like Ni, Co, Mn, Zn, and Ce may achieve results that are equivalent to those of noble metal-promoted catalysts, they are regarded as suitable catalyst promoters. It has been discovered that Ni has greater deoxygenation performance and endurance than noble metal catalysts with greater C–C or C–O bond cleavage activity.[34–36] This is corroborated by a previous study in which a Ni-promoted catalyst produced a diesel selectivity of 80% at 390 °C in inert environments.[37,38] However, Ni-based catalysts favor excessive cracking, leading to poor coking activity, which can limit their stability and yield. Thus, previous studies have investigated the modification of Ni by adding Co metal, which demonstrated that deoxygenating the palm fatty acid distillate over the Co/AC catalyst produced 91% hydrocarbon fuel.[39,40] Notably, the Ni–Co catalyst has been shown to have a synergistic effect that can increase the DO activity even at low temperatures.[41,42]

It has also been shown that the catalyst support plays a significant role owing to its physicochemical properties and electronic interactions, which would affect the rate of the reaction and increase the yield of the desired deoxygenated product. γ-Al_2O_3, SiO_2, and TiO_2 are typically utilized as catalyst supports owing to their excellent oxygen storage capacity and intrinsic redox properties, which make them capable of facilitating the activation of oxygenated compounds.[13,43,44] However, catalyst supports with high acid strength such as zeolite (H-ZSM-5) and sulphated zirconia (SO_4^{2-}/ZrO_2) were prone to promote excessive cracking, as well as severe coke formation and deposition, which resulted in rapid deactivation. To decompose the carboxylic group in vegetable-based oil, moderately acidic supports such as iron oxide supports are needed. The use of iron oxide as a support can also minimize the weight loss and make the catalyst easier to separate owing to its magnetic ability. Iron oxide has high oxyphilic effects, and redox reactions make it easier to break C–C and C–O bonds and boost the efficiency of the oxygen-removing agent.[45–47] In addition, it also reduces polymerization and accentuates cracking and char generation. The presence of Lewis acid sites on iron oxide supports aids in reducing carboxylic acids to aldehydes, while Brønsted acid sites facilitate cracking and hydrogen transfer reactions.[48–50] Therefore, the present work focuses heavily on the advancement of bimetallic nickel–cobalt-supported catalysts on iron oxide for catalytic deoxygenation of second-generation crops in the absence of H_2 atmosphere.

1.1. Development of green fuels

Therefore, the creation of clean and renewable energy sources is gaining popularity. The United Nations adopted ''Transforming our World: the 2030 Agenda for Sustainable Development'' on September 25, 2015, with the goal of promoting global sustainable development and ensuring that ''no one is left behind''. For this initiative to be successful, it is crucial that the economic, social, and environmental aspects of sustainable development are interconnected.[51,52] In addition to this initiative, the European Union has embraced the European Green Deal, which presents a growth strategy aimed at transforming the organization into a modern and competitive economy. The primary

objectives are to maximize resource efficiency and, notably, to achieve net-zero greenhouse gas emissions by the year 2050.[28,51,53] In order to limit global warming by 1.5 °C over pre-industrial levels, the 2015 Paris Agreement calls for a reduction in greenhouse gas emissions, which is something that the green deal supports.[54–56] From what has been discussed thus far, it is evident that the development of green fuels is a topic of great importance that also has favourable environmental effects.

Global energy consumption is at an all-time high due to changing lifestyles and a growing population. Currently, fossil fuels are the primary energy source. However, it was expected that fossil fuel resources would eventually run out because they are known to be non-renewable. According to a study published in the Statistical Review of World Energy, if global energy consumption continues to rise, the world's reserves of petrol and oil will run out in 41 and 63 years, respectively. Furthermore, the use of petroleum contributes significantly to the release of greenhouse gases (GHGs), which affect human health and the environment by causing sea-level rise, glacier retreat, and climate change.[57–60] The global average temperature rises as a result of the climate system radiating more positively due to an increase in greenhouse gases. This is supported by statistics showing that atmospheric CO_2 levels have increased from 277 parts per million in 1750 to 417 parts per million in 2019. globally, leading to a 2 °C increase in temperature over the pre-industrial revolution levels.[61–63] Ice sheets and glaciers will also melt as global temperatures rise, endangering millions of people with diseases, such as malaria, starvation, flooding, and water shortages. Consequently, there has been a national focus on developing renewable energy sources in an attempt to mitigate the negative impacts of the issues caused by the use of conventional fuels.[64,65]

Energy derived from naturally occurring processes that replenishes itself is referred to as renewable energy.[66,67] The examples of such processes include solar, wind, biomass, geothermal and hydropower resources (tidal and wave).[66,68] Renewable energy is superior to fossil fuels in many different ways, such as an endless supply, lowering the risk of atmospheric pollution by minimizing the emission of sulfur, carbide, and dust, and reducing the consumption of natural fossil fuels.[69,70] Moreover, renewable energy is clean, green, and low in carbon, along with a reduction in solid waste release and the protection of water resources. Recently, renewable energy has been widely used to generate electricity and energy of approximately 24.5% and 19.3%, respectively, and has been used in the industrial and domestic sectors.[71–73] Renewable energy can also be used to develop value-added products such as cosmetics and perfumes from fatty acids of fermenting sugars, food additives, and nutritional supplements from algae, plastics, lubricants, surfactants (oleo-furan), fertilizers, biogas, and renewable natural gas.[74–76] Furthermore, the development of green fuels in the transportation industry has significantly increased the use of renewable energy sources such as biomass (Fig. 1).

1.1.1. Sustainable aviation fuel (SAF)/bio-jet fuel. Air transportation plays a crucial role in the daily lives of developing countries. Civil aviation is a rapidly expanding mode of transportation and one of the fastest-growing areas in the industry.[80,81] In 2019, the International Air Transport Association (IATA) reported that air travel by people in emerging nations is expected to increase by up to 10% annually, resulting in a significant growth of 44% over the following 20 years.[80,82] The exponential expansion of air transport has resulted in a corresponding increase in environmental impacts, particularly the depletion of fossil fuels as its principal energy source. However, these challenges require special attention and consideration. The U.S. Department of Energy (DoE) forecasted that the commercial jet fuel market will expand to more than

Categories	Biomass Sources	Production Process	Biofuel	Common Catalyst Type
First Generation	 Sunflower Wheat Corn	Biochemical (fermentation, transesterification, esterification)	Bioethanol	Enzyme catalyst, microorganisms (yeast)
			Biodiesel	Homogenous (NaOH, KOH, HCl, H_2SO_4) and heterogenous catalyst (CaO, dolomite, $AlCl_3$, WO/ZrO_2)
Second Generation	 Jatropha Ceiba PFAD	Biochemical Thermochemical	Bioethanol Biodiesel Bio-jet fuel/ Sustainable Aviation Fuel (SAF)	Bioethanol and biodiesel commonly used catalyst similar to first generation
Third Generation	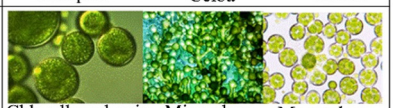 Chlorella vulgaris Microalgae Macroalgae			Bio-jet fuel/sustainable aviation fuel (SAF) used heterogenous catalyst such as Pd/C, zeolites, transition metal oxides
Fourth Generation	 Genetically engineered feedstocks with genomically synthesized microorganisms			

Fig. 1 An overview of each type of green fuel generation.[77–79]

230 billion gallons by 2050, which the current existing petroleum could not withstand; thus, another alternative approach to replace this petroleum fuel has been widely studied. This rise not only causes fossil fuels to diminish over time but also leads to an increase in CO_2 emissions.[83] Statistics studies from EIA show that global aviation emissions represent 2% of global GHG emissions, which rose in 2022 to reach nearly 80% in 2019 (Fig. 2), which is around ~1000 MMT of CO_2, and as forecasted by the International Civil Aviation Organization (ICAO), the value would triple by 2050.[84–86] To overcome this issue, researchers worldwide have extensively studied and explored alternative approaches to replace fossil fuels in various sectors, including aviation.[52,87]

An effective approach is to advance and implement sustainable aviation fuels (SAFs). The SAF, commonly referred to as bio-jet fuel or biokerosene, is a liquid hydrocarbon alternative to hydrocarbons in the C_8–C_{16} boiling point range. It shares similar properties with traditional fuels, and is formulated for current aircraft usage.[88–90] SAF is distinguished by its markedly reduced carbon impact compared with that of the traditional jet fuel. SAF typically achieves a significant decrease in carbon dioxide emissions, typically falling within the range of 50–80% as opposed to the conventional jet fuel sourced from fossil fuels. The extent of this decrease depends on the specific feedstock and production method used.[91,92] The primary objective of the carbon offsetting and reduction scheme for international aviation (CORSIA) is to offset any excess emissions over the established limitations by 2020 through the purchase of carbon credits from various businesses.[70,93,94] In addition, it specifies the sustainability criteria for the raw materials used. To be certified as sustainable, a fuel must adhere to the sustainability guidelines established by the CORSIA. These requirements include reduction of carbon emissions, enhancement of water quality, consideration of soil and air quality, and adherence to land and human rights. The proposal functions as an interim measure until the aviation sector can devise and use more environmentally sustainable technologies to mitigate carbon emissions. SAFs must comply with specific fuel property standards to ensure efficient absorption. These properties include energy content to improve aircraft performance, density to optimize fuel load and payload capacity, viscosity to ensure smooth engine operation, flash point for safe handling, freezing point for cold climate operations, low sulfur content to reduce emissions, and specific distillation characteristics for compatibility with aircraft engines.[95–97] Achieving an appropriate balance between these characteristics is crucial for the advancement of SAFs that not only comply with precautions and operational demands but also have a positive environmental impact and assist in the future of greater sustainability for the aviation sector.

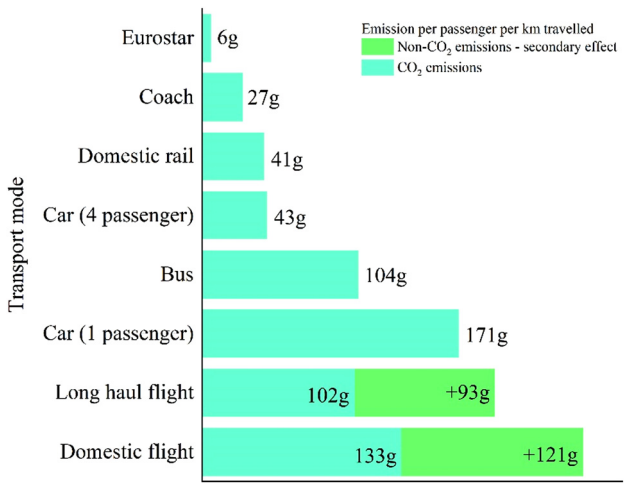

Fig. 2 Emissions from different transportation modes per passenger per kilometre travelled.

Jet A-1 is the conventional jet fuel that serves as a reference point for the SAF in terms of its molecular makeup and overall fuel characteristics.[98–100] Jet A-1 is typically composed of C_8–C_{16} hydrocarbons. It is abundantly composed of paraffinic chains such as iso-, cyclo-, and *n*-paraffins, followed by aromatics.[83,98] Given their low freezing points, superior thermal conductivities, and particular powers, iso-alkanes are the preferred alternatives. Cycloalkanes, however, satisfy certain requirements owing to their density and ability to swell. Both iso-alkanes and cycloalkanes offer the advantages of providing specific energy density, assuring thermodynamic durability; lowering specific emissions; boosting cargo capability; and prolonging endurance.[83,101] Although aromatics are less packed with energy than the alkane group elements of jet fuel, these components are nevertheless required to keep the nitrile rubber sealant on airplanes from expanding excessively to minimize fuel leakage.[102,103] The key factors determining the fuel qualities of the standard are its H/C ratio of 2, lower heating value (LHV) of 43.2 MJ kg^{-1}, and complete absence of oxygen.[83,98,102,104] The chemical properties of aviation fuels, including Jet A, are of critical importance, as they directly determine the fuel's efficiency, safety, and environmental footprint. The compatibility of fuel molecules with engines for aircraft and equipment is crucial for effective discharge of energy, efficient ignition, and safe flight operations. Furthermore, strict compliance with aviation fuel specifications based on molecular functions is crucial for meeting rigorous industry regulations and guaranteeing consistency and dependability throughout the aviation industry. The chemical composition of aircraft fuels is intricately linked to their energy content, ignition characteristics, fluctuation, ignition point, thawing point, and pollutant features.[98,102,105] Hence, a crucial area of research involves developing and refining the molecular composition of SAFs to closely resemble those of traditional fuels. This enables improved fuel efficiency, reduced emissions, and a smaller carbon footprint than conventional fossil-based aviation fuels. Hence, it is imperative to thoroughly understand and assess the molecular functions of synthetic candidates for SAFs to authorize their use in aircraft. This will help promote sustainable aviation practices, improve aircraft performance, and reduce environmental impact.[83,106] The ASTM D7566, which includes the rigorous criteria necessary for SAF, received its initial route approval in 2009. The processes authorized according to ASTM D7566 are listed in Table 1. The aviation sector is responsible for approximately 3% of global GHG emissions, and has long been recognized as one of the major contributors of the

Table 1 ASTM standard on the production group of sustainable aviation fuel (SAF)

ASTM D7566	Conversion process	Possible feedstocks	Blend limit (%)	Year
A1	Fischer–Tropsch synthetic paraffin kerosene (FT-SPK)	Coal, natural gas, biomass	50	2009
A2	Hydroprocessed ester and fatty acid (HEFA-SPK)	Vegetable oil, animal fat, waste oil	50	2011
A3	Synthesized iso-paraffinic (SIP)	Starch, carbohydrate, cellulose	10	2014
A4	Fischer–Tropsch synthetized paraffin kerosene with aromatics (FT-SPK/A)	Coal, natural gas, biomass	50	2015
A5	Alcohol to jet synthesized paraffin kerosene (ATJ-SPK)	Biomass from ethanol or isobutanol production	30 50	2016 2018
A6	Catalytic hydrothermolysis jet fuel (CHJ)	Fatty acids, fatty acid esters, vegetable oil	50	2020
A7	Hydroprocessed hydrocarbons, esters and fatty acids (HC-HEFA-SPK)	Algae	10	2020

transportation sector to global warming.[107–109] With almost 37% of the world's jet fuel consumption going to the US, this country is the largest user.[110,111] China is projected to overtake the United States as the largest worldwide market for jet fuel and air passengers by 2029.[112,113]

An illustration of the chemical equation used to describe the catalytic deoxygenation of WCO is shown in Fig. 3. The fatty acid composition profile of WCO revealed that the vast majority of its constituents were derivatives of the C_{18} and C_{16} fatty acids. This was the case for most of the constituents. In principle, the deCOx procedure can eliminate the carboxyl and carbonyl groups present in C_{18} and C_{16} fatty acid derivatives. This results in the production of hydrocarbon fractions that are mostly composed of *n*-heptadecenes (*n*-C_{17}) and

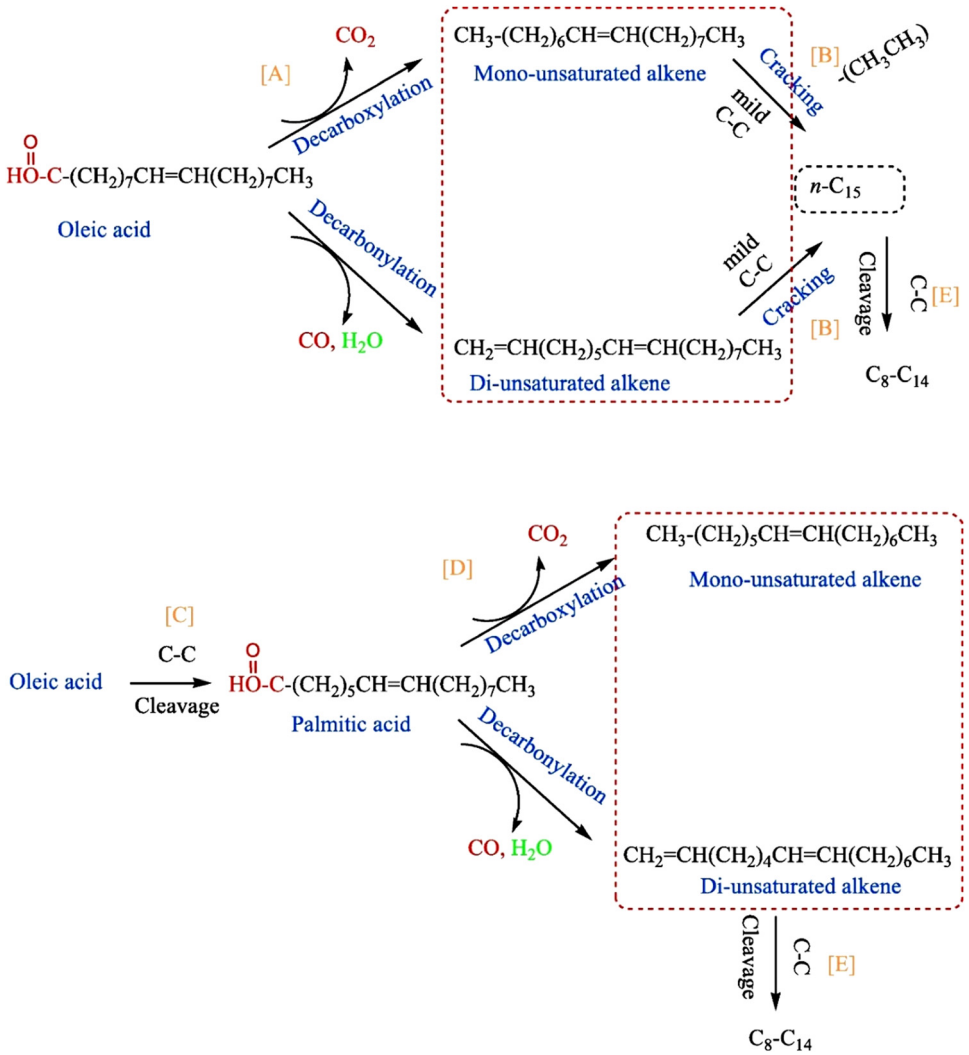

Fig. 3 Proposed deoxygenation reaction pathway for the deoxygenation of WCO to hydrocarbon over CaO–La_2O_3/AC catalysts.

n-pentadecenes (*n*-C_{15}), in addition to the production of byproducts (CO_2, CO, and H_2O) (reactions A and D). During the course of the present study, a significant proportion of the *n*-C_{15} fraction was recovered as opposed to mixtures of *n*-C_{15} and *n*-C_{17}. This discovery provides evidence in favor of the idea that a mild cracking pathway is likely to occur. This route finally led to C–C cleavage of the *n*-C_{17} fraction into the *n*-C_{15} fraction (by the elimination of ethane) (Reaction B). It has been hypothesized that bimetallic CaO–La_2O_3 phases are responsible for the enhancement of certain deCOx-mild cracking pathways. The cracking activities of the CaO/AC and La_2O_3/AC catalysts, which resulted in the synthesis of the *n*-C_{11} fraction, demonstrated that CaO and La_2O_3 were responsible for the cracking ability of CaO–La_2O_3/AC. This was confirmed by the cracking activity of these catalysts. Another option is the C–C cleavage that occurs on fatty acid derivatives, which leads to the production of C_{16} fatty acids (reaction C). Subsequently, the fatty acid derivatives were subjected to a selective deCOx reaction, which ultimately led to the production of *n*-C_{15} hydrocarbon products (reaction D). Because it is impossible to avoid the cracking reaction, the hydrocarbons commonly go through the process of C–C cleavage, which leads to the creation of the short-chain hydrocarbon *n*-(C_8–C_{14}) (reaction E). This is because the cracking reaction cannot be avoided.[114]

The suggested process for the catalytic deCOx of synthetic organic compounds is shown in Fig. 4. This method makes use of a NiO–CD catalyst.[115] The proposed chemical pathway was constructed using the hydrocarbon composition of the SO-based green fuel produced from the deCOx reaction and the fatty acid content of the indicated reactant, as determined by GC–MS analytical data. Both of these factors were considered when designing the route. The fatty acids in SO were responsible for most of the fatty acids in the feedstock. SO contained the following fatty acids: 40.1% oleic acid, 29.4% palmitic acid, and 14.1% stearic acid. The composition of this feedstock led to the production of green fuel, which contained a sizable quantity of hydrocarbons with designations C_{15} and C_{17}. This particular type of diesel was produced. Given this result, it can be concluded that the production of hydrocarbon derivatives in C_{15} and C_{17} is facilitated by deCOx of sulfur dioxide in the presence of a NiO–CD catalyst. In the first procedure, oleic acid was hydrogenated, leading to the synthesis of steric acid as an intermediate product (Fig. 3). During the process, water gas shift (WGS) is the important pathway that creates significant amounts of *in situ* hydrogen throughout the reaction, in which oleic acid's double bonds are saturated completely as a result of the WGS pathway. Moreover, the NiO–CD catalyst accelerated the hydrogenation process by making it easier to break the carbon–oxygen bonds. As a result, oxygen atoms will be removed from the molecules of synthetic organic compounds (SO). In the next step, active sites composed of NiO and CaO on the dolomite catalyst support will cause this steric acid to undergo a deCOx reaction. In accordance with procedures 2 and 3, the decarboxylation and decarbonylation (deCOx) process removes carbon dioxide, carbon monoxide, and water from the stearic acid carbon chain. This may lead to the synthesis of heptadecane (C_{17}) and *n*-heptadecene (*n*-C_{17}). The carbon chain was eliminated as a result of this reaction. Based on the information shown in pathways 4, 5, and 6, more C-single bond cleavage would produce pentadecane, *n*-pentadecene, and lighter hydrocarbons with C_8-single bond C_{14}. To achieve this, heptadecane and *n*-heptadecene were employed as solvents. This was supported by the findings of research conducted by prior studies on the removal of carbon dioxide from fatty acids using a NiO catalyst.[116,117] Route 7 releases hydrogen peroxide and carbon monoxide, which allow palmitic acid to undergo a decarbonylation process that ultimately leads to the synthesis of pentadecane. The mechanism that leads to the production of *n*-pentadecene is the decarboxylation of palmitic acid, which is controlled by pathway 8. A second C–C cracking reaction of these C_{15} hydrocarbons

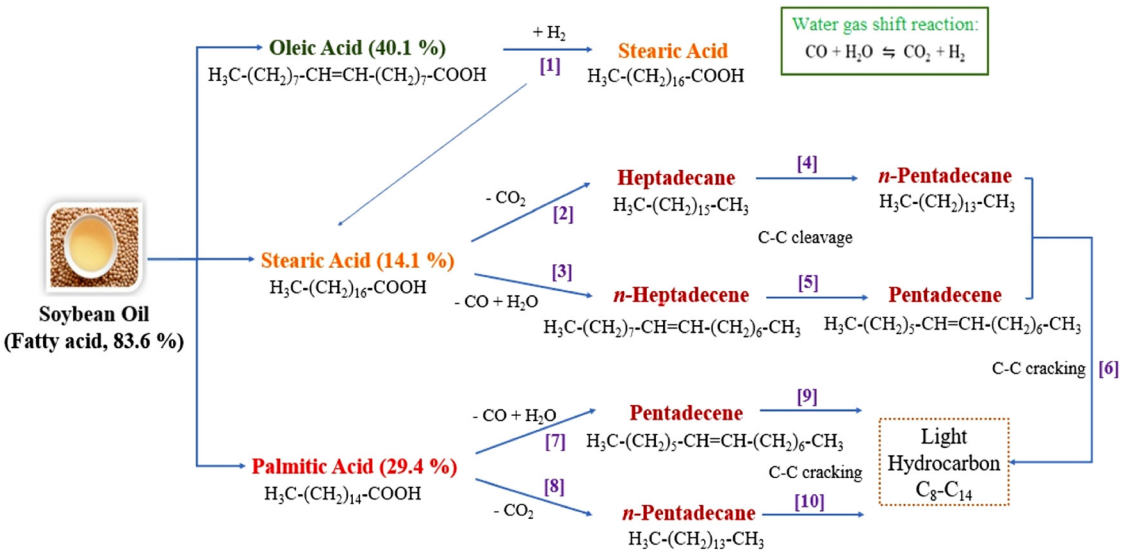

Fig. 4 Proposed catalytic deoxygenation reaction mechanism of soybean oil using an NiO–CD catalyst.[118]

would result in a lighter hydrocarbon with a carbon range of C_8 single bond C_{14}, as demonstrated in routes 9 and 10. This occurs in a moderate environment. Decarboxylation and decarbonylation processes are preferred by the 1–10 approaches that have been suggested for the catalytic deCOx of SO, according to the produced NiO–CD catalyst.

1.1.1.1. Fischer–tropsch hydroprocessed synthetic paraffinic kerosene (FT-SPK). Syngas is transformed into liquid hydrocarbon fuels *via* the Fischer–Tropsch (FT) approach. The standard FT technique consists of six steps: feedstock pretreatments, waste gasification, vapour conditioning, gaseous acid elimination, FT synthesis, and syncrude purification. The raw material was initially dried and treated to reduce humidity and particle size before it was gasified. Gasification followed the prior treatment of the biomass. Temperature, type of biomass used, gasifying agent used, particle size, heating velocity, working strain, equivalency proportion, enzyme addition, and reactor design are some of the variables that affect the quantity and characteristics of syngas produced.[119] Gasification of FT always occurs at a high temperature (approximately 1300 °C) with high-purity oxygen and steam. For gasification, the common gasifier reactors are the fluid bed, moving or fixed bed, and entrained flow systems.

Additional research has analyzed different types of gasifier reactors in detail, and it has been suggested that ash and tar can be removed using a syngas cooling system next to the gasifier, which uses direct quench technology.[120] The syngas is injected into an acid gas removal system after the gasification process to eliminate the sulfur, CO_2, and H_2S present in the gaseous form of acid. Eliminating CO_2 may improve the economy and efficiency of the downstream synthesis process, whereas eliminating H_2S will keep the catalyst clean. The gas is then sent to a gas conditioning unit *via* a water–gas shift (WGS) reaction, where the correct ratio of CO and H_2 is adjusted. The H_2/CO ratio plays a significant role in the FT process, where it enters the reactor and produces the major product. Carboxylic acids, ketones, ethers, alkenes, and alkanes are the products of two main reactions that occur during FT: CO and H_2. Recycled FT gas and unconverted syngas may be returned to the FT reactor following reformation, where refining the liquid products is necessary to create several types of fuels and surplus gas can be utilized for electricity generation. The degree of selectivity of the catalysts is crucial for the target hydrocarbons.

There is another way to divide FT synthesis into low- and high-temperature procedures.[121] Fuel, solvent oil, and olefins are the principal byproducts of high-temperature FT, and lubricating base oil, naphtha fractions, diesel oil, and kerosene are the principal byproducts of low-temperature FT. When the FT temperature is too low, large volumes of methane are produced as a by-product. The typical pressure range for the Fischer–Tropsch (FT) method is between one and several tens of atmospheres, where elevated pressures can lead to the formation of longer hydrocarbon chains.[122]

Fe, Co, Ni, and Ru are frequently used as catalysts in the FT process.[123,124] Ru has good selectivity and catalytic activity, but its high cost prevents frequent utilization.[125] The most popular catalysts for industrial production are Fe-based catalysts that have a long lifetime but a high space-time yield and Co-based catalysts that are effective at allowing carbon chains to form, their byproducts contain fewer oxygen-containing molecules, and carbon deposition is difficult.[122] Alkali metals, alkaline earth metals, copper, and other transition metals are common promoters that can be employed to modify the catalytic activity and efficiency.[126–128]

The primary challenges associated with the main difficulties related to the FT-SPK pathway are the adoption of less complicated gasification methods, which often results in a decrease in the quality of the syngas. However, using plasma gasification for the manufacture of high-quality syngas requires a significant upfront investment for economic viability. Currently, commercially accessible biomass-derived gasified aircraft fuels are scarce.[129] Another significant cost factor is the essential "cleanup" of raw syngas before the Fischer–Tropsch synthesis.[130] This cleanup process involves multiple steps to eliminate various contaminants, and the complexity and cost increase owing to feedstock variability and varying levels of contaminants. In addition, adverse economics and unresolved syngas clean-up difficulties prevent commercial plants from manufacturing FT fuels *via* the BTL method.[131] Additional costs and uncertainties to the process also come from the collection facilities from various places, the relatively inadequate heat amount, and the inconsistent amount and quality of the fuel.[132] Considering the drop-in efficiency, the absence of volatile substances in FT products may cause issues with fuel seepage because elastomer seals may not expand sufficiently.[133]

The FT-SPK/A technology, which enhances the aromatic content of the FT fuel produced, was approved according to ASTM D7566 Annex 4. It is crucial to consider that fuels with high H/C ratios and low O/C ratios can be utilized to calculate the energy source content.[134] Fuels with larger aromatic compositions have higher specific energies. FT fuels do not release aerosol emissions of sulfur dioxide (SO_2) or sulfuric acid (H_2SO_4) because of the thorough cleanup of intermediate syngas. As a result, the rate of impurity deposition decreases, allowing hot-path components (including turbines and combustors) to operate longer before requiring maintenance.

1.1.1.2. Synthetic paraffinic kerosene from hydroprocessed esters and fatty acids (HEFA). The HEFA process is implemented for manufacturing bio-jet fuels by subjecting triglycerides (TGs), both saturated fatty acids (SFAs) and unsaturated fatty acids (UFAs), plant-based oils, residue from cooking oils, and animal-derived fats to hydrotreatment. Typically, this procedure consists of two steps. UFAs are initially converted into SFA by catalytic hydrogenation, during which the TGs undergo a H_2 elimination reaction and produce a fatty acid.[135] By hydrodeoxygenating and decarboxylating the SFA, C_{15}–C_{18} paraffinic chains are produced.[136] Propane, H_2O, CO, and CO_2 are the co-products. Noble metals on zeolite or oxide supports were initially implemented as catalysts for this phase; however, with catalyst deactivation by poisoning, the production of cracking species

and process costs increased, with the focus shifted to other transition metals such as Ni, Fe, Cu, Mo, Co, and Fe, or composite bimetallic catalysts.[137–140]

In the subsequent stage, the paraffinic hydrocarbons are subjected to a process called targeted hydrocracking and deep isomerization, resulting in the production of fuels that contain highly branched alkanes. Activated carbon, Al_2O_3, and zeolite molecular sieves are frequently used as catalysts in this step, together with Pt, Pd, or other expensive metals.[141–144] A moderately acidic zeolite catalyst that supports Ni exhibits good activity. However, a highly acidic catalyst causes over-cracking and lowers the yield of isomers. Fractionation was used to separate the combined liquid fuels into naphtha, light gases, paraffinic kerosene (jet fuel), and paraffinic diesel. Triglycerides were hydrocracked in a single step by Azkaar *et al.* using Ru-modified faujasite zeolite catalysts.[145] When hexadecane was utilized as the feedstock, they were able to obtain a high yield of jet-fuel range hydrocarbons (71%) with a reasonably high selectivity using 2.5 wt% Ru deposited on a hierarchical micro-mesoporous USY zeolite to complete deoxygenation and cracking in a reactor.[145] To convert used cooking oil into a jet green fuel, Li *et al.* suggested using a nickel-based mesoporous zeolite Y catalyst.[146] High jet-range alkane yields of 40.5% and low jet-range aromatic hydrocarbon yields of 11.3% were achieved at an optimal temperature of 400 °C. Using a three-stage catalytic method, Wu *et al.* created jet fuel from vegetable oils based on triglycerides that contained aromatic components.[147] The first step involves catalytically cracking vegetable oils over a zeolite catalyst into light aromatics. Second, by alkylating light aromatics with the help of an ionic liquid, C_8–C_{15} aromatics are created. Third, by hydrogenating aromatics for 6 h at 200 °C and 5 MPa over a Pd/AC catalyst, the aromatics were transformed into saturated cycloparaffins. As they are high-energy green fuels, bio-jet fuels made by HEFA can be used in aircraft engines without blending. The fuel has a high cetane number, strong cold flow characteristics, high thermal stability, and less tailpipe smog; however, it has a low aromatic concentration, which makes it less lubricating and more prone to fuel leaks.[148]

1.1.1.3. Alcohol-to-jet synthetic paraffinic kerosene (ATJ-SPK). A range of events including dehydration, oligomerization, hydroprocessing, and distillation can be employed to create green fuels from alcohols such as methanol, ethanol, or higher alcohols.[149,150] Ethanol, butanol, and isobutanol are commonly used in commercial manufacturing as intermediaries to convert biomass to jet fuel. It usually involves a four-step upgrading procedure to produce hydrocarbons from alcohols in the aviation fuel range. A middle distillate is created by oligomerizing olefins in the presence of catalysts after the alcohol is first dehydrated to form olefins. The jet-fuel-ranged hydrocarbons are created by hydrogenating middle distillates, followed by distillation.[151,152]

Al_2O_3, transition metal oxides, zeolites, and heteropolyacid catalysts are frequently used as ethanol dehydration catalysts.[153–155] Phung *et al.* conducted a comparison between alumina and silica alumina in the context of commercial zeolite catalysts used for ethanol dehydration.[156] H-zeolites are undoubtedly more active on a catalyst weight basis when compared to silica alumina and alumina. The ethylene output from H-FER and faujasite was maximum (99.9%) at 573 K.[156] Ethylene was then subjected to a catalytic oligomerization procedure in which either homogeneous or heterogeneous catalysts were used. When the reaction conditions were optimized, the selectivity for linear-olefins was 96%. For ethylene oligomerization, Shimura *et al.* created a heterogeneous catalyst composed of NiO/SiO_2–Al_2O_3, which is extremely active, selective, and stable.[157] After hydrotreatment and isomerization, these oligomers can transform into branched alkanes, from which distillation can yield jet fuel. One or more olefins such as 1-butene, *cis*-2-butene, *trans*-2-butene, and isobutene can be produced when isobutanol is dehydrated.[158–160] The common catalyst for dehydrating isobutanol involves the use of γ-Al_2O_3 with its moderate acidity. However, catalysts such as inorganic acids, metal oxides, zeolites, and acidic resins have also been identified. Kim and colleagues investigated the dehydration of 1-octanol using the Al_2O_3 catalyst.[161] It was discovered that the crystal phase changes also affected the strong Lewis acid sites and catalytic activity of Al_2O_3, thus increasing the 1-octanol and octene yield.[161] Dehydration is followed by the oligomerization of isobutene to produce jet-range alkenes. Phosphoric acid impregnated on solid supports was a pioneering industrial catalyst for the oligomerization of light olefins, and more catalysts have been studied in recent years, including sulfonic acid resins, acid solids like sulfated zirconia and sulfated titania, nickel-doped zeolites and nickel supported on sulfated zirconia.[157,162–164] Since they have both Lewis and Brønsted acid sites, zeolites are among the most appealing stable acid catalysts; however, they are easily deactivated during oligomerization. The catalysts for isobutene oligomerization were mesostructured aluminosilicates, according to Fang *et al.*[165] The catalyst was durable, and possessed strong acidic sites with high strength. The data show that Ni ions and acidity dominate the product distribution at 523 and 723 K, respectively, where micropore acidity benefits reactions at 723 K, whereas mesopores have an advantage at 523 K.[165]

Butanol can also be converted into jet fuel by using the same process as isobutanol and a similar catalyst. Zeolite, zirconium, solid acid catalysts, HPW ($H_3PW_{12}O_{40}$), and mesoporous silica groups are commonly used catalysts for the dehydration of butanol. To synthesize butenes *via* butanol dehydration, Buniazet *et al.* used a mesoporous material made from ferrierite as the catalyst.[166] The catalyst was discovered to have excellent catalytic activity, selectivity, and stability, with selectivity for linear butenes higher than 80%.[166] Next, hydrogenation and distillation are used to transform the by-products into the jet fuel.

1.1.1.4. Synthetic iso-paraffins from hydroprocessed fermented sugars (SIPs). The SIP method utilizes fermentation to transform carbohydrates into fuels resembling alkanes. This approach differs from the alcohol-to-jet process, which requires an alcohol intermediate. It is based on the advancement of genetic engineering and screening techniques, which allow for the modification of the way bacteria metabolize sugar.[167]

Fermentation products vary widely, but they are largely influenced by the type of substrate used, the fermentation method applied, and the microorganisms involved.[168–170] Through sugar fermentation, the mevalonate pathway in yeast cells can be used by Amyris' biochemical technology to produce farnesene. Farnesene is a hydrocarbon molecule that can take the role of petrochemicals in a range of products, including diesel and jet fuel.[171] SIP conversion has been described in detail by Davis *et al.*, who studied that SIP included six main steps: pretreatment and conditioning, enzymatic hydrolysis, hydrolysate clarity, biological conversion, product purification, and hydroprocessing.[172] The commercialization of the biological conversion of sugar to aviation fuel is carried out by LS9 company.[173] LS9 has focused on creating a method to directly produce alkanes *via* a single-step fermentation process, except for the fatty acids that are generated aerobically *via* the fatty acid biosynthesis pathway. This method produces diesel without the need for hydrogen, hazardous inorganic catalysts, high pressures, higher temperatures, or complicated unit operations.[174,175] Further research is needed on the other intermediates produced during sugar fermentation. Owing to the low temperature of fermentation and the SIP's limited (10%) fuel blend, both these factors result in a low energy input. It is also noted as being more appropriate for manufacturing valuable compounds.

1.1.1.5. Catalytic hydrothermolysis jet (CHJ-SPK). The catalytic hydrothermolysis jet (CHJ-SPK) pathway received ASTM certification in 2020 for blending limits up to 50%.[129] It is based on hydrothermal liquefaction (HTL) technology for the conversion of lipid feedstocks such as fatty acid esters and free fatty acids. However, the processing steps for HTL and bio-crude upgrading are still in the pilot stage of development.

1.2. Generation of feedstocks for green fuel production: from first to advanced biofuels

More than 350 oil-bearing crops are found worldwide and have the potential to be used as sources for biodiesel production. This is considered to be one of the most important variables in the manufacture of green fuels. The choice of feedstock is a critical factor that significantly impacts the overall complexity of the production process, the severity of the operating conditions, and the overall profitability of renewable fuel production. Phan & Phan emphasized the importance of selecting bio-energy feedstock with precision, as the cost of these raw materials can represent up to 75% of the total expenses associated with biofuel production.[176] The feedstock should ideally meet two primary criteria: cost-effectiveness in terms of production and scalability in terms of production volume. The accessibility of raw materials for the production of biofuels is contingent upon the climatic conditions, geographical positioning, local soil quality, and agricultural methods employed in a given country. Numerous fuel crops and land biomass have been researched and considered as potential sources of feedstock for the development of sustainable fuels. Three generations of feedstocks act as sources for achieving sustainable green fuel development and decreasing the oil dependency of the transport industry. They are known as first-, second-, and third-generation feedstocks.

The composition of vegetable oil is a crucial criterion for determining its appropriateness as a feedstock. The oil composition determines the quality of the resulting green fuel. Diverse varieties of consumable vegetable oils, along with inedible oils containing distinct fatty acid contents, are employed in the manufacturing of green fuels. The primary fatty acids found in both edible and inedible oils are oleic, linoleic, stearic, and palmitic acids. The oils contain fatty acids that can be classified into two categories: saturated and unsaturated fatty acids. The first group consisted of stearic, palmitic, and dihydroxystearic acids, whereas the second group consisted of oleic, linoleic, ricinoleic, palmitoleic, linolenic, and eicosenoic acids. The government stopped producing first-generation biodiesel in 2007 in response to a debate over its possible negative social effects, including food safety and environmental contamination.[177] Recent years have seen significant potential for the sustainable development and emission reduction of third-generation biodiesel, which is mostly sourced from microalgae. Nevertheless, increasing the output of third-generation biodiesel to satisfy the urgent energy requirements of nations such as China remains a challenge.[178,179]

1.2.1. First-generation feedstocks. First-generation feedstocks that consist of edible oil crops, such as rapeseed, soybean, sunflower, palm, and coconut oil, can potentially be converted into green fuel *via* thermochemical processes. Table 2 shows the fatty acid composition of the edible oil feedstock containing high unsaturated fatty acids, which is expected to generate long carbon chains of mainly C_8–C_{20} fractions *via* a selective deoxygenation reaction, as one carbon will be removed from the parent fatty acid chain of the feedstock. For instance, rapeseed oil and sunflower oil have been widely used as the main sources of green fuel production in Europe. This can be confirmed by Rogelio *et al.*, who produced renewable diesel-based hydrocarbons on three bifunctional catalysts (Pt/H-Y, Pt/H-ZSM-5, and sulfided NiMo/γ-Al_2O_3) using rapeseed oil at certain parameters. The results revealed that NiMo/γ-Al_2O_3 gave the highest yield of green fuel, successfully converting rapeseed into green fuel.[180] Yuitsu *et al.* successfully produced green fuels from rapeseed oil under conditions of 300 °C/1 MPa (H2 pressure) with Pd/C for 120 min in a yield of 92 mol%.[181] Soybean oil has also been a major source of green fuel using different catalysts such as Pt/SAPO-11 and NbO_4P.[182,183] Coconut oil is commonly used in Asian countries, particularly the Philippines, whereas palm oil is predominantly used in Malaysia and Indonesia.[184] Malaysia is ranked as the second-largest exporter of palm oil following Indonesia. Malaysia generated approximately 17.7 million tonnes of palm oil across 4.5 million hectares of land.[185–187] Edible oils play a dual role, acting as essential raw materials for motor fuels while also supplying crucial nutrients that should not be disregarded. As an illustration, soybeans have a high protein content (35–40%) that contains all the necessary amino acids needed for the development and growth of individuals, supporting excellent health at every stage.[188] Furthermore, soybean oil contains a

Table 2 Types and fatty acid compositions of potential edible oil feedstocks

Feedstock	Palm	Soybean	Sunflower	Corn	Coconut
Primary sources	Malaysia & Indonesia	U.S.A.	Europe	U.S.A.	Philippine
Availability (mill metric tonnes)	65.5	53.7	16.6	60	61.4
Price (USD)* (Nov 2017) (per metric ton)	688	772	1000	300	1523
Oil in seed or kernel (%)	30–60	15–20	25–37	48	65–72
Saturated fatty acid	48	14	11	16	90
Unsaturated fatty acid	50	81	89	84	9
Acid value (mg KOH g^{-1})	0.5	0.6	<1.1	0.223	<3

significant amount of linoleic acid, which is a type of omega-6 fatty acid required for the diet of all mammals. This fatty acid is present in soybean oil at a concentration of 51%, as well as in rapeseed oil at a concentration of 22.3%, and plays a crucial role in reducing the risk of cardiovascular illness.[189] However, palm oil's substantial quantity of saturated nutrients can function as antioxidants, which aid in lowering the likelihood of specific tumor forms. Although it has been demonstrated that different types of edible oils can be used as raw materials for green fuel production, there is ongoing controversy surrounding the use of food resources for automotive fuels. This practice has the potential to disrupt the global food supply and demand market, jeopardize food security, and contribute to rising prices of staple foods in impoverished and developing nations. Similarly, it gives rise to significant environmental concerns, such as the pollution of soil and water, the obliteration of ecosystems, the dissemination of agricultural illnesses and pests, and long-term sustainability challenges related to low energy and cultivation yields for crops such as corn, sugarcane, and soybeans.[190–194] Thus, the ability of fuel crops to replace fossil fuels and achieve sustainable production is questioned. Thus, scientists have begun to focus on relatively non-food-based feedstocks that are inexpensive and economically viable. One potential approach to decrease the use of vegetable oils for diesel generation is to use non-edible oils.

1.2.2. Second-generation feedstocks. The global interest in non-edible oil resources is driven by their abundance, especially in barren areas that are not suited for growing food crops.[195,196] They provide numerous benefits such as the eradication of food competition, a decrease in deforestation rates, improved efficiency, enhanced environmental sustainability, the generation of profitable secondary products, and substantial cost-effectiveness compared to edible oils. Considerable consideration has been given to the long-term effects of global food or fuel issues on the use of edible oil as a green fuel source.[197] Due to their high oil content, availability, and capacity to survive in deserted territories and harsh climates, non-edible plant oils have drawn considerable attention as a new generation feedstock. Additionally, geographical weather has a significant impact on growth.[198] Therefore, they may be cultivated with less extensive care, thus lowering the cost of production. A number of non-edible plant species, including trees, also have extended life spans, some of which can reach 100 years, which is encouraging for the sustainability of the food supply. Well-known non-edible crops such as palm kernel oil, *Jatropha curcas* oil (JCO), ceiba oil, and sterculia oil have been widely used in the manufacturing of liquid green fuels, particularly in the production of biodiesel. It was discovered that non-edible plant seed or kernel raw materials have a higher oil content than raw materials from food plant sources. Table 3 shows the free fatty acid values of non-edible oils, in which ceiba oil had the highest oil content (25–28%), followed by tung oil and cotton seed oil (16–20%). The majority of the oils were classified as non-edible because they contained significant quantities of free fatty acids (FFAs), which include a higher proportion of unsaturated fatty acids than saturated carbon, as indicated by the breakdown of fatty acids in inedible oil. This suggests that deoxygenating such feedstocks could produce a product primarily composed of unsaturated hydrocarbon fractions.

Jatropha curcas L. is a non-edible crop belonging to the Euphorbiaceae family, with a small tree or large shrub up to 5–7 m tall. *Jatropha curcas* is indigenous to tropical America, but it is currently widely distributed in numerous tropical and subtropical areas across Africa and Asia.[199] This crop exhibits resilience in challenging climates and soil conditions, such as non-arable and desert soils with little requirement for energy and water resources; it is easily established and demonstrates rapid growth and longevity, producing seeds for a span of 50 years. This jatropha plant also contains various parts with medicinal values and is often used for erosion control.[200] Jatropha, the wonder plant, produces seeds with an oil content of 20–60% and kernels with 40–60%, reported to be 1590 kg ha^{-1}. Jatropha oil is rich in fatty acids and comprises chains ranging from C_{16} to C_{18}. These carbon chains have a structure similar to that of diesel fuel, making them a highly promising potential source of oil. Additionally, jatropha plants have additional benefits such as ability to sustain extreme weather, substantial fat content, affordable price of kernels, quick span of development, and swift development.

The perennial herb *Sterculia foetida* L. is a member of the Sterculiaceae family and is referred to as a waterproof oil. This plant is indigenous and is highly suited to tropical and subtropical regions. The typical lifespan of this plant exceeds 100 years. This plant is a tall, upright deciduous tree that can reach a height of 40 m and girth of 3 m. Its branches are organized in whorls and spread horizontally. This oil seed has numerous applications, serving not only as a culinary ingredient, but also as an illuminant in the pharmaceutical, soap-making, and surface–coating industries. The desiccated seeds contained 51.8% fat, 12.1% carbohydrate, 21.6% protein, 5% sugar, 5.5% cellulose, and 3.9% ash. The husks provide oil that is light yellow with a fat content constituting 50–60% of its composition. The identified fatty acids are oleic acid (20.5%), linoleic acid (12.9%),

Table 3 Types of inedible oils along with free fatty acid (FFA) contents

Oil properties	Sterculia	Palm kernel oil	Ceiba
Acid value (mg KOH g^{-1})	11.9	3.4	11.9
FFA value (%)	5.9	1.7	5.9
Fatty acid composition of oil (%)			
Caprylic acid (C8: 0)	—	6.5	—
Decanoic acid (C10: 0)	—	10.9	—
Lauric (C12: 0)	0.1	7.5	0.1
Myristic (C14: 0)	0.1	32.6	0.1
Palmitic (C16: 0)	19.2	19.8	19.2
Palmitoleic (C16: 1)	0.3	—	0.3
Stearic (C18: 0)	2.6	7.9	2.6
Oleic (C18: 1)	17.4	10.2	17.4
Linoleic (C18: 2)	39.6	—	39.6
Linolenic (C18: 3)	1.5	7.9	1.5
Arachidonic (C20: 0)	0.56	0.3	0.56
Malvaloyl (C18: CE)	18.5	—	18.5
Others	0.34	—	0.34

palmitic acid (11.9%), sterculic acid (6.8%), and margaric acid (2.3%).

Ceiba pentandra L., commonly referred to as kekabu or kapok, is a member of the Malvaceae family. It originated in Southeast Asia and grew in Southeast Asia, India, Sri Lanka, and tropical America. The tree was cultivated in a naturally occurring humid and sub-humid tropical environment, and it is typically resistant to drought. The trees bear leathery, ellipsoid, and hanging capsules, which contain seeds with an oil content of 25–28% (w/w) of each fruit, while the trees yielded 1280 kg ha^{-1} of oil. This plant has a low nutritional value because it contains a large amount of fiber. Tye's study revealed that its fibre comprises 34–64% cellulose and holds significant promise for the production of cellulosic ethanol.[201] These fibers are commonly used as filling materials such as beds and pillows.[202] This plant contains a distinctive pair of cyclopropane fatty acids (malvalic acid) that exhibit higher reactivity than the polyunsaturated carbon bond when exposed to ambient oxygen. Therefore, this hydrocarbon chain decreased the ability of *C. pentandra* oil to resist oxidation. According to Bindhu *et al.*, cyclopropane fatty acids (specifically malvalic acids) result in higher viscosity and faster oxidation than palmitic acid.[203]

Malaysia is a major global supplier of palm oil, accounting for 28% of global production and 33% of global exports.[204] Although palm oil has long been used to produce biodiesel, Malaysia has begun to focus on developing jet fuel based on palm oil due to the current crisis and increasing demand.[205] However, the growth of palm oil has resulted in additional environmental problems. The renewable feedstock used to make jet fuel should not have a large carbon chain impact due to indirect land-use change (ILUC).[93] However, oil palm has a significant advantage over other feedstocks because it is more economically viable to produce and yield a higher amount of oil than other feedstocks.[206,207] In addition, it can provide a more stable source of income and has an economic life of over 20 years.[208] As the palm oil sector develops, it will contribute to reducing poverty and promoting economic progress in emerging nations.[209] Because palm oil is widely available in Malaysia, its use as a renewable resource to produce bio-jet fuel is both possible and highly profitable.

For cooking purposes, palm oil is obtained from the fleshy portion of the fruit through a straightforward streaming and pressing process, whereas palm kernel oil (PKO) is obtained from the fruit kernel. Palm oil is a tropical perennial plant that grows in low-lying and humid areas such as Malaysia, Indonesia, and Thailand. The palm oil has been reported to reach a maximum height of 20–30 minutes and the tree has a single stem and is unbranched.[210] Moreover, the fruit can be obtained from the farmed oil palm for 40–50 years starting in the fourth year of growth producing up to 2000 fruitlets with the juicy orange-reddish-colored fruits.[210] In addition, palm oil is a high oil yield crop that produces approximately 10 times more oil than soybeans, with an average annual production of 4–5 tonnes of oil/ha/year.[211] At room temperature, crude palm oil is present in a semi-solid state, and is composed of lauric acid (48%) and myristic acid (6%), which have good oxidative stability and acute melting points and are abundant in palm kernel oil.[212] Palm oil, with its economical price and maximum output per acre among all vegetable oil feedstocks, is a sustainable resource that holds promise for green fuel production.[213,214] Typically, two types of natural oils are derived from fruits: palm oil and palm kernel oil. These oils have distinct chemical and physical properties. Furthermore, crude palm kernel oil (CPKO), which is obtained through extraction, can be further refined into refined palm kernel oil (PKO) *via* mechanical pressing or the use of solvents such as hexanes. Refined palm kernel oil is commonly utilized in non-edible products such as cosmetics, personal care items, and soaps due to its chemical composition, physical properties, and similarities to coconut oil.[215] PKO exhibits a significant proportion of lauric acid (C12: 0) at approximately 50%, which distinguishes it from palm oil, which is generally composed of palmitic acid (C16: 0) and oleic acid (C18: 1) at approximately 40% each. Despite the greater cost of CPKO compared to palm oil, this disparity has been diminishing owing to the implementation of policies that promote the expansion of farmed areas for palm in green fuel programs. Consequently, a sustainable supply of CPKO is readily generated.[216,217] Hence, these data are intriguing and compelling for investigating PKO as a sustainable raw material for BHK production in comparison to palm oil because its fatty acid chain has a carbon atom count within the range often found in kerosene.

1.3. Types of reactions and processes

1.3.1. Hydrodeoxygenation/hydrocracking (HDO). As stated earlier, it is not recommended to directly use renewable sources for fuel, owing to engine compatibility issues with renewable green fuel. As a result, various enhancement techniques, including hydrodeoxygenation, have been devised to generate green energy compatible with modern infrastructures. Hydrodeoxygenation involves the conversion of unsaturated fats in vegetable-based oils to saturated fats. The process involves the removal of oxygenated molecules from triglycerides using heterogeneous catalysts at a precise temperature and high pressure while using H_2 gas to cleave the C–O bonds.[147,218] Generally, the reaction begins with the conversion of the carboxyl group into a carbonyl functional group. The reduction process involves the hydrogenolysis of the

carbonyl bond, resulting in the formation of an aldehyde molecule. This process occurs through the adherence of oxygen molecules to the active sites, which is followed by the dissociation of hydrogen from these sites. The oxygen atom is then eliminated from the active site in the form of water, while the aldehyde undergoes reduction to form a primary alcohol and reacts with hydrogen to yield an alkane and water.[219] The main approach for achieving ultimate elimination involves dehydration, which results in the formation of alkenes. Conversely, alkanes are generated through hydrogenation. The rate-limiting process involves the transformation of the carboxyl group into a carbonyl group. The reaction progresses *via* the following sequence: first, reduction to an aldehyde, then reduction to an alkane, and finally reduction to an alcohol. The two stages of HDO are in opposition, and when the catalyst comes into contact with highly adsorbed acids, it can hinder the adsorption of alcohols and result in a shift in the selectivity towards deoxygenation.[220] The technique relies heavily on H_2, and hence, requires a continuous flow of H_2 to achieve the desired result. The primary objectives of HDO are to reduce the O/C ratio and concurrently increase the H/C ratio.[221] The catalytic support also plays a pivotal role in determining catalyst selectivity. Supports exhibiting greater acidity demonstrated improved effectiveness in the dehydration of alcohol functional groups.

$$C_nH_{2n}O_2 + 3H_2 \rightarrow C_nH_{2n+2} + 2H_2O \quad (1)$$

The outcome was that the *n*-alkane generated the same number of carbon atoms as the starting fatty acids in triglycerides, making *n*-alkane green fuels more desirable as sustainable fuels with superior qualities than traditional diesel-based fuels (such as a high cetane number).[26,222,223] In addition, two potential side reactions may occur during the HDO process: the water gas shift reaction and methanation reaction. These processes result in an increase in hydrogen intake.[224] The primary volatile by-products resulting from the HDO of TG-based oils are CO_2, CO, H_2, and C_3H_8.[225,226] Unfortunately, the disadvantage of the hydrodeoxygenation process is its high cost, which is mostly caused by the significant amount of hydrogen used in the process.[227] Consequently, extensive studies have been conducted to develop a new cracking method for the generation of certain diesel fractions in an atmosphere with free hydrogen, known as deoxygenation.

1.3.2. Deoxygenation process (DO). Deoxygenation involves two processes occurring simultaneously (decarboxylation and decarbonylation), in which oxygenated molecules are removed from triglycerides to produce by-products (CO, CO_2, and H_2O), which can then be used to create hydrocarbons resembling fuels in the absence of H_2 gas. Decarboxylation is the process of removing a carboxyl group, where oxygen (O_2) is expelled as carbon dioxide (CO_2) from the carbon chain of TGs.[228] Meanwhile, the decarbonylation reaction has two primary reaction pathways: β-elimination and γ-hydrogen transfer.[228] β-Elimination is a chemical process that results in the production of carboxylic acids and unsaturated glycol difatty esters (UGDE) from triglycerides (TGs). Subsequently, the hydrogenation of UGDE results in the release of fatty acids and the formation of a lesser quantity of straight paraffin chains.[229] However, the γ-hydrogen transfer process initiates the unravelling of the C–C bond within the acyl group, leading to the emergence of a terminal olefin that is less than two carbons than the fatty acids. This process predominantly yields alkanes as the main product and releases CO_2 as a by-product.[228] The primary outcome of the decarboxylation reaction is alkanes, with carbon dioxide produced as a secondary by-product.

Conversely, the decarbonylation reaction involves the elimination of a carbonyl group to generate a paraffin molecule that has a single less carbon than the TGs and generates carbon monoxide as a by-product.[229] During decarbonylation, fatty acid intermediary states release formic acid as the primary output instead of CO_2.[229] Subsequently, the process of formic acid decomposition might occur through two concurrent pathways: dehydration and hydrogenation. Carbon monoxide (CO) and water (H_2O) were released during dehydration. In contrast, dehydrogenation produces carbon dioxide (CO_2) and hydrogen gas (H_2), which are used to generate alkenes or olefins.[18] The equations are depicted as follows:

$$\text{Decarboxylation: } C_nH_{2n}O_2 \rightarrow C_{n-1}H_{2n} + CO_2 \quad (2)$$

$$\text{Decarbonylation: } C_nH_{2n}O_2 + H_2 \rightarrow C_{n-1}H_{2n} + CO + H_2O \quad (3)$$

Remarkably, this reaction has several advantages over hydrodeoxygenation, despite the fact that both processes successfully produce green fuel and jet fuel. First, deoxygenation uses inexpensive catalysts and requires little to no H_2, making it more economically desirable. In contrast, hydrodeoxygenation employs H_2 gas to saturate unsaturated hydrocarbons and removes O_2 as H_2O to generate renewable fuel.[230,231] For this reason, hydrodeoxygenation uses H_2 more than deoxygenation; thus, production costs and operating expenses for hydrodeoxygenation are higher than those for deoxygenation. Moreover, the use of H_2 in the reaction also leads to environmental issues, making HDO environmentally unfriendly. Finally, the decarboxylation pathway improves the catalytic stability, as no water is produced during the reaction. Acid-heterogeneous catalysts are essential for the production of green fuels. For oxygen removal from fatty acids by C–O cleavage *via* a deoxygenation process, highly acidic catalysts are employed to dramatically boost the product yield and selectivity.

1.4. Catalyst development for deoxygenation reactions

1.4.1. An overview of catalysts. Catalysts are crucial for expediting certain chemical processes, hence enhancing performance and maximizing output standards and productivity.[232] A catalyst is a material that accelerates the progress of a chemical reaction toward equilibrium without significantly consuming itself. However, the equilibrium of the process is unaffected by the catalyst. In 1835, Berzelius first used the term ''catalyst'' to describe a concept that might explain a variety of occurrences that appeared to be unrelated to one another.[233] For instance, it has been demonstrated that the production of alcohol from plant materials is achievable when ferments are added in small

quantities. When one or more reactants and catalysts form a chemical bond, new routes for the conversion of these reactants into products are created, allowing the catalyst to be renewed. Additionally, only chemical reactions that are thermodynamically viable can benefit from catalytic activity. A catalyst performs its function in both forward and reverse reactions when the reaction is reversible.[234] The catalyst should be able to continuously cycle between the reactant and reactant catalyst without depletion. Various alkali-, acid-, and enzyme-based catalysts have been used to produce green fuel.[235–239]

In reality, the catalysts must be regenerated and changed. Manufacturing catalysts is a significant industry; billions of dollars' worth of catalysts are sold each year globally. The catalysts can be solids, liquids, or gases. Most modern catalysts consist of fluid or solid surfaces. Homogeneous catalysis refers to catalytic reactions that occur in a single gas or liquid phase, characterized by the homogeneity of the phase in which they occur. Heterogeneous catalysis refers to the process of catalysis occurring in mixtures consisting of several phases, such as a gas–solid mixture. The catalytic activity of a catalyst is a measure of the speed at which the catalytic process occurs. It can be expressed as the rate of the catalytic reaction, a rate constant, or as the conversion or temperature necessary for a certain reaction under predetermined conditions. The ability of the catalyst to focus a reaction on specific products was measured by selectivity. Selectivity cannot be defined by a single definition, but is sometimes referred to as the ratio of activities. It is the ratio of the rate of the desired reaction to the total rate of all reactions that use the reactants. The distribution of products is another way to describe selectivity. In addition to being assessed for activity and selectivity, the stability of the catalysts was assessed. The rate at which the activity or selectivity is lost in a catalyst is gauged by its stability. Essentially, stability can be measured by the rate at which deactivation occurs, such as the pace at which the desired catalytic reaction changes or the rate at which the temperature of the catalyst must be adjusted to compensate for the loss of activity. Catalysts that have become inactive are often subjected to treatment to revive or restart their functionality. The regenerability of a catalyst refers to the extent to which it can be successfully restored; however, its definition is ambiguous.

1.4.2. Homogeneous *vs.* heterogeneous catalysts. Industrial catalysts frequently exhibit intricate compositions and structures. The catalyst is composed of catalytically active phases, supports, binders, and promoters. The most frequently used metals, metal oxides, and metal sulphides are catalytically active substances in solid or liquid form. On rare occasions, they are employed in purest forms. There are some crucial aspects that need to be considered when choosing suitable catalysts for deoxygenation, such as acidity, basicity, surface area, pore size, pore volume, and crystallite size. Traditionally, homogeneous acid or alkali catalysts have been employed to create green fuels, especially in biodiesel production. Homogeneous catalysts are catalysts that are in the same phase as reactants, principally by a soluble catalyst in solution (liquid–liquid form), where either acid or alkaline depends on the properties of the substances used, such as HCl, H_2SO_4, NaOH, and KOH. These types of catalysts are more desirable as they are affordable and yield more products even in a short time of reaction.[240,241] This was confirmed by the study of Abhishek using H_2SO_4 as a catalyst for the conversion of *S. obliquus* lipids to FAME, which yielded 96.68% at low temperatures.[242] This was also aligned with the investigation of Ogunkunle using KOH to *trans*-esterify milk bush seed oil, which showed nearly complete methanolysis with a FAME value of 94.33% under optimal conditions.[243] However, some problems occur when using homogeneous catalysts, including difficult separation, instrument corrosion, requirement for extensive cleaning, contamination, and expensive materials.[244,245] As a result, research is primarily focused on finding suitable catalysts that are easy to separate, have high conversion efficiency, and cause less corrosion to the reaction vessel in addition to the fact that chemical reactions can occur on the surface of these catalysts such as heterogeneous catalysts. Heterogeneous catalysts are catalysts that are in distinct phases from reactants, such as solid–liquid form or solid–gas forms. Heterogeneous catalysts have also been divided into basic and acidic types, yet this hetero-catalyst is in solid or powder form that can be repeatedly recycled and easy to discretize. Therefore, it might serve as a catalyst for promoting eco-friendliness by minimizing hazards, reducing catalyst usage, preventing losses, and enhancing the efficiency and sustainability of the catalysts.[246] This could be verified by comparison with Abhishek, which showed no cycle of reusability for H_2SO_4, while three reusability cycles were performed for the tungsten zirconia catalyst and achieved a FAME conversion of 94.58%.[242] This was also corroborated by another study by Nurul Saadiah, which revealed that the reaction over the CaO/SiO_2 catalyst reached 87.5% at 2 h along with the seventh reuse cycle, with a slightly remarkable reduction in yield.[247]

Heterogeneous catalysts encompass both monometallic and bimetallic systems, which are typically dispersed on various supports to enhance their activity and stability. These catalysts can be broadly classified based on their active components into noble metals, nitrides, sulfides, phosphides, carbides, and non-noble metal catalysts. Monometallic catalysts, defined by the presence of a single active metal or metal promoter supported on a support, are widely recognized for their straightforward synthesis, facile characterization, and cost-effectiveness. These catalysts offer well-defined active sites and have demonstrated considerable efficacy across a range of catalytic processes, including hydrogenation and methanation, particularly when employing transition metals such as Ni, Pd, or Pt. For example, Huang *et al.* reported the selective deoxygenation of lauric acid over a Pt/TiO_2 monometallic catalyst at 30 °C under 1 bar H_2 with LED irradiation (365 nm, 18 W), achieving an impressive 93% selectivity toward n-C_{11} hydrocarbons, underscoring the catalyst's efficiency under mild reaction conditions.[248] Despite these promising outcomes, monometallic catalysts frequently encounter intrinsic limitations, including restricted catalytic activity, selectivity, and stability when exposed to harsh operational environments. For instance, Ni-based monometallic catalysts are prone to sintering and carbon deposition during

deoxygenation, leading to catalyst deactivation, secondary reaction and diminished performance.[249] Moreover, although precious metal catalysts such as Pt exhibit high intrinsic activity, their high cost and scarcity pose significant barriers to large-scale industrial deployment. These challenges underscore the imperative for continued research aimed at enhancing the durability, efficiency, and economic viability of monometallic catalysts, particularly for applications demanding robust and sustainable catalytic systems. Table 4 highlights the prior studies on homogeneous and heterogeneous catalysts.

In contrast, bimetallic catalysts leverage the synergistic interactions between two different metals, which can significantly enhance the catalytic performance by improving the activity, selectivity, and resistance to deactivation. The addition of a secondary metal can modify the electronic and geometric properties of the primary metal, stabilize active sites, and promote better dispersion, leading to superior catalytic behaviour. For instance, Tan *et al.* studied on the catalytic deoxygenation of stearic acid into biofuels using a FeNi/AC catalyst. The results demonstrated the best catalytic performance with a stearic acid conversion of 99% and a linear C_{17} selectivity of 94%.[250] This shows that bimetallic catalysts have been shown to have high conversion along with the increase in the efficiency performance of catalysts owing to the synergistic interaction between the two active metals and the existence of equal base–acid properties in the catalysts. Despite these advantages, bimetallic catalysts present challenges related to their synthesis and structural control, such as preventing phase segregation, dealloying, and ensuring uniform metal distribution. Moreover, the complexity of these systems complicates mechanistic understanding and scale-up for industrial use. However, these obstacles are gradually overcome by new developments in synthesis techniques, such as controlled co-impregnation, atomic layer deposition, and additive manufacturing, as well as computational modelling methodologies, such as density functional theory (DFT) and machine learning. These developments make it possible to rationally build bimetallic catalysts with precisely regulated composition and structure, offering specialized activity, selectivity, and durability for a range of uses in chemical synthesis, energy, and environmental remediation. Although monometallic catalysts are still useful in applications where simplicity and economy are important considerations, bimetallic systems are becoming increasingly more popular in catalysis because of their better tunability and capacity to overcome the inherent drawbacks of single-metal catalysts.

1.4.3. Noble metal catalysts. Noble metal catalysts such as Pd, Pt, Rh, and Ru have been widely employed in the DO reaction. The data indicate that these noble metal catalysts are promising with high catalytic activity and selectivity during the DO reaction, as they contain unfilled d-electron orbitals, making it easy to adsorb reaction species at lower temperatures. Among these metals, Pd with high dispersion properties has been recognized as the catalyst that selectively produces more products towards paraffin chain formation due to its high dispersion properties. Table 5 presents an overview of recent research focused on the deoxygenation of natural oils and analogous model compounds into diesel-range hydrocarbons, highlighting the predominant role of noble metal catalysts in advancing this field over recent years. This was studied by Why *et al.* to investigate the effect of Pd metal on three different supports, which are carbon, vanadium oxide and zeolite, on the generation of bio-jet fuel from WCO. The results exhibited Pd/C has highest yield ~99% with 73% of jet fuel selectivity.[251] The fuel properties were also studied, indicating that the produced liquid product achieved the ASTM standard by having better low-temperature fluidity at 15 °C and combustion effect, which is due to the high paraffinic hydrocarbon selectivity with low aromatic contents. Further examination of the variation ratio of blended Jet A-l has also been investigated.[252] Notably, the bio-jet fuel catalyzed by the Pd/C catalyst with P20%J80% showed the best ratio. This was because of the chemical composition, which contained ~73% bio-jet fuel (~73%), ~24% iso-paraffins, and a small molecular weight of non-paraffinic compounds compared to other ratios, making the properties similar to those of the existing jet fuel. Srihanun *et al.* also corroborated that monometallic Pd on an alumina support can produce a high green fuel yield of 86%, but the addition of Fe to the catalyst increases the performance of the catalyst, yielding 96% green fuel with high selectivity.[186] Apart from Pd, Pt has been widely used as a catalyst for the production of green fuels. Zheng showed that bimetallic Pt–Ni has higher stability and activity owing to the synergistic effect of Pt–Ni along with the promotion of C=O hydrogenation and improved Ni dispersion. The results discovered that bimetallic catalysts produce 52.67% and 40.25% of hydrocarbons and aromatics, respectively, while lowering the coke deposition to 7.26%.[253] This was also supported by Janampelli *et al.*, who revealed the conversion of the 4Pt-8MoOx/ZrO_2 catalyst to a green fuel at a lower temperature of 200 °C, making it a favorable DO catalyst.[254] Other metals such as Re, Ru, and Rh have also been employed as catalysts with superior catalytic performance, making them desirable as catalysts for green fuel production.[255–258] However, the high cost of noble metals has hampered their widespread industrial

Table 4 Literature studies on homogeneous and heterogeneous catalysts

Catalyst	Feedstock	Conditions	Product distribution (%)	Ref.
H_2SO_4	*S. obliquus*	60 °C, 4 h, 30 : 1, 10 wt%	96.68	242
KOH	Milk bush seed oil	65 °C, 2 h, 9 : 1, 3 wt%	94.33	243
CaO/SiO_2	Palm oil	60 °C, 2 h, 3 wt%, 15 : 1	87.5	247
Ni/AC	WCO	N_2-60 mL min^{-1}, 500 °C, 15 min	24–85	249
FeNi/AC-500	Stearic acid	N_2-360 °C, 1 h	Conversion – 88 C_{17} – 97%	249
Ni–Fe/ZSM-5/SAPO-11	Palm oil and triolein	H_2-60 bar, 300 °C, 2 h	Palm oil-62 Triolein-64	142

Table 5 Research on the deoxygenation of natural oils and other analogous model molecules to diesel-ranged hydrocarbons over noble metals, which has been the main focus in recent years

Catalyst	Feedstock	Conditions	Product distribution (%)	Ref.
Pt/ZIF-67/zeolite 5A bead	Palmitic acid	300 °C, 20 bar CO_2, 2 h, batch reactor	n-C_{15} = 92	260
Pt/NMC	Lauric acid	300 °C, without H_2, 3 h, mini-batch reactor	n-C_{11} = 99	261
Pt/HAP-AE	Stearic acid	260 °C, 10 bar N_2, 4 h, batch reactor	n-C_{17} = 91	262
PtSn/SnO_x	Stearic acid	320 °C, 10 bar N_2, 4 h, batch reactor	n-C_{11} ≅ 94 n-C_{15} ≅ 92	260
Pd/C	Stearic acid	260 °C, 28 bar H_2, 6 h, batch reactor	n-C_{17} =: 92 n-C_{18} ≤ 1.0	263
Pd/HPA-SiO_2	Soybean oil	200 °C, 10 bar H_2, 24 h, batch reactor	n-C_{15}–C_{18} ≅ 90	264
Pd@PPN	Stearic acid	150 °C, 20 bar H_2, 14 h, batch reactor	n-C_{17} = 84 n-C_{18} = 6	265
Al-modified Pd@SiO_2	Methyl palmitate	260 °C, 30 bar, 5 h, batch reactor	n-C_{15} = 28 n-C_{16} = 71	266
Ru/C ($ZnCl_2$ starch)	Microalgae oil	140 °C, 50 bar H_2, 6 h, batch reactor	n-C_{17} = 93	259
Ru-Re_{10}/TiO_2	Ethyl stearate	220 °C, 30 bar H_2, 2 h, batch reactor	n-C_{17} = 22% n-C_{18} = 70%	267
Ru/$La(OH)_3$	Jatropha oil	240 °C, 40 bar H_2, 8 h, batch reactor	n-C_{17} = 65% n-C_{15} = 12%	268
SiNA-Rh	Stearic acid	200 °C, 10 bar H_2, 24 h, microwave reactor	n-C_{17} = 94% n-C_{18} ≅ 1	257

applications. Moreover, earlier research has shown that adsorbed chemical intermediates, such as carbon monoxide, heavy organic compounds, and carbonaceous deposits, can poison the active metal site of palladium, making it more prone to deactivation. Thus, another alternative way to substitute into more effective compounds has been researched.

Research on the utilization of Ru in the hydrodeoxygenation process of microalgae oil was carried out by Ali *et al.*[259] At a low reaction temperature of 140 °C, a high heptadecane yield of 93% was achieved over a mesoporous carbon-supported Ru (Ru/C) catalyst derived from starch. Furthermore, it would be desirable to design catalysts that are impervious to contaminants to convert WCO. Xu and colleagues successfully synthesized an exceptionally active Ru–HAP catalyst by using an ion-exchange method. With this catalyst, it was possible to hydrogenate renewable oils into long-chain alkanes at relatively low temperatures (the conversion was completed at 200 °C). At least five recycling cycles demonstrated the high stability of the Ru/HAP catalyst, as well as its high tolerance to a variety of pollutants such as salts, sugars, and amino acids. Both these attributes have been proven. Apart from its application in the hydrogenation of many oil sources, such as WCO, palm oil, and jatropha oil, this catalyst has also shown a high degree of tolerance. Metastable calcium carboxyl phosphate was produced as a result of the widely distributed Ru nanoparticles anchored on the HAP substrate and absorbed fatty acids. The significant role of this component was directly responsible for the high activity and stability of the Ru/HAP compound. A number of authors have also noted that substituting another metal or metal for Ru in catalysts may alter product selectivity. For example, Zhou *et al.* investigated the effect of Re incorporation into Ru/TiO_2 catalysts in the context of the selective deoxygenation of ethyl stearate and found that it produced a promotion effect. Their results showed that the addition of Re had a promoting effect. The catalyst, which consisted of 1 wt% Ru/TiO_2 in the absence of Re, produced a substrate conversion of 98%. Additionally, a strong selectivity toward n-$C_{17}H_{36}$ (n-C_{18}/n-C_{17} = 0.5) was demonstrated by the catalyst. The catalyst was also able to achieve this conversion. The ratio of n-C_{18} to n-C_{17} may rise significantly if the amount of Re in the mixture is increased from 0.5 to 10 wt%. This suggests that there is room for the ratio to increase further. Over the course of their investigation, they learned that the addition of Re increases the number of weak acid sites and promotes Ru growth. They arrived at this conclusion during the course of their investigations.

1.4.4. Non-noble metal catalysts

1.4.4.1. Metal carbide (CS)-, phosphide (P)-, nitride (N)-, sulfide (S)-based catalysts. This has progressively deviated the research effort toward the development of cheaper and more efficient catalysts with high catalytic activity, such as non-noble metals which are tabulated in Table 6. This involves the development of non-noble metal-based catalysts, such as carbides, sulfides, nitrides, and phosphides, on catalyst supports for the conversion of TGs and model compounds into hydrocarbons. Thikhamporn *et al.* reported on Ni–Mo sulphide catalysts producing the highest C_{14}–C_{18} yield of 75.3 wt% with recyclability up to 4 cycles. This might also be due to the high acidity, which leads to high activity.[269] Moreover, sulfured catalysts such as NiMo-PS/MgO–Al_2O_3 and NiMo-CS/AC catalyst have been observed, and the results showed that octadecane and heptadecane are main products, in which NiMo-PS/MgO–Al_2O_3 is more favourable that might be related to the metal oxyphilic capacity.[270] Furthermore, the inclusion of P and CS could promote the catalysts' structure, allowing a sulphide to prevail on the surface of both catalysts, thus presenting high catalytic activity with different active sites.[271] However, some issues emerged while carrying out HDO using sulfided-based catalysts such as an impairment catalytic activity in the earlier reaction time of corresponding catalyst and the necessity for more prominent process conditions such as pressure and temperature, thus making it unfavorable to be used in this reaction.

Table 6 Literature studies on metal carbide (CS)-, phosphide (P)-, nitride (N)-, sulfide (S)-based catalysts for the production of green fuels

Catalyst code	Feedstock	Conditions	Solvent	Product selectivity	Ref.
$NiMoS_2$	Palm oil	*T*: 300 °C, *t*: 2 h, *P*: 30 bar H_2, batch reactor	*n*-Decane	*n*-C_{15} = 22 *n*-C_{16} = 20 *n*-C_{17} = 30 *n*-C_{18} = 28	269
Ni_3S_2	Palmitic acid	*T*: 300 °C, *P*: 50 bar H_2, batch reactor	Dodecane solvent-free	*n*-C_{15} = 94 *n*-C_{16} = 6	276
Ni–MoS_2	Palmitic acid	*T*: 300 °C, *P*: 50 bar H_2, batch reactor		*n*-C_{15} = 45 *n*-C_{16} = 55	276
Sulfided ReNiMo/*y*-Al_2O_3	Oleic acid	*T*: 350 °C, *t*: 1 h, *P*: 40 bar H_2, batch reactor		*n*-C_8–C_{12} = 4 *n*-C_{13}–C_{18} = 77	277
$Ni_2P/A1_2O_3$	Palmitic acid	*T*: 300 °C, *P*: 40 bar H_2, *t*: 1 h, flow reactor	Solvent-free *n*-Hexane	*n*-C_{15} = 76 *n*-C_{16} = 23	278
$MoP/A1_2O_3$	Palmitic acid	*T*: 300 °C, *P*: 40 bar H_2, *t*: 1 h, flow reactor		*n*-C_{15} = 3 *n*-C_{16} = 22	278
Ni_2P/AC	Palm oil	*T*: 350 °C, 40 bar H_2, *t*: 6 h, flow reactor		*n*-(C_{13}–C_{20}) = 98	279
NiC	Coffee oil	*T*: 400 °C, *P*: 40 bar H_2, *t*: 5 h, batch reactor		*n*-(C_8–C_{16}) = 42 *n*-(C_{13}–C_{20}) = 23	280
MoWC/C	Canola oil	*T*: 250 °C, *P*: 450 psi H_2, *t*: 2 h, batch reactor		*n*-C_{18}: 50 *n*-C_{17}: 34	265
$Mo_{2.56}CN_{0.50}$	Palmitic acid	*T*: 300 °C, *P*: 40 bar H_2, *t*: 1.2 min, fix-bed reactor	*n*-Decane	*n*-C_{16} = 86	281

Carbides are non-noble-metal–supported catalysts that can be used to produce hydrocarbons. Tran *et al.* demonstrated the effect of bimetallic carbides on the production of diesel-range hydrocarbons using canola oil, and the results showed that Mo-W carbides/C catalysts converted more than 95% with a cracking ratio of <3% at a low temperature of 250 °C.[265] Another study by Fei *et al.* examined the efficacy of molybdenum carbide nanoparticles on a carbon nitride support (MoC/CN) catalyst. The results showed impressive performance, with a conversion rate of 94.3% and a selectivity rate of 90.3% at 310 °C. This success can be attributed to the presence of more active sites, enhanced dispersion of active sites by the abundance of pyridinic and pyrrolic N onto molybdenum, and incorporation of Mo metal.[272] Nevertheless, the carbide catalyst surface's degradation and accumulation of carbon could result in the reduction of active sites, which could reduce the catalyst's performance. Therefore, the production of green fuels has enabled the use of nitride-based catalysts. Nitride and carbide catalysts possess numerous similar structural characteristics; however, nitride catalysts tend to be more oxidation-resistant. Wang examined the conversion of methyl palmitate (MPA) to green fuels using a Co_3Mo_3N catalyst, and the data obtained showed the highest yield (99.5%) with selectivity to hexadecane of up to 95% under mild conditions.[273] This might be due to the interaction of Co–Mo nitrides with the unique dual-site fining of the electronic and structural configuration of the Co_3Mo_3N catalyst, thus leading to the desired hydrodeoxygenation route with high stability up to 72 h. Another study also confirmed that nitridation of the catalyst plays a pivotal role in its properties, thus increasing the activity of the catalyst. This might be due to the excellent dispersion of active metals and promoters on the support and the formation of γ-Mo_2N species, thus successfully hydroprocessing rapeseed oil with high efficiency.[274] Phosphide-based catalysts have been extensively studied for the production of green fuels. Kaewtrakulchai investigated the effect of transition metal phosphide-supported porous biochar on the hydrocracking of bio-jet fuels.[275] The results showed that Fe–P produced a high percentage of paraffin while lowering the aromatic content from 21% to 14% owing to its high acidity, surface area, and catalyst dispersion.[275] However, increasing the number of active sites can promote the isomerization of short chains, leading to the formation of branched paraffins (iso-paraffins). In addition, the high acidity of the Fe–P catalyst leads to excessive fractions that result in a high proportion of undesirable products, such as C_4 and C_5 gaseous hydrocarbons.[275] Ruangudomsakul also examined the hydrogenation on mixed-phase nickel phosphide catalysts. Remarkably, the Ni_xP_y catalyst produced more green fuels than commercial Ni_2P owing to the presence of mixed Ni_2P and $Ni_{12}P_5$ in Ni_xP_y.[187] It was noticed that more favored decarboxylation and decarbonylation processes produced C_{15} and C_{17} alkanes as the major products, in which the presence of dominant phase Ni_2P might have an impact. Thus, catalysts constructed from transition metal oxides (TMOs), such as Ni, Cu, and Mo, have been progressively explored for the oxygen deprivation of fatty acids to straight hydrocarbons of gasoline- and kerosene-range hydrocarbons, as well as for the green fuel-like approach.

Ketene intermediate (3) was produced as a consequence of the activation of the fatty acid molecule on the sulfur vacancy site of Ni–MoS_2 (1 → 2). This process is illustrated in Fig. 5. A Mo cation and a nearby basic sulfur atom, which engaged in the C–O cleavage and α-proton abstraction processes, respectively, were utilized to produce this intermediate. The goal of the interaction between the carbonyl carbon and Mo cation was to improve the synthesis of C_{15} hydrocarbons. This interaction resulted in the weakening of the C–C bond and an increase in the proportion of ketene species with DCO (3). Because the sulfur anions on MoS_2 are less basic and have fewer electrons than those on Ni–MoS_2/Ni_3S_2, there may be a change in product selectivity on MoS_2, which could explain why ketene species production is restricted (3). This may be related to the fact that MoS_2 exhibits distinct product selectivity. However, although

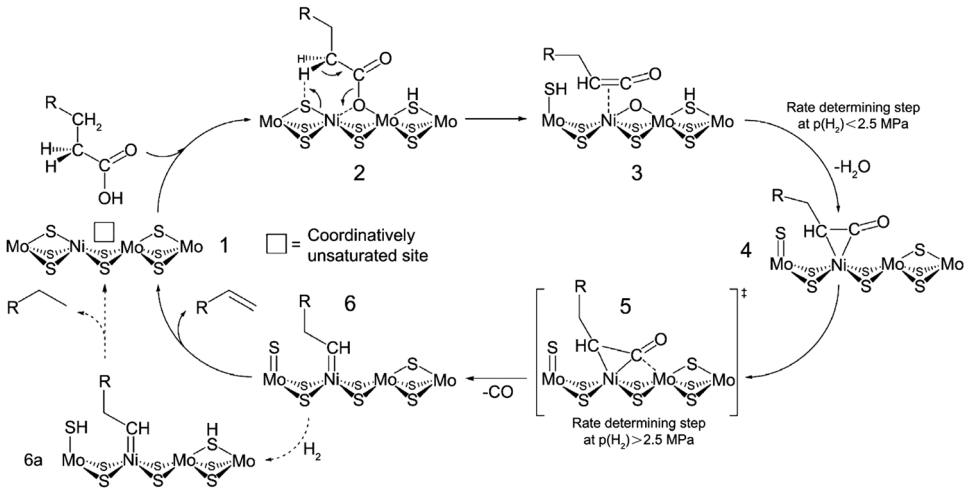

Fig. 5 Hypothesized mechanism for the decarbonylation of fatty acids on Ni–MoS_2. Reprinted with permission from ref. 276.

these compounds can be used to achieve high selectivity for desired products, the use of metal sulfides presents a number of environmental challenges. Consider sulfur as an example. Under hydrothermal conditions, sulfur can leak into the reaction fluid. The sulfur may be absorbed into the liquid fuel product or precursor as a result of this leaching. This might cause the catalyst to become inactive, which would shorten its lifespan and add to the environmental contamination.

1.4.4.2. Transition metal oxide (TMO)-based catalysts

1.4.4.2.1. Ni-based catalysts. Among TMOs, Ni has sparked interest due to comparable performance and endurance comparable to noble metal catalysts in the conversion of triglycerides and fatty acids to hydrocarbon molecules. Furthermore, this Ni species is easily synthesized, resulting in cost-effective production, exceptional hydrogen activation capabilities, and favorable electrical properties that can induce chemical reactions reminiscent of precious metals (*e.g.*, Pd and Pt), including the unravelling of C–C or C–H bonds in hydrocarbon processes.[34] This supports the findings of Zhang by using phosphotungstic acid loaded on a Ni/MCM-41 (HPW-Ni/MCM-41) catalyst, and it was shown that Ni metal catalyzed methyl palmitate through hydrodeoxygenation and dehydrogenation of methyl palmitate to produce 1-pentadecene and then produced jet fuel-ranged hydrocarbons with an increment yield of 86% with selectivity to *n*-alkanes and iso-alkanes of 47% and 8%, respectively. Moreover, Lee investigated a Ni/Al-SBA-15 catalyst under a N_2 atmosphere at 20 bar and 280 °C for 2 h, and the data revealed that 83% conversion to jet fuel hydrocarbon from methyl palmitate showed that Ni metal alone could successfully produce high conversion due to acidic sites due to Ni. In contrast, Tan examined under H_2 conditions for 4 h at 330 °C, and the results revealed that the exposed Ni_2P/Zr-SBA-15 catalyst produced a hydrocarbon yield of approximately 61–74%. Another separate study using a non-edible oil, karanja oil, has been conducted by Ramesh *et al.* in a H_2 atmosphere, showing that more than 90% jet fuel was produced using a NiMoS/Ti–K catalyst for 6 h reaction time. Ni-MOF catalysts have also been employed to produce jet-fuel hydrocarbons using different linkers, as illustrated by Zhu *et al.* using 1,3,5-benzenetricarboxylate denoting catalyst as Ni-BTC/MCM-41, which was observed to produce only 53% jet fuel selectivity. In addition, Cheng *et al.* produced a Ni-DOBDC catalyst using 2,5-dihydroxy terephthalic acid as linkers, and 82% of the jet fuel-like products were produced. However, extensive prior research has demonstrated that monometallic Ni-based catalysts often yield low amounts of gasoline- and kerosene-range hydrocarbons due to severe coke formation, which significantly hinders catalyst stability. As a result, these catalysts can become deactivated, lowering overall hydrocarbon yields. This could be seen in the investigation of Hunsiri, which produced ~71% yield using the Ni/Beta catalyst under a H_2 atmosphere. Furthermore, Kuttiyathil demonstrated jet fuel yields ranging from 40–70% using a Ni/Zeo catalyst, whereas Li reported yields of 24–85 wt% with a Ni/AC catalyst, with both experiments performed under N_2 atmospheres. Although both studies were performed at 500 °C, the yield was not too high, which might be due to the sintering of the Ni species at high reaction temperatures. Hence, adding a second metal such as La, Ce, or Co strongly stabilized the active Ni sites and increased the Ni dispersion, thus improving the selectivity to the desired hydrocarbons.[282,283] A thorough summary of earlier research on Ni-based catalysts for the generation of sustainable aviation fuels (SAFs) is provided in Table 7.

1.4.4.2.2. Co-based catalysts. It is interesting to note that despite Co's lower acidity than Ni, Co-based catalysts behave differently from Ni-based catalysts. Further research on the effects of Co revealed a stronger selectivity for the decarboxylation pathway. Table 8 provides a thorough summary of previous study findings on Co-based catalysts for the generation of green fuel. According to a recent report on the deoxygenation of PFAD over acid–base catalysts, the results revealed that the Co/AC catalyst demonstrated the best level of deoxygenation efficiency and excellent selectivity towards the synthesis of the liquid product (n-C_{15} + n-C_{17}).[39] Further study by de Barros *et al.* revealed that the Co/EAC catalyst presented almost 98.4% conversion of jet-fuel hydrocarbon from macauba pulp oil.

Table 7 Previous literature on Ni-based catalysts for SAF production

Catalyst	Feedstock	Reaction condition	Yield (%)	Reusability cycles	Ref.
Phosphotungstic acid HPW-Ni/MCM-41	Methyl palmitate	H_2-2 MPa, 390 °C, 6 h	86	NA	284
Ni/Al-SBA-15	Methyl palmitate	N_2-20 bar, 280 °C, 2 h	83	NA	285
Ni_2P/Zr-SBA-15	Jatropha oil	H_2-45 bar, 330 °C, 4 h	61–74	NA	286
Ni-BTC/MCM-41(1,3,5-benzenetricarboxylate)	Methyl palmitate	H_2-2 MPa, 390 °C, 6 h	53	NA	287
Ni/NH_4-Beta	Palm olein	H_2-30–40 bar, 300–360 °C, 4–8 h	>62	NA	288
Ni/SiO_2–ZrO_2	Biobased difurfurilydene acetone	H_2-2 MPa, 280 °C, 24 h	65	NA	289
Ni–Fe/ZSM-5/SAPO-11	Palm oil and triolein	H_2-60 bar, 300 °C, 2 h	Palm oil-62 Triolein-64	NA	142
Ni-DOBDC (2,5-dihydroxy terephthalic acid)	Methyl palmitate	CO_2-2 MPa, mass ratio of 1 : 40, 430 °C, 8 h	82	NA	290
NiMoS/Ti–K	Karanja oil	H_2-30 bar, 350 °C, 6 h	>90	NA	291
Ni/Beta	Palm olein	H_2-40 bar, 320–360 °C, 5 h	71–74	NA	292
Ni/Zeo	Salicornia bigelovii seeds	N_2-80 mL min^{-1}, 300–500 °C, 10 min	40–70	NA	293
Ni/AC	WCO	N_2-60 mL min^{-1}, 500 °C, 15 min	24–85	NA	249

Gamal examined PFAD using $Co_{10}Mo_{10}$/AC under a N_2 flow, with a yield of 92%.[294] Asikin *et al.* further confirmed that a Co_5W_{10}/silica alumina catalyst using tung oil could achieve an 84% yield within the jet fuel range, retaining this high performance over four reuse cycles with only minor reductions in yield and *n*-C_8–C_{16} selectivity. Athirah *et al.* reported achieving an 83.4% yield during the deoxygenation of coconut oil under N_2 using a CoO–NiO/kaolin acid–base catalyst. Nonetheless, monometal Co-based catalysts show low catalytic activity as Co species favor the decarboxylation pathway. This supports the results of Choo *et al.* (2020) on the effects of several TMO catalysts supported on zeolite Y. The Co-Y catalyst exhibited the lowest transformation (58%) for the deoxygenation of triolein to green fuels in a H_2-free environment. This was also aligned with the investigation by Muangsuwan *et al.* on CoMo/Al_2O_3, with the lowest yield of ~20%. Furthermore, Baharudin reported that Co/SBA-15 yielded only 16%. However, bimetallic Ni–Co/SBA-15 showed the highest hydrocarbon content (88.1%), with a high selectivity to jet fuel. This might be caused by a synergistic interaction between the high hydrogenolysis capacity of Ni and the reduced Brønsted/Lewis acid, which encouraged decarboxylation and prevented the cracking and polymerization of heavy hydrocarbons. This was confirmed by Safa *et al.* using Co(10 wt%)–Ag(10 wt%)/AC, revealing 92% hydrocarbon yield with 8 consecutive runs, as silver metal favours the decarbonylation along with decarboxylation by Co, resulting in high performance for catalytic activity, thus producing high yields with high selectivity. Thus, it is advised to use bimetallic materials such as Ni–Co catalysts that produce synergistic effects on the acid–base sites of both metal species, boosting the catalyst's stability with high deoxygenation activity and simultaneously inhibiting coke formation. Furthermore, a catalytic support is crucial for augmenting the effectiveness of metal promoters in catalysts by strengthening catalyst reliability, facilitating metal dispersion, and reducing deactivation.

1.4.5. Catalyst supports. The choice of a suitable catalyst support is essential in catalyst conception, as it can affect the specific reaction route selected, including the acid/base properties, interactions between the metal and support, and geometric configuration. This choice also affects the distribution of products and enhances the efficiency of the supported catalysts, ultimately leading to increased catalytic activity. Prior research has demonstrated that the physical characteristics of the catalyst support can alter the distribution of active sites throughout its surface and

Table 8 Literature review on Co-based catalysts for green fuel production

Catalyst	Feedstock	Reaction condition	Yield (%)	Reusability cycles	Ref.
Co/AC	Palm fatty acid distillate	350 °C, 1 h, 3 wt%	~72%	NA	39
Co/SBA-15	Palm fatty acid distillate	350 °C, 3 h, 10 wt%	~50	NA	294
Co/SBA-15	PFAD	N_2-10 wt%, 350 °C, 2 h	Co/SBA-15 (16) Ni–Co/SBA-15 (88)	5	35
Co/EAC	Macauba pulp oil	H_2-30 bar, 350 °C, 4 h	98	NA	295
$Co_{10}Mo_{10}$/AC	PFAD	N_2-3 wt%, 350 °C, 1 h, 50 mL min^{-1}	92	6	294
Co_3O_4/$Si_2O_3Al_2O_3$	Jatropha and palm oil	H_2-2/30 bar, 250/300 °C, 6–8 h	67–74	NA	296
Co-Y	Triolein	Partial vacuum-100 mbar, 380 °C, 2 h	58	NA	297
BOMoCo	Waste cottonseed oil	N_2-500 °C, 2 mL min^{-1}	~60	NA	298
Co(10 wt%)–Ag(10 wt%)/AC	Coconut shell waste	N_2-1 wt%, 350 °C, 2 h	92	8	299
CoMo/Al_2O_3	Palm empty fruit bunch (PEFB)	H_2-2 MPa, 300–350 °C, 1 h, 10 wt%	~20	NA	300
Co_5W_{10}/silica alumina	Tung oil	N_2-350 °C, 2 h, 5 wt%	84	4	301
Co–Mo/Al_2O_3	Neem seed	N_2-1 atm, 350–550 °C, 30–240 min	47–53	NA	302
CoO–NiO/kaolin	Coconut oil	N_2-330 °C, 2 h, 5 wt%	83	NA	303

affect the interaction between the support and the active site. The support might exhibit chemical inertness or interact with the active component, which is the true catalyst. The reactions that occur between the active catalyst and the support material affect the selectivity and activity of the catalyst. The support material indirectly assists in the catalytic reaction process by adsorbing the reactants near the embedded catalysts, even though it does not directly participate in the reaction. Additionally, the metal support plays a vital role in modifying the chemical properties of the catalysts and adjusting the activity of the catalytic reaction, while also improving the dispersion of the active metal.

Additionally, common catalysts are mostly composed of porous supports.[304] Most supports are robust solids that can be manufactured with various surface areas and pore-size distributions. Catalyst supports require chemical robustness, substantial surface area, and the capability to efficiently disseminate metal or metal oxide particles on their surfaces, especially when noble metals are used as catalyst promoters. Supports provide the catalyst with its physical framework, appearance, mechanical robustness, and specific reactivity, particularly for bifunctional catalysts. The performance of supported metals is affected by the surface chemical composition, namely the functional classes, as well as the physical characteristics of the surfaces. Considering these requirements, a range of oxide- and carbon-based elements have been used as materials to support catalysts.

Among these materials, zeolite has been used as a catalyst support in the DO reaction because of its high acidity, strictly uniform pore diameter, and high surface area. However, the strong acidity that leads to the deposition of carbonaceous materials on the active sites makes it prone to catalyst deactivation. Thus, AC has gained researchers' interest in producing highly feasible catalyst supports for the DO reaction as a low-cost and highly porous material. Nonetheless, it is difficult to reactivate, and the appearance of inorganic impurities such as potassium, sulfur, and nitrogen, which require prior pretreatment, makes it undesirable for use as a catalyst support.

Thus, another catalyst material was chosen to act as a catalyst support in the DO reaction: an oxide support. This is because of its superior oxygen retention ability and inherent redox characteristics, which enable it to aid in the activation of oxygenated molecules. γ-Al_2O_3, SiO_2, and TiO_2 are typically used as oxide catalyst supports because they are common materials for hydroprocessing conventional fuels. Inevitably, the cracking process requires the support of acidic catalysts, because they provide more sites for oxidized chemical consumption or H_2 breakdown. Moreover, the acidity of the support can enhance the C–O hydrogenolysis activity. However, it is not suggested to employ strong acid support catalysts, such γ-Al_2O_3, since this might lead to significant degradation of the catalyst by promoting the development of coke and an indiscriminate breaking reaction. Consequently, it is essential to employ a moderately acidic material, such as an iron-based catalyst, in order to solubilize the carboxylic group present in the vegetable-derived oil.

1.4.5.1 Properties of iron elements as catalyst supports. Iron (Fe) is the fourth most abundant transition element in the Earth's crust, which is safe for the environment and an incredibly important metal to society.[305] Iron in its pure form exhibits malleability and ductility, with a melting point of 1538 °C. It has a solid density of 7.87 g cm^{-3} and exhibits magnetic characteristics. Despite its apparent prevalence, pure iron metal is rarely used in our surroundings. Instead, a substantial quantity of iron collected from its ore is employed in the production of various alloys, such as steel, which incorporates carbon. The primary ores utilized for iron extraction include hematite, limonite, magnetite (a magnetic ore), and siderite. This shows that the Fe element exists in various oxidation states, including 0, +1, +2, and +3, which leads to different forms, including Fe, FeO, Fe^{2+}, Fe^{3+}, FeOOH, Fe_2O_3, and Fe_3O_4, due to electron transition that has different physical and chemical properties suitable for different types of reactions.[305–307] These classes of materials are widely feasible, reliably manipulable, environmentally sustainable, and simply produced through the use of various techniques.

As it is commonly found in the Earth's crust, making it a low-cost production material, Fe-based catalysts have been widely applied in medical, biological, and chemical applications, such as magnetic resonance imaging (MRI) and manufacturing pigments. Furthermore, it has been employed as a heterogeneous catalyst in various advanced oxidation processes (AOPs) such as catalytic ozonation, Fenton oxidation, electrocatalysis, photocatalysis, Fischer–Tropsch process, gasification and sulphate radical-based AOPs as well as the adsorption of some contaminants.[308–315] These studies show that Fe-based catalysts exhibit high catalytic activity along with a strong affinity for oxygen, favoring redox reactions and making them desirable for producing green fuel. It also appears that Fe-based catalysts have better water–gas shift reactions with a lower H_2/CO ratio and strong oxophilic effects, making it easier to break C–O bonds by binding to oxygen from C═O of oleic acid.[316] The strong attraction between the oxygen-deprived spaces within the iron oxide species enables them to enhance the adhesion and activation of oxygenated compounds more effectively than Ni.[317] This is supported by a prior study by Peng *et al.*, who found that by adjusting the Ni/Fe ratio, bimetallic Ni–Fe catalysts allowed for high phenolic conversion and greatly improved selectivity to phenol or cyclohexane.[318] According to another study by Deplazes *et al.*, the selectivity for toluene increased, while the selectivity for cyclic components on the deoxygenation of *m*-cresol decreased.[319] In addition, Fe-based catalysts improve the surface area and dispersion of host metal elements, enhance the yield and selectivity of the product, and act as electronic/chemical promoters to alter metal catalysts. Widayat *et al.* showed that the biodiesel yield reached 86.78% using α-Fe_2O_3–Al_2O_3 as a catalyst.[320] Furthermore, Zhang *et al.* investigated the impact of a Fe_2O_3 catalyst on the ignition and pollution properties of a diesel engine. They observed noteworthy conversion rates of 72.3% for NO and 76.1% for NO_x in an engine powered by diesel fuel.[321] Given its significance in promoting eco-friendly fuel substitutes, NO_x emissions are a crucial factor. The Euro VI standard has implemented harsh regulations, mandating a 95% decrease in NO_x emissions from heavy-duty diesel engines. This is due to the fact that 90% of NO_x emissions are known to come from the combustion of fossil fuels, with diesel engines

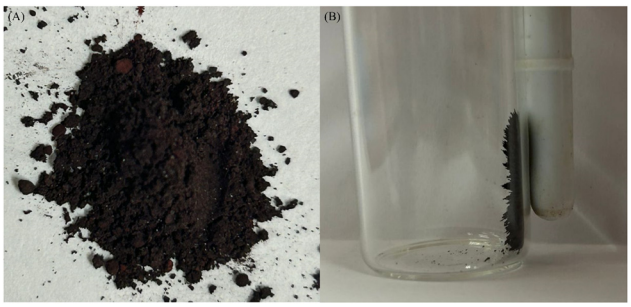

Fig. 6 Images of (A) the prepared Fe_3O_4 catalyst and (B) Fe_3O_4 catalyst attracted to a magnetic bar.

being responsible for 70% of these emissions. These regulations highlight the significant potential of Fe_2O_3 as a catalyst.[322,323]

However, an ineffective separation method could result in catalyst loss and reduce the reusability cycle of the reaction, making the catalyst less favorable (Fig. 6). Therefore, magnetic materials including Fe_3O_4 serve as viable substitutes for catalyst support components due to their cost-effectiveness, simplicity of synthesis and functionalization, minimal toxicity, and ability to be readily recovered using an external magnetic field.[324–326] Additional beneficial characteristics of these magnetic iron oxide nanoparticles include an enhanced saturation field, substantial surface area, high number of functional groups, and remarkable thermodynamic and chemical durability.[327–330] In addition, using a magnetite catalyst not only preserves the magnetic features, but also increases the recovery rate while maintaining its catalytic strength and reusability. Magnetic catalysts have been widely applied in various applications.[331–336] Prior research has also demonstrated that magnetic catalysts have superior catalytic activity in the generation of biodiesel compared to homogeneous catalysts. This is attributed to the magnetic characteristics of the particles, which lead to improved efficiency and durability.[325,337] In addition to its cost-effectiveness and high catalytic activity, this magnetite catalyst has a remarkable impact on carbon combustion. It rapidly forms highly reactive iron oxide condensation sites, which occur faster than carbon particles. Consequently, it reduces the activation energy for soot formation and alters the chemistry of fine particle emissions. This leads to an increase in alkane, organic carbon, and fragments components, particularly in the manufacturing process of renewables fuel such as SAF and green fuels.[338,339] Nevertheless, magnetic elements tend to form larger clusters because of their electromagnetic dipole–dipole attractions, which inhibit the effective dispersion of the magnetic catalyst and, thus, affect its surface area.[340,341] Thus, this magnetic catalyst requires the inclusion of a metal promoter to avoid agglomeration. The study focuses on synthesizing synergistic acid–base Ni–Co loaded on the Fe_3O_4 surface to produce high hydrocarbon yields with selectivity towards diesel-range, gasoline-range, and kerosene-range hydrocarbons *via* a deoxygenation reaction under N_2 conditions using a non-edible oil.

1.4.6. Deoxygenation of bimetallic Ni–Co supported on Fe-based catalysts. Fig. 7 illustrates the mechanistic roles of nickel, cobalt, and iron in the deoxygenation reaction, highlighting how their synergistic interactions contribute to high yields and enhanced catalytic efficiencies. Nickel (Ni) is the primary site of hydrogen dissociation in the deoxygenation of triglycerides and fatty acids. It efficiently cleaves molecular hydrogen (H_2) into atomic hydrogen, which is necessary for further hydrogenation processes (Pathway I). Ni also promotes the hydrodeoxygenation (HDO) and decarbonylation (deCOx) pathways by facilitating the breakage of C–O bonds within fatty acid chains (Pathway II).[342] These routes eliminate carbon monoxide (CO) and water (H_2O), respectively, as forms of oxygen. Significantly, Ni sites are essential for reducing the activation energy barriers related to these bond-breaking processes, which makes it possible for triglycerides to be efficiently converted into hydrocarbons. However, by promoting the breakage of C–C bonds and the elimination of carbon dioxide (CO_2) as a by-product, cobalt (Co) primarily supports the

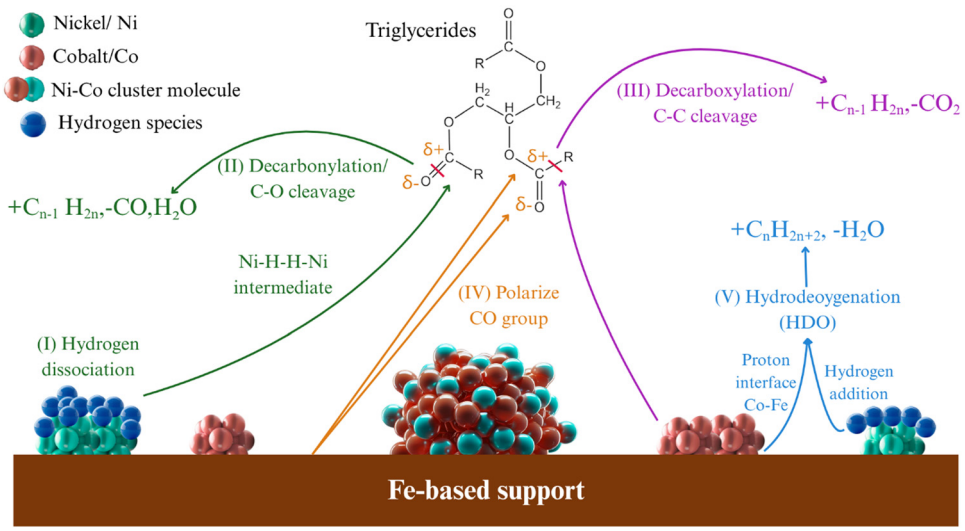

Fig. 7 Diagrammatic representation of the mechanistic functions of iron, cobalt, and nickel in the deoxygenation process.

decarboxylation route (Pathway III).[343] Oxygenated intermediates are further stabilized by the catalyst's oxygen vacancy concentration and redox flexibility, preventing coking-induced catalyst deactivation. For example, earlier research has shown that Ni supported on SAPO-11 produces a greater percentage of C_8–C_{18} alkanes ($\sim$26%) than Co/SAPO-11 catalysts ($<$20%), underscoring the different catalytic functions of these metals.[344] However, to attain the best activity and selectivity, monometallic systems' catalytic efficacy is sometimes insufficient on its own. This restriction emphasizes the need to create bimetallic catalysts, in which the electronic structure of the catalyst is substantially altered by the synergy between Ni and Co. By optimizing reactant and intermediate adsorption and lowering activation barriers for both C–C and C–O bond breakage, this change improves selectivity toward jet fuel-range hydrocarbons (C_8–C_{16}).[100]

Meanwhile, the iron oxide (Fe_3O_4) support contributes additional functionality by providing Lewis acid sites (Fe^{3+} centers) that polarize carbonyl groups in triglycerides.[100] This polarization lowers the activation energy required for decarboxylation and decarbonylation reactions (Pathway IV). Moreover, the dynamic redox cycling between Fe^{2+} and Fe^{3+} promotes the formation of oxygen vacancies, which facilitates efficient oxygen removal and helps maintain catalyst stability and activity.[345] Mechanistically, hydrodeoxygenation (HDO) involves proton transfer at Co–Fe interfacial sites and hydrogen addition at Ni sites, leading to the formation of water and saturated hydrocarbons (Pathway V). Thus, by successfully balancing the deCOx and HDO routes through complementing electrical and structural alterations, the Ni–Co/Fe_3O_4 catalyst system improves deoxygenation efficiency. Co encourages C–C cleavage and stabilizes oxygen intermediates, Ni activates hydrogen and cleaves C–O bonds, while the Fe_3O_4 support supplies necessary acid sites and oxygen vacancies. These elements work in concert to enhance catalyst performance, stability, and selectivity, which makes this system extremely promising for the production of renewable fuels.

1.5. Deactivation of catalysts

The automobile and commercial catalytic industries face a persistent and significant concern regarding catalyst degradation and the progressive reduction in catalytic activity in which the replacement of catalysts can result in considerable capital expenditures. Deactivation has a substantial impact on the functioning, architecture, advancement, and investigation of commercial catalytic systems. Any process that is adequately regulated gradually encounters a decline in its activity. A wide range of physical and chemical elements may play an important role, and they can be divided into four broad categories: poisoning, metal leakage, sintering, and coking.

1.5.1. Sintering. Sintering, also known as thermal degradation, is a time-dependent thermal process that causes catalysts to undergo molecular and physical modifications. This incorporates alterations in the catalyst's surface area resulting from factors such as crystallite growth, support loss, or chemical transformation that occurs during active phase–support reactions. Sintering is commonly occurred at elevated reaction temperatures exceeding 500 °C with the assistance of moisture vapor. This sintering could be caused by metal or support sintering, where there are three main processes involved: high-temperature vapor transport, atomic migration, and crystallite migration. While vapour transportation occur during support sintering, both crystallite and atomic migration typically happened during metal sintering. The process of crystallite growth begins with the complete crystallite migrating over the support surface, followed by collision and amalgamation, the process by which elements combine to create a single mass. Meanwhile, metal atoms separate from crystallites and migrate across the support surfaces before being ensnared by larger crystallites. This process is known as atomic migration. The substance evaporated and condensed into water particles during vapor movement. Water vapor has a major impact on the porosity of the catalysts because the water particles obstruct the active sites, resulting in a surface area of the catalyst that is less active. As a result, less of the surface was exposed to the reactants, reducing the surface-to-volume ratio. Two illustrative scenarios of restricting steps in the sintering process are the disengagement of metal-containing compounds from metal crystallites and the entrapment of atomic metals on the support surface. However, these examples are excessively straightforward and have failed to consider the possibility that these mechanisms operate concurrently and collaborate *via* multifaceted physical and chemical processes.

The sintering process is influenced by several key elements, including temperature, environment, metal type and dispersion, types of promoters, as well as catalyst surface and permeability. Sintering commonly occurs at numerous stages of a catalyst's life cycle, such as through the calcination process in synthesis and catalytic regeneration. As this sintering process is thermally induced, increasing the reaction temperature exponentially increases the sintering rate of the catalyst. Thus, using a stabilizer support or high thermal stability of the support will aid in minimizing the structural collapse or modification of the morphology of catalysts. This is because the sintering rates of the porous molecules are low as the crystallite diameter decreases, approaching the pore size. Dickinson and team studied the conversion of guaiacol from *o*-cresol *via* hydrodeoxygenation at 653 °C and a H_2 pressure of 305 bar using a Ni/SiO_2–Al_2O_3 catalyst. The results showed that sintering occurred after a higher temperature was projected, increasing the particle size of Ni to be increased up to 36 nm from 3.8 nm after the reaction, resulting in a 20% decrease in guaiacol conversion within 400 min.[346] Apart from that, Kim *et al.* reported the loss of active metal sites during HDO of Pt/Zr–P, in which the surface area deduced to 5 $m^2\ g^{-1}$ after 114 h of reaction time. This demonstrates that support materials with a substantial surface area undergo an alteration in phase, transitioning into a form with a smaller surface area owing to the loss of Pt metal during the reaction.[347]

Indeed, under a H_2 atmosphere, the stability of noble metal crystallites often decreases as the metal melting temperature decreases. Rh > Pt > Ir > Ru is the order in which the metal stability decreased under O_2. The degree of unpredictability of the metal oxides is determined by their volatility and the durability of the metallic oxide-support association. In addition, by taking up defect sites or generating new phases, additives and

impurities can affect the thermal characteristics of the support. For example, the sintering process can be accelerated by alkali metals such as barium, nickel, calcium, and lanthanum oxides, which produce spinel phases that are thermally resistant. Additionally, chlorine promotes sintering and particle formation in titanium and magnesium at elevated temperatures. This sintering process induces the closure of pores, leading to the encapsulation of the active metals and a subsequent decrease in the efficacy of the catalyst.

1.5.2. Coking. In addition to sintering, coking is a deactivation mechanism that affects the catalytic activity of the catalysts. Coking is a process in which species within the fluid state are physically deposited onto the surface of catalysts, obstructing their pores or active sites and resulting in a decline in activity. Catalytic fouling transpires when solid deposits obstruct the adsorption of reactants by suffocating the pore spaces and active sites.[348] At a more advanced stage, catalyst particles have the potential to dissolve, leading to the possibility of reactor gaps becoming clogged. Carbonaceous material- and coke-forming processes include chemical absorption of different carbons or concentrated hydrocarbons, which can function as catalyst inhibitors. However, one of the most notable examples is the mechanical deposition of carbonaceous species, such as carbon and coke, in porous catalysts. While coke is created by the breakdown or precipitation of carbon chains on catalyst surfaces, carbon is usually the result of CO disproportionation and is composed primarily of polymerised heavy hydrocarbons.[348] In these processes, many forms of carbon and coke are produced, each with its own unique shape and reactivity. When the temperature drops below 250 °C, carbon dioxide will dissociate on metal surfaces to generate adsorbed atomic carbon. Increasing the temperature causes more amorphous, reactive carbon to develop in the 250 °C $> T <$ 600 °C range, and more refractory, less reactive graphitic carbon to form at $T >$ 600 °C.[349] These carbonaceous species structures formed in the catalytic processes depend on the type of catalyst, reactant and reaction.

It has been suggested that the increased catalyst acidity tends to encourage the development of coke deposits.[350] Ausavasukhi also investigated the hydrodeoxygenation of *m*-cresol to form benzene, toluene, and xylene.[351] A pool of condensate products was found on the surface of the Ga/ZSM-5 catalyst, which resulted in coking during the reaction. This finding was also confirmed by Zanuttini *et al.*'s study, in which coke formation occurred during deoxygenation of *m*-cresol over Pt/γ-Al_2O_3.[352] Increased catalyst acidity has been reported to facilitate the formation of coke deposits.[353,354] Regarding the hydrocarbon processes, coke deposits exhibit an olefinic pool rather than a phenolic pool. Adsorbed polyaromatics produced by olefin cyclization, alkylation, and oligomerization constitute the olefinic pool,[355]Additionally, studies have found that coke formation during hydrogenolysis over Pt catalysts supported on Al_2O_3, CeO_2, La_2O_3, and ZnO is attributed to the oligomerization of acetol.[356,357] Similarly, it has also been found that spent MoO_3 catalysts for the HDO process contain carbonaceous species including soft coke and oxycarbidic carbon.[358,359]

Temperature-programmed oxidation (TPO) and thermogravimetric analysis (TGA) are commonly used to analyze coke deposits on spent catalysts, providing insights into the quantity and composition of coke based on desorption behavior. In order to remove coke, carbonaceous species must be burned or oxidized on a catalyst at a temperature that increases. The amount of coke included in the catalyst would be represented by the total weight loss in TG following the coke elimination. Similarly, the TPO peak resulting from the conversion of coke into CO_2 by oxidizing processes provides details about the quantity and temperature at which coke oxidizes. Various carbon species can be distinguished using this method based on their thermal reactivity in the presence of oxidation.[360,361] TPO is a promising technique since it can represent total coke morphologies and uses minimal powder-like coke samples.

Coking is caused by various factors such as acidity or basicity of the catalyst or the presence of molecules containing oxygen in the deoxygenated product.[362–364] Recent research has indicated that the presence of robust acidic regions on the catalyst enhances the formation of large polyaromatic molecules. These compounds serve as precursors for coke formation and are generated *via* the processes of aromatization, polymerization, and polycondensation. This was noted in research by Choo *et al.* on the implementation of supported zeolite Y catalysts for the deoxygenation of triolein to green fuels.[297] The results revealed that a large amount of Brønsted acidity in the zeolite Y catalyst produced higher concentrations of intermediates that tended to form coke, simultaneously lowering the catalytic activity of the zeolite Y catalyst.[297] The coking performance was remarkable when a significant amount of unsaturated feed was used in the deoxygenation process. Unsaturated species may act as inhibitors by firmly adhering to the layer of catalyst and/or by engaging in the creation of coke, thus concurrently lowering the activity of reaction.[135,365] Other studies have shown that 17 wt% of coke was discovered on spent Ru/C using TGA analysis during HDO of guaiacol. The coking resulted from the deposition of polyaromatic hydrocarbons, which decreased the conversion within 5 h reaction time.[366] Notably, rich phenolic-oxygen-containing species during the reaction could lead to severe coking activity.[367] Consequently, modified supports featuring a greater pore size or a moderate acid strength can improve the C–O hydrogenolysis activity while reducing coking. The latter strategy minimizes secondary reactions of deoxygenated products. Nevertheless, when the coking effect intensifies and the reaction proceeds, these catalysts remain susceptible to catalytic renewal.

1.5.3. Poisoning. The chemisorption of reactants, products, or contaminants on active sites deactivates the catalyst and renders them inaccessible for the catalytic reaction to occur, which results in poisoning. This process, known as chemisorption, involves the bonding of undesirable compounds to the catalyst's active sites, which can change the surface's geometric structure, physically obstruct the active sites, change their chemical makeup (chemical reconstruction), and affect the electronic capacities of other species to dissociate and adsorb on the catalyst surface.[367] Numerous prevalent carcinogens consist of inorganic anions that exhibit a high inclination for adsorption onto the outside surfaces of metal catalysts, in

conjunction with organic functional groups. This comprises organic molecules (nitrogen-containing compounds, carbon monoxide, halides, cyanides, sulfides, and phosphates). Various factors can influence catalyst poisoning, including the production of volatile substances in the reaction (reactive byproducts, inhibitors, contaminants, corrosive substances, and moisture), the presence of a catalytic framework that promotes adsorption, and the occurrence of profound circumstances (high temperature and pressure) that can lead to structural changes and unwanted side reactions.[367]

In deoxygenation processes, certain chemical species may perform as toxins by deactivating the metal catalysts. As an illustration, the application of sulfide, phosphide, or chlorine-based starting materials may result in the degradation of catalysts. This could be attributed to the strong binding of these substances on metals, which hinders or alters the subsequent adsorption of reactants. Mortensen *et al.* studied the effects of sulfur, chlorine, and potassium on nickel-based catalysts for hydrodeoxygenation.[268] It was revealed that without impurities, Ni/ZrO_2 could withstand over 100 h operation; however, employing Ni/ZrO_2 into a sulfur compound results in complete loss of activity and rapid deactivation of the catalysts. In addition, exposing the Ni/ZrO_2 catalyst to a chlorine compound causes the Ni particles to be sintered, thus deactivating the catalyst.

Apart from that, water, which is one of the by-products in deoxygenation and hydrodeoxygenation processes, might interfere with the major reactions occurring on the active sites of catalysts by aggressively adhering to their surfaces. Literature reports on phenol hydrodeoxygenation over Mo_2C/ZrO_2 catalysts indicate that water can oxidize Mo_2C to MoO_2, leading to a decline in HDO activity and a reduction in yield to 19% after 80 hours of continuous operation.[368] In addition, Li *et al.* followed the trend in which water oxidizes phosphide into phosphate and lessens the activity while covering the active sites of phosphide.[369] Furthermore, Li *et al.* reduced the activity when covering the phosphide's active sites, continuing the trend where water oxidizes phosphide into phosphate.[268] Asikin *et al.* observed that while using an active Co–CaO clamshell catalyst to deoxygenate triolein under free-H_2 conditions, the reaction resulted in the conversion of the catalyst into an inactive $CaCO_3$ phase.[370] Similar results were noted for MgO catalysts, where MgO underwent a reaction and was transformed into an inactive carbonate phase ($MgCO_3$).[371] It has been observed that the ingestion of toxic gases will be prominent when the deoxygenation process is conducted completely within an enclosed reaction environment.

1.5.4. Leaching. Leaching, according to the IUPAC definition, involves the dissolution of active substances from an immobile phase, such as a catalyst, towards a partially soluble fluid.[372] The progressive reduction in the number of active sites caused by this leaching ultimately leads to the elimination of catalytic activity, which occurs when the active phase components, especially metal fragments, are extracted from the catalyst. Both high-temperature chemical reactions and solubilization in liquid media can induce leaching. Catalyst leaching can be caused by the following: (i) solvents that are destructive or indistinguishable with the catalyst; (ii) stringent reaction conditions characterized by elevated temperature, high pH, extended duration, and rapid oxidation/reduction rates; and (iii) catalyst's structure, choice of catalyst support, and synthesis method. Degradation that occurs through leaching when aggregate or supported catalysts are employed can be elucidated through chemical transformations or direct dissolution in a solvent.[373] In catalysts with low solubility in water, metal oxide, hydroxide, and carbonate substances dissolve quickly in solutions due to their hydrophilic nature, and this process is known as solubilization, which occurs as these chemicals are forced into the solutions.[373] Hydrotalcites, which are a type of layered double hydroxide with the chemical formula $Mg_6Al_2CO_3(OH)_{16}\cdot 4H_2O$, can selectively remove Mg from solid base catalysts such as MgO when they are dissolved in water.[374] Conversely, leaching *via* chemical alteration may arise when the elements of the catalyst combine with the substances involved in the process to produce a soluble or passive substance. This may be because metal oxide catalysts, which are more hydrophilic under hydrothermal conditions, generate hydroxides. Similarly, the release of active phases from the support can be attributed to the solvolysis of the metal–oxygen link.[375]

The deoxygenation process may result in the leaching of active metal when exposed to acidic hydrothermal conditions, where H_2O is produced as a side-product and the feedstock contains a significant amount of acidic oxygenates, which include acetic acid and formic acid. After 300 h of reaction, approximately 10% of the Ru metal was eliminated from the RuSn/C catalyst during the conversion of levulinic acid to γ-valerolactone at 453 K and 35 bar.[376] Zhao *et al.* demonstrated the existence of acidic conditions that exacerbate the leaching of Ni metal.[377] As the leaching conditions were shifted to a 15 wt% acetic acid solution, the quantity of Ni leaked increased. Specifically, for the Ni/HZSM-5 catalyst, the concentration rose from 5 ppm to 580 ppm, while for the Ni/Al_2O_3-HZSM-5 catalyst, it increased from 1.5 ppm to 690 ppm after 90 hours.[377] This demonstrates that leaching inevitably leads to consequences including the depletion of active sites. Nonetheless, the degradation of supported metal catalysts can potentially be mitigated through the use of metals and supports with more robust metal–support interactions.[377]

1.5.5. Catalysts' stability. Catalyst deactivation processes critically undermine catalyst stability, thereby limiting their industrial applicability. To address these challenges, various strategies have been developed to mitigate deactivation and enhance catalyst durability. One effective approach involves incorporating stabilizing elements to form more robust phases, as irreversible phenomena such as metal leaching and sintering pose significant obstacles to catalyst longevity. For example, the incorporation of SiO_2 as a structural promoter in core–shell $Pd@Al_3$-$mSiO_2$ catalysts has been demonstrated to effectively protect the active metal from sintering and leaching, thereby preserving catalytic performance.[266] Similarly, Liu *et al.* reported that introducing SiO_2 into Ni_2P–Pd/α-Al_2O_3 catalysts enhanced stability by a factor of three, underscoring the critical role of support modification in catalyst robustness.[378]

Coking remains one of the most prevalent deactivation pathways during deoxygenation reactions. To counteract coke formation, the rational catalyst design focusing on structural optimization, thermal regeneration, and strengthened metal–support interactions is essential. For instance, doping Ni catalysts with erbium (Er) has been shown to improve coke resistance during the hydrodeoxygenation of jatropha oil, attributed to reduced Ni particle sizes and the generation of surface oxygen vacancies that inhibit carbon deposition. In another study, the incorporation of lanthanum (La) into Ni/SiO_2 catalysts led to the formation of La_2O_3 and $La_2O_2CO_3$ phases, which effectively suppressed coke accumulation and significantly enhanced catalyst stability and reusability.[379]

Regarding catalyst poisoning, strategies aim to minimize the adsorption strength of poisons or transform them into less harmful species. For example, Rabaev *et al.* demonstrated that adding the amine surfactant hexadecylamine during SAPO-11 crystallization inhibited hydrothermal desilication, markedly improving the hydrothermal stability of the catalyst.[380] Despite these advances, deactivation remains a complex issue requiring further investigation, particularly through the development and optimization of regeneration protocols such as thermal, chemical, and reductive processes that can partially restore catalyst functionality. Nevertheless, repeated regeneration cycles often lead to gradual performance deterioration. Therefore, ongoing research prioritizes the development of catalysts with enhanced thermal stability, coke resistance, and regeneration capability. Such advancements are pivotal for realizing sustainable and economically viable bio-jet fuel production technologies, ensuring that catalysts maintain high performance over extended operational lifetimes.

1.6. Factors affecting the reaction conditions

This section explores various factors affecting the DO process, including feedstocks, reaction environment, reaction temperature, catalyst amount, and the use of solvents. The discussion focuses on how these parameters potentially impact the efficiency and selectivity of biomass deoxygenation, ultimately affecting the production of green fuels.

1.6.1. Reaction temperature. One of the key variables that determines the products generated during hydrotreatment is the reaction temperature. According to a study by Bezergianni *et al.*, the yield of gasoline increased with the reaction temperature, going from 0% at 330 °C to 10.2% at 398 °C, depending on yield conversion to the desired product along with selectivity, eradication of heteroatom components, and saturation point of the double bond.[381] Higher temperatures cause the oil to fracture, which converts the heavier diesel molecules into lighter gasoline molecules. In contrast, the amount of oxygen recovered was insignificant when the temperature was low, and it exhibited a substantial increase as the temperature increased, accompanied by the absence of heteroatoms such as nitrogen and sulfur in the resulting liquid product.[381] Another study by Anand and Sinha discovered that while hydrocracking triglycerides over a sulfided CoMo catalyst, the triglycerides initially transformed into oligomerized hydrocarbons at lower temperatures; however, as the temperature increased, C_{15}–C_{18} hydrocarbons were produced.[382] In addition, while hydrotreating pomace oil, Pinto *et al.* examined the gas and liquid compositions.[383] It was noted that an increase in the utilization of hydrogen at higher temperatures over extended periods of time led to a 22% increase in the quantity of lighter gaseous hydrocarbon mixtures. This suggests that the increasing temperature promoted an extensive cracking reaction, thus producing a more gaseous product.[383] Further evidence shows that decarboxylation and decarbonylation reactions may have been encouraged by the rise in temperature resulting from the 30% and 40% increases in CO and CO_2, respectively. At 300 °C, only 3% of the light fractions contained fatty acids, 96% of which were transformed into hydrocarbons. The hydrocarbon content increased to 99% as the temperature increased to 430 °C, and the fatty acids decreased. However, at 300 °C, the heavier fractions produced only 50% hydrocarbons and 47% fatty acids; 90% of the hydrocarbons were converted when the temperature reached 430 °C, but only 10% of the fatty acids were converted.[383]

A study by Simacek *et al.* also showed that rapeseed oil was converted almost completely at 310 °C, whereas it was fully converted at 360 °C.[384] In a different study, Kikhtyanin *et al.* discovered that, while using Pd/SAPO-31 as a catalyst, the ideal temperature range for fully converting sunflower was 320–350 °C.[385] Hancsok, however, was able to fully convert sunflower at 350 °C using a $Pt/HZSM\text{-}22/Al_2O_3$ catalyst.[386] Furthermore, a study was undertaken by Bezergianni *et al.* to investigate the influence of the reaction temperature on the hydrotreatment of compounds comprising heavy gas oil (HGO) and waste cooking oil (WCO), in which a NiMo catalyst was employed and other variables remained constant throughout the experiment.[387] In their study, they used 70/30 HGO/WCO feedstock at 350 °C to achieve a maximum conversion of 48%. The researcher also discovered that the HGO concentration of a combination decreased with increasing conversion across the board.[387] Lower temperatures were associated with decreased hydrogen consumption because only reactions related to saturation and heteroatom removal occur there, although cracking also occurs. Srifa *et al.* conducted research on hydrotreated palm oil that was subjected to a temperature of approximately 270 °C. The outcome of this process is oil solidification at room temperature. The solidified product is mainly composed of palmitic and stearic acids, supplemented by trace amounts of triglycerides.[388] Therefore, these results show that the product solidifies at ambient temperature during the hydrotreatment process at temperatures below 270 °C.

A substance produced by increasing the temperature further consists of molecules of hydrocarbons, lipids, or fatty acids that are freely present. The higher molecules break down into smaller molecules when the reaction temperature is high.[389] For the majority of the feedstock, it was found that increasing the reaction temperatures accelerated the rate of DO. Nevertheless, in the majority of circumstances, there is a significant decrease in the selectivity for DO at elevated temperatures, which is caused by an increased generation of aromatic products and a higher rate of heat degradation. This emphasizes the necessity of determining an optimal reaction temperature that balances the selectivity and

rate of dissolved oxygen. In addition, the reaction temperature has minimal influence on selectivity towards the desired DO pathways, such as deCOx or HDO, yet the specific catalyst chosen influences the direction of the DO pathway.

1.6.2. Reaction time. Residence time is defined as the ratio between the mass of the liquid input rate and the weight of the catalyst in the reaction mechanism.[389,390] The reaction time metric is a fundamental aspect in the production of green fuel. Throughout each experiment, this characteristic is consistently researched, and the aggregate results show that conversion rates grow in direct correlation with the response times. The range of reaction times can be adjusted from 30 min to 48 h, and possibly longer. Significantly, the maximum reaction varies depending on the reaction components, including the feed, catalyst used, temperature, and pressure. An investigation conducted by Srifa *et al.* examined the impact of residence period on the production of hydrocarbon-diesel-fuel such as crude palm oil (CPO) using a 5% Pd/C catalyst.[391] By extending the reaction period from 0.25 to 5 h, they discovered that the optimal diesel output of 91% occurred around the 3-hour period.[391] Mohammed *et al.* also revealed that the Pd/AC catalyst produced the highest 93% conversion of diesel-like fuel from waste cooking oil over 2 h reaction time.[392] Gamal *et al.* also investigated the effect of the residence time of the $Co_{10}Mo_{10}$/AC catalyst on the production of renewable diesel from the palm fatty acid distillate (PFAD), which contains 55.69% palmitic acid (C_{16}) followed by 22.76% oleic acid (C_{18}).[294] The parameter was studied over a period of 1 to 4 hours. Results showed a progressive increase in yield from 75% to 92% between 1 and 2 hours, along with diesel selectivity increasing from 70% to 89%.[294] Furthermore, Ding *et al.* examined the effectiveness of methyl laurate on a Co/ZSM-5 catalyst.[393] The outcomes illustrate that the Co/ZSM-5 catalyst successfully converted methyl laurate into dodecane, with 68% selectivity for C_{11} and 18% selectivity towards C_{12} alkanes at 280 °C with 4 hours reaction period.[393] In addition, it was observed that prolonged reaction times enhanced the production of CO gas by favoring the decarbonylation route.[394] Further cracking of the deoxygenated liquid product resulted in an increase in lighter fractions, which were almost similar to those of sustainable aviation fuels composed of C_8–C_{16}. Therefore, it is obvious that sufficient retention times are necessary to provide optimal interaction between the precursor and catalysts in order to produce the desired products including diesel-like fuel or kerosene-like fuel and gasoline-like fuel.

Unfortunately, it is not recommended to have a prolonged reaction time, considering the adverse effects on product selectivity. It has been reported that prolonging the reaction time causes the fatty acid to split into a lighter hydrocarbon fraction, decreasing the yield due to increased C–C cleavage, which aggravates the lighter hydrocarbons. This is because extended reaction times resulted in higher yields of undesirable side products such as ethane and methane, as long-chain hydrocarbons continued to break down into shorter hydrocarbons. Ramezani *et al.* reported that as the reaction period was extended, the products experienced side reactions, including cracking, isomerization, cyclization, and dimerization, resulting in a reduction in the amount of the desired hydrocarbons.[395] These results are consistent with Sahar *et al.*, who found that the Pd/C catalyst's conversion of green fuel dropped to only 52% after 4 hours.[392] This can also be seen from Azira's finding, where when the reaction duration of the NiCo/SBA-15 catalyst was increased to 3 h, the selectivity towards bio-jet fuel started to decrease.[396] This was probably due to the widespread cracking of fatty acids, resulting in the production of shorter hydrocarbon chains.[396] Another study also showed that up to 4 h of reaction time, the yield was reduced to ~60% as a more undesirable side product such as gaseous or char was formed, resulting in the build-up of chemicals from undesirable side reactions (condensation, cyclization, and re-polymerization), obstructing the active centers of the reaction sites.[294]

However, a shorter contact period resulted in insufficient time for the catalyst to initiate the deoxygenation reactions. Nevertheless, a contact period that was too brief resulted in an inadequate amount of time for the catalyst to initiate the DO process. Itthibenchapong *et al.*[394] reported that a shorter residence time in a solid–liquid reaction system implies an elevated liquid hourly space velocity (LHSV) across the reagent and catalyst. This can result in a decrease in HDO generation and an increase in deCOx output.[394] This also aligns with Mezaal's findings on palm oil conversion to renewable fuel using a scale-derived hydroxyapatite (HAP) catalyst, where the reaction time was varied from 30 to 240 minutes using a one-variable-at-a-time (OVAT) approach.[397] The data showed that the HAP catalyst produced less than 30% of the hydrocarbon yield during the 30 min reaction period. In addition, another researcher carried out a study on the DO reaction by $Ag_2O_3(10)$–$La_2O_3(20)$/AC nanocatalyst on WCO, and the results indicated that less than 60% of hydrocarbons were produced in 30 min.[398] Syazwani further stated that the initial biodiesel production was hindered by a poor yield due to insufficient mixing and dispersion of the feedstock and methanol within a short timeframe.[399] The aforementioned studies suggest that achieving the optimal reaction time is crucial for enhancing the deoxygenation activity through decarboxylation.

1.6.3. Catalyst type and amount used. Homogeneous and heterogeneous catalysts are the two main types of catalysts used in the manufacture of bio-jet fuels. However, heterogeneous catalysts, which do not require any additional mechanisms for removal from green fuel products, are the most widely employed catalysts. Two categories of catalysts are used in heterogeneous reactions: noble metal and transition metal catalysts. These catalysts are supported by SBA-15, zeolites, carbon, and alumina.[35] Compared to transition metals, noble metal catalysts are more expensive and have a shorter lifetime. Based on the observations by Morgan and colleagues, who found that the 20Ni/C catalyst demonstrated better deoxygenation promotion by generating C_8–C_{17} fractions (>80%) than noble-metal-promoted catalysts when deoxygenating various feedstocks (triolein tristearin, soybean oil).[400] This demonstrates that transition metals can also boost the production of green fuels. Basicity and acidity also play an important role in the production of green fuels.

The high acidity of the catalyst improved the elimination of oxygen and the breaking of C–C bonds, leading to augmented generation of linear hydrocarbons. However, an excessive number of acidic sites can cause aggressive cleavage of C–C bonds, leading to the creation of undesirable side products such as CO, CO_2, CH_4, and CH_2. This reduces the selectivity for the desired product. Furthermore, excessive acidity might result in deactivation of the catalyst due to coking, which subsequently reduces the effectiveness of the catalyst.[401] Basic sites, recognized for incorporating coke-inhibiting species, effectively facilitate decarboxylation pathways and strongly resist CO adsorption, reducing coke formation and contributing to greater catalyst stability.[398,402] However, the basic sites that appear to be inactive for decarbonylation pathways are often unfavorable to produce hydrocarbons, thereby reducing the yield. Therefore, it was proposed that the production of catalysts with a synergistic interaction between the acidic and basic sites could improve the catalyst stability and increase the deoxygenation activity.

Furthermore, the amount of catalyst employed in the DO reaction can significantly influence the rate of the reaction, quantity of the desired product produced, and selectivity of the products. A previous study discovered that the use of a Pd/C catalyst for eliminating oxygen from stearic acid had a substantial impact on the speed of the reaction and the selectivity of the intended products (*n*-heptadecane and heptadecene).[403] The impact of the catalyst dosage on the DO of stearic acid into dodecane was investigated under a helium flow at a temperature of 300 °C and a pressure of 6 bar. The data showed that the conversion and reaction rates increased monotonically as the amount of catalyst was altered.[404] Further experiments were conducted using different quantities of the $NiMo/Al_2O_3$ catalyst ranging from 0 to 0.126 g. The results demonstrated that increasing the amount of catalyst led to an increase in the yield and selectivity towards straighter hydrocarbons, while reducing the formation of intermediate and undesired side products.[405] This may be due to the higher number of available active sites on the catalyst surface when a higher amount was used. This was confirmed when Arvela and colleagues found that 4 wt% Pd/C catalysts yielded a higher yield and selectivity towards *n*-heptadecane during the deoxygenation of tall oil fatty acids.[406] Conversely, when a small amount of catalyst is used in DO reactions, polymerization occurs, thereby enhancing the production of aromatics and other unwanted by-products. This can be seen in Chen's study, which showed that polymerization occurred when less silver nanoparticle catalyst was used for the production of CO_2 in exhaust gas.[407] Hence, the precise quantities of the catalyst play a critical role in defining the highest possible amount and quality of the specified hydrocarbon output. In addition, higher concentrations of the catalyst resulted in a reduced rate of catalyst deactivation and an increased preference for *n*-alkanes. This demonstrates that the production and selection of an optimal catalyst are crucial for maximizing the output of the desired product.

1.6.4. Types of feedstocks. Usually, deoxygenation experiments are conducted using various types of feedstocks, such as triglyceride-based oil and algae biomass. Model compounds have also been selected as feedstock because of the similar molecular structures of vegetable oils.[408–410] Some examples include various fatty acids such as behenic acid, palmitic acid, and stearic acid, as well as fatty acid esters such as stearic acid ethyl ester. The utilization of saturated fatty acids involves decarboxylation to generate linear hydrocarbons with enhanced selectivity, while unsaturated fatty acids undergo hydrogenation followed by decarboxylation to produce *n*-heptadecane, with stearic acid acting as the intermediary product.[231] Furthermore, the composition of the chosen feedstocks is also a significant factor that dictates the composition and quality of the ultimate products generated throughout the process. These hypotheses could be validated by conducting studies involving multiple raw materials, such as stearic acid, soybean oil, and PFAD, with a Pd-based zeolite catalyst in an environment free of H_2, and the results demonstrated the highest bio-jet fuel yield.[411] Further investigation was conducted on the HDO of a model compound of palmitic and stearic acid by using Pd onto a mesoporous carbon catalyst with a dodecane solvent at 300 °C, and the results demonstrated that the conversion rates of both feedstocks were identical.[412] This outcome is consistent with that which had been observed for the DO of heptadecanoic acid, stearic acid, nonadecanoic acid, arachidic acid, and behenic acid.[413] The main liquid products of the catalytic deoxygenation of palmitic acid and stearic acid were *n*-pentadecane and *n*-heptadecane, respectively. These findings demonstrate that using saturated feedstocks instead of unsaturated feedstocks consistently provides benefits for DO experiments.

Similar experiments using commercial Pd/C catalysts have been conducted using saturated and unsaturated feedstocks with dodecane as the solvent at 300 °C for 360 min.[403] The initially observed reaction rates for stearic acid (0.63 mmol min^{-1} $g_{cat}{}^{-1}$) and stearic acid ethyl ester (0.70 mmol min^{-1} $g_{cat}{}^{-1}$) were both slightly higher than those for behenic acid (0.36 mmol min^{-1} $g_{cat}{}^{-1}$). The degradation of stearic acid ethyl ester by the Pd/C catalyst was more pronounced than that of stearic acid. This may be interpreted as stearic acid ethyl ester with a conversion of only 38%, whereas stearic acid reached 60%, which may be attributed to the increased production of unsaturated products that diminish the selectivity for *n*-alkanes. The presence of additional unsaturated molecules in the substrate or output may result in their adsorption onto the surface of the catalyst because of the C=C scission of the alkyl chain, which promptly renders the catalyst inactive. An additional investigation was conducted on bimetallic layered double hydroxides (LDHs) and Ni/Al_2O_3 catalysts under N_2 conditions.[414] The results indicated that soybean oil exhibited the greatest propensity for coking and cracking reactions, confirming that a greater concentration of unsaturated chemicals in the reactant increases the probability of undesirable coking and cracking.[414] In addition, the presence of unsaturated compounds serves as a bridge for cyclization and dehydrogenation events that produce undesirable aromatic products.[231] Previous research suggests that the deoxygenation of stearic acid ethyl ester (SAEE) leads to the formation of carbon monoxide (CO) as the primary gaseous constituent because of the stability of the ethoxy group

in SAEE.[18] The coexistence of these effects in the DO process, caused by the presence of unsaturated molecules in the feedstock, can result in noticeable catalyst deactivation, reduced DO activity, and a large decline in hydrocarbon selectivity. Therefore, it can be deduced that using saturated feedstocks in DO processes can improve DO activity and the selectivity of the products.

1.6.5. Reaction environment. It is commonly acknowledged that the reaction atmosphere has a major impact on the reaction route in deoxygenation research. Deoxygenation and product selectivity improved noticeably in the presence of H_2. Heriyanto reported a green fuel yield of approximately 78% using NiMo/γ-Al_2O_3 at 400 °C for 4 h under a 60 bar H_2 environment.[415] Another study by Frida *et al.* reported that NiO/$NbOPO_4$ yielded 86% conversion of renewable diesel from palm oil, with a C_{15} selectivity of 58%.[416] Further study by Tang and colleagues also revealed high jet fuel components, comprising 55% of C_8–C_{16} using a magnetic Ni–Fe/SAPO-11 catalyst on rapeseed oil.[417] In addition, the Ru/HAP+ HZSM-5 catalyst produced ~92% hydrocarbon yield in an H_2 environment.[418] While the utilization of H_2 can enhance the conversion and hydrocarbon output, it also results in an escalation in operational expenses. Due to the elevated H_2 pressure, the use of costly specialised equipment becomes necessary, and it is also linked to potentially significant safety concerns with hydrogen recycling in the enlarged facility. Consequently, deoxygenation in an inert environment, such as nitrogen (N_2), becomes a more attractive option.

This can be seen in Elaine's report on the deoxygenation of palm kernel oil (PKO) using a Pd/C catalyst. Pd/C produced a significant quantity of liquid product (~99%) with a favorable level of selectivity for jet paraffins (~73%) that had attributes similar to Jet A1.[251] An additional investigation conducted by Azira Razak focused on producing jet fuel from WCO at 350 °C for a duration of two hours, while maintaining a 5% catalyst loading. According to the findings, the 5Ni5Co/SBA-15 and 5Ni5Co/SBA-15-SH catalysts showed outstanding activity by producing around 78–80% hydrocarbon with selectivities ranging from 78 to 92%.[396] In a previous study, Xing evaluated the impact of the reaction conditions on the deoxygenation of oleic acid using a Ni/HZSM-5 catalyst at 360 °C.[419] The findings demonstrated that, while the synthesis of C_8–C_{15} alkanes was boosted in a N_2 atmosphere, yielding approximately 65.05 mol% in a H_2 atmosphere, the yields were reduced due to the catalytic cracking effect, yielding 49.67 mol%. Additionally, when H_2 was increased from 2 MPa to 4 MPa in a H_2 environment, more aromatic hydrocarbons were formed, the molar proportion of straight chains decreased, and the N_2 pressure ranging from 1–4 to MPa remained unchanged.[419] This implies that lowering N_2 did not significantly alter the product and that no olefins were found in N_2, but more aromatic compounds were found when H_2 was present. Based on these results, it is possible to produce green fuel without relying on an external source of H_2.

There is a significant relationship between the atmospheric conditions and the performance of the process as well as the solvent-free deoxygenation pathway. There are situations in which the hydrogen concentration can potentially play a significant role in determining the predominant reaction route. Decarboxylation, decarbonylation, and hydrodeoxygenation are processes that significantly increase the amount of hydrogen required. It was because of this that the current situation came about. With the increase in the initial hydrogen pressure, both the hydrodeoxygenation activity and the product yields improved considerably. During the hydrodeoxygenation process of the model chemical, insufficient stoichiometric hydrogen is present to complete the conversion into the hydrocarbons that are required. This is a concern, because hydrocarbons are expected to be produced. The concentration of linearly saturated C_{15}–C_{18} hydrocarbons was found to be 48.6% in an autoclave batch reactor that included 40 bar of pure hydrogen, according to Malins *et al.*[420] During this time, hydrogen was free of impurities. However, when the pressure was increased to 60 and 100 bars, the concentration of hydrogen increased to 91.7% and 93.3%, respectively.[421] This occurred because of the increasing hydrogen content.

It is possible that the composition of the product changes as a result of a different primary reaction pathway. According to the information provided in a previous study,[296] shorter hydrocarbons are formed when an inadequate supply of hydrogen in the state makes the cracking process easier to carry out. For the purpose of conducting an experiment to explore the effects of air conditions on the deoxygenation of oleic acid, an autoclave batch reactor became the instrument of choice, and Fig. 8 illustrates the results of the study.[419] The effects of air quality were investigated during the course of the study. In addition to preventing the cracking reaction, hydrogen sulfide (H_2S) improves the production of the required hydrocarbons. Using a semi-batch quartz reactor with a capacity of 50 mL and partial vacuum of one bar, oleic acid was decarboxylated to produce unsaturated 8-heptadecene. The production of shorter olefins was accomplished using a straightforward procedure that involved a cracking event. It has been demonstrated that a C–C bond is more thermodynamically stable than a C=C bond,[422] which explains why a situation like this does exist. The deoxygenation of oleic acid results in the production of gaseous carbon monoxide, carbon dioxide, and water as byproducts. A number of additional processes, including water–gas shift (WGS), Fischer–Tropsch synthesis, and methanation, were incorporated into the system after it was previously extended. It is possible that this results in an increase in the hydrogenation of olefins, which, in turn, may lead to the generation of more hydrogen. The formation of linear hydrocarbons is possible *via* hydrogenolysis, a process that occurs during the deoxygenation of cyclic molecules in the presence of hydrogen.

Previous experiments, discussed in this paragraph, have shown that deoxygenation is more effective when air contains hydrogen. Increasing the amount of hydrogen present in the process facilitates the improvement of the hydrodeoxygenation route and decreases cracking, which ultimately results in an increase in the yield of saturated linear hydrocarbons. The addition of hydrogen at a high pressure increases the cost of the process. To improve the performance of the catalysts and

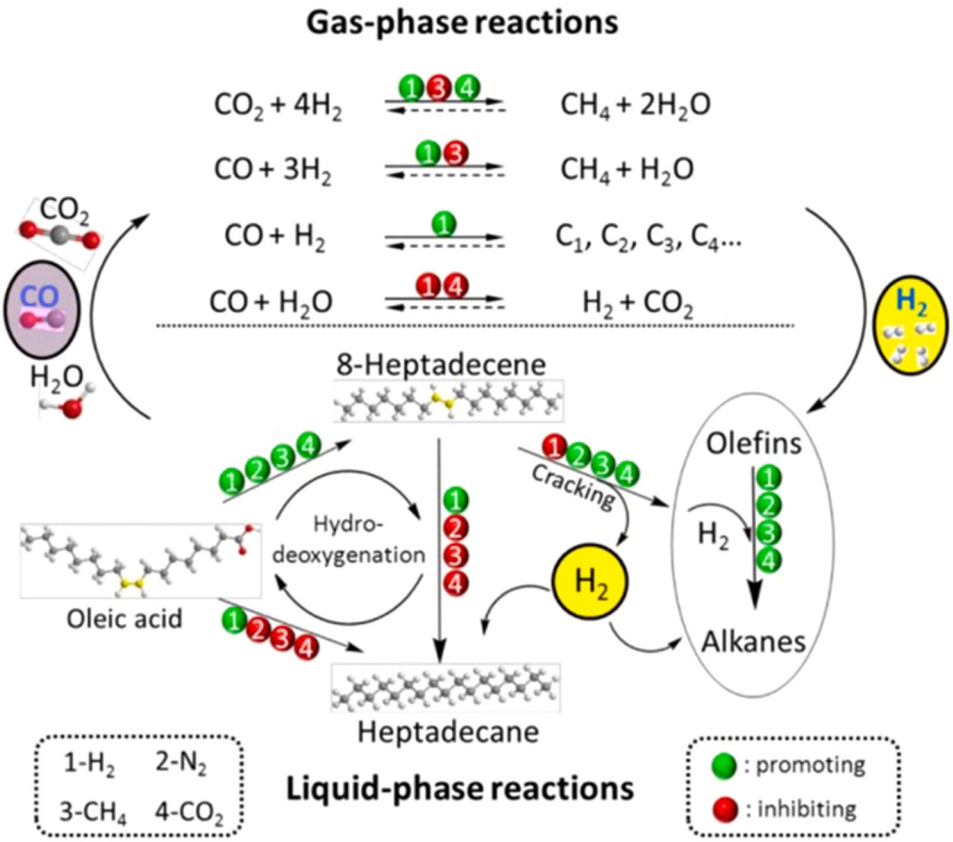

Fig. 8 Impact of four distinct reaction gasses on the reaction route that leads to the deoxygenation of oleic acid. This reference is protected by copyright.[419]

the effectiveness of deoxygenation, research is being conducted in inert settings.

1.7. Recent developments and future outlook of deoxygenation reactions for the production of renewable biofuels

In contemporary times, petroleum fuel plays a significant role in the domains of transportation and industries, both of which are indispensable in the daily lives of people worldwide. Demand was anticipated to rise in tandem with the growing population throughout the period of globalization. Transportation, which includes petrol, jet fuels, and diesel fuels, is one of the major sectors that consumes most of the energy worldwide. This has accelerated economic progress in every country. Nevertheless, a negative consequence of this use is the release of greenhouse gases, particularly carbon dioxide (CO_2), by direct combustion. Carbon dioxide (CO_2) contributes directly to climate change and global warming. Moreover, this petroleum-based fuel originates from restricted sources and is expected to be depleted in a few decades owing to its extensive consumption to satisfy the rising demand. Therefore, there is a critical need for renewable, sustainable, and alternative green fuels that can replace petroleum-based diesel in terms of their lack of pollution, economic attractiveness, and ability to reduce waste. Green fuels derived from renewable sources, such as corn oil, palm oil, animal fats, sunflower oil, and microalgae, can effectively mitigate CO_2 emissions by absorbing and using CO_2 for the photosynthetic cycle. During the initial stages of renewable energy production, the product was referred to as a first-generation green fuel, with a primary focus on biodiesel production through transesterification or esterification procedures.

This hypothesis might be substantiated through an examination conducted by Gideon *et al.*, which focused on the production of biodiesel using tall oil fatty acids (TOFA) and experimenting with different types of catalysts.[423] The data reported that on a homogenous catalyst, sulfuric acid (H_2SO_4) obtained 96.76% FAME under optimum conditions of 55 °C using 0.5% catalyst concentration for 1 h with a methanol/oil ratio of 15/1. Furthermore, while using a heterogeneous catalyst called Amberlyst BD20 ion-exchange resin, a conversion rate of 90% was achieved under the following conditions: methanol-to-oil ratio of 20.8/1, catalyst amount of 23.4% relative to the oil mass, and reaction period of 4.7 hours at a constant temperature between 75 and 80 °C. Abhishek also investigated the impact of the W/ZrO_2 catalyst on the conversion of microalgal lipids to 94.58% and found that it could be utilized for up to three rounds without any noticeable loss of catalyst.[242] Notably, the majority of the fuel characteristics of biodiesel obtained comply with the specifications set by ASTM 6751 and EN 14214 standards.

Nonetheless, biodiesel is not ideal as a direct replacement for B-100 because the inclusion of oxygen atoms in biodiesel results in the formation of sediments and polymers, in addition to the viscosity of the fuel. This could result in injector fouling and filter clogging. The primary difficulties associated with FAME biodiesel are its instability during long-term storage, small ignition point, poor oxidation resistance and susceptibility to autoxidation at room temperature. These issues arise from the presence of mono- and poly unsaturated fatty acids, making biodiesel prone to oxidative deterioration.[424]

Therefore, second-generation green fuels have been created with the aim of fully substituting fossil fuels. This green fuel, referred to as SAF or bio-jet fuel for air transportation, possesses a paraffinic molecular framework similar to that of conventional diesel or kerosene/gasoline fuels. Green fuel is favorable because of its higher thermal temperature, energy density, cetane number, high stability, and low oxygen content, making it better in quality than biodiesel. Many studies have been conducted, and a few processes have been certified for producing jet fuel owing to certain properties. However, to date, only up to 50% of jet fuel is blended with petroleum fuel, and the use of HEFA and FT fuels may lead to performance concerns.[425,426] The lack of aromatic compounds in these fuels leads to a reduced emission of particles, and it can also cause fuel pump leakage owing to insufficient expansion of the elastic polymers.[425] Nevertheless, the manufacture of hydrocarbons containing significant amounts of aromatic compounds and cycloparaffins for aviation applications must comply with the rigorous standards specified in ASTM D1655, which establishes the requirements for aviation turbine fuel.[427] Hence, the ASTM D7566 standard includes the addition of FT-SPK plus aromatics (FT-SPK/A) to increase the aromatic content to a maximum of 20 wt%. Despite this, the fuel composition is still unsuitable for consumption by aircraft turbine engines until it is blended with commercial jet fuel. The economic viability of HEFA procedures was proven by the substantial fuel output (86–91% feedstock) observed in previous studies.[428,429]

In the early development of second-generation green fuel, hydrodeoxygenation followed by selective cracking/isomerization was chosen as the favorable pathway to produce a high yield of the product. This process uses a non-edible resource with high TG or FFA contents. In addition to utilizing non-edible oils for the production of second-generation SAFs, there are various other alternative feedstocks and technologies worth considering. These alternatives include lignocellulosic biomass, municipal solid waste (MSW), and oil derived from microalgae. A study reported by Yani *et al.* showed hydrodeoxygenation by a $NiO/NbOPO_4$ catalyst with green fuel yields ranging from 69% to 82% with the highest selectivity with 58% of C_{15} followed by C_{12} (15.04%).[416] However, the calorific value (44.03 MJ kg^{-1}) was higher than that reported by Orozco but acceptable by the Indonesian National Standard (43 MJ kg^{-1}).[430] An additional study conducted by Tsiotsias *et al.* revealed that the use of a Ni/CeZr catalyst for 20 h of continuous operation at a temperature of 300 °C resulted in approximately 80% of C_{15}–C_{18} hydrocarbons, which is considered to be acceptable.[431] The data also showed high selectivity for C_{17}, revealing the dominance of the deCOx pathway.[431] In another separate study, Makcharoen examined the production of bio-jet fuel by using crude palm kernel oil with a 5% Pt/C catalyst and showed 58% bio-jet fuel yield with selectivity towards n-C_8–C_{16} around 28%.[141] Nonetheless, the cold flow properties were found to be poor; thus, the addition of HZSM-5 to the Pt/C catalyst promoted cracking, aromatization, and isomerization, resulting in a reduction in the freezing point to 30 °C and aromatic content to 8%, thus shifting the boiling range of the liquid product. Research has shown that involving H_2 into the HDO process improves the catalyst's longevity and reduces carbon emissions in the form of CO and CO_2 yet these methods necessitate a substantial amount of H_2 to produce desirable hydrocarbons.

Instead of employing expensive hydrodeoxygenation techniques, deoxygenation with N_2 could be a viable alternative for producing second-generation green fuels. This method offers substantial economic benefits compared with the conventional hydroprocessing methods. A study conducted by Aziz *et al.* examined the transformation of Nyamplung oil into green fuels by employing a NiAg/ZH catalyst at 350 °C for 3 h. Their results showed a petrol selectivity of 4%, a kerosene selectivity of 5%, and a green fuel selectivity of 62%.[432] Further research by Why *et al.* employed a Pd/C catalyst to convert jet fuels from PKO, which demonstrated the highest yield (99%) and favorable jet paraffin selectivity (~73%) but a lower aromatic concentration, resulting in a higher fuel blend.[251] This clearly shows that the noble metal catalyst has high potential as the best catalyst for green fuel production.

However, the use of noble metals as catalysts is disadvantageous owing to their high manufacturing costs. Therefore, future prospects for green fuel production involve enhancing the quality, removing oxygen, increasing the yield, and improving the selectivity toward diesel or jet fuel chains. Additionally, efforts should be made to improve the properties of SAFs by adjusting the aromatic content to the desired level without compromising the yield. Furthermore, the aim is to reduce production costs by using non-noble metal catalysts and eliminating the need for external H_2. Researchers have developed substitute catalysts made of non-noble elements to prevent the consumption of precious metal catalysts. Numerous investigations have indicated that catalysts made of nickel can be as efficient as noble metals in the manufacturing of environmentally friendly diesel fuel for the above-mentioned reasons. As a result, Ni metal has been created because of its superior features, such as a large number of active sites and high acidity, which enhances the effectiveness of the catalyst. In addition, monometallic Ni catalysts have a high impact on excess cracking, producing more undesirable products and leading to catalyst deactivation during coke formation. Hence, the development of bimetallic catalysts with a second metal added to suppress coke formation and enhance hydrocarbon production has been extensively investigated. The objective of future green fuel production involves lowering manufacturing expenses in order to achieve a commercially feasible scale of equipment that is both economically viable and yields high catalytic activity. This can be accomplished in two ways. The first

option is to employ economical or industrial scrap of transition metals such as Ni and Co, as the predecessor for the catalyst. Palm kernel oil (PKO) is a refined waste output that can also reduce the rivalry between energy, supply, and sustenance. Furthermore, by advancing catalysts or implementing technology that eliminates the need for an external hydrogen supply, it is possible to reduce the operational pressure and the amount of hydrogen consumed.

2. Conclusion

Deoxygenation represents a potentially viable alternative method for the production of biofuels from renewable feedstocks, in particular the conversion of non-edible oils such as ceiba and palm kernel oil (PKO) into hydrocarbon-fuel-like fuels that are identical in chains and comparable in quality to conventional fuels. However, numerous obstacles must be overcome before attaining this objective. The primary emphasis of research has been on the deoxygenation of inedible feedstocks. Nevertheless, the composition of biomass oil is intricate, frequently comprising various free fatty acids and esters. Therefore, further research should be conducted on novel catalysts by using non-noble metals such as iron-based catalysts and catalytic deoxygenation processes tailored to various biomass feedstocks. Iron is the fourth most abundant transition element in the Earth's crust. It is environmentally safe and plays a crucial role in society as a significant metal. Furthermore, catalysts containing iron (Fe) exhibited a more efficient water gas shift process, characterized by a lower hydrogen-to-carbon monoxide (H_2/CO) ratio and a strong affinity for oxygen. This affinity facilitates the breaking of carbon–oxygen (C–O) bonds by binding to the oxygen atom in the C═O group of oleic acid. These iron oxide species possess a robust affinity for oxygen-deprived regions, allowing them to increase the adhesion and activation of oxygenated compounds more efficiently than nickel. However, the selectivity and activity of catalysts during the conversion of biomass feedstock into biofuels may be impeded by the complex composition of these materials. Catalyst deactivation is an additional significant obstacle in the deoxygenation process. Irrespective of the catalyst composition (noble or non-noble metal), the formation of even a negligible amount of coke leads to toxicity and causes deactivation. The major findings of this review are that bimetallic NiCo catalysts on magnetite supports demonstrate high efficiency in converting PKO into SA, achieving significant kerosene-range selectivity through deoxygenation. Additionally, optimizing the catalyst design and exploring alternative feedstocks are crucial for improving the energy efficiency, reducing environmental impacts, and ensuring the scalability of SAF production. Future research should focus on developing novel, iron-based catalysts to enhance the deoxygenation of complex biomass oils, ensuring greater efficiency and selectivity while reducing catalyst deactivation. Additionally, efforts should be directed toward creating catalysts resistant to coke formation or those that can be easily regenerated to optimize the sustainability and economic viability of biofuel production. Consequently, in the future, it is necessary to develop novel catalysts that are resistant to coke formation or can be regenerated *via* straightforward processes. As previously stated, economic factors support the advancement of catalysts composed of iron-based catalysts.

Conflicts of interest

The authors declare no conflicts of interest.

Data availability

No primary research results, software or code has been included and no new data were generated or analysed as part of this review.

Acknowledgements

This research was financially supported by the Ministry of Higher Education, Malaysia, for niche area research under the Higher Institution Centre of Excellence (HICoE) program (JPT(BKPI)1000/016/018/28 Jld.3(2) & NANOCAT-2024E), the PUTRA grant-UPM (Vot No. 9344200), MOSTI-e Science (Vot No. 5450746), and Geran Putra Berimpak (GPB) UPM/800-3/3/1/GPB/2018/9658700.

References

1 J. Rosen, *New York Times*.
2 S. H. H. Al-Jaberi, U. Rashid, F. A. J. Al-Doghachi, G. Abdulkareem-Alsultan and Y. H. Taufiq-Yap, *Energy Convers. Manage.*, 2017, **139**, 166–174.
3 A. G. Alsultan, N. Asikin Mijan, N. Mansir, S. Z. Razali, R. Yunus and Y. H. Taufiq-Yap, *ACS Omega*, 2021, **6**, 408–415.
4 *Climate Change - NASA Science*, **https://science.nasa.gov/climate-change/**, (accessed 28 December 2024).
5 N. A. M. Aziz, R. Yunus, H. A. Hamid, A. A. K. Ghassan, R. Omar, U. Rashid and Z. Abbas, *Sci. Rep.*, 2020, **10**, 1–17.
6 X. Y. Ooi, W. Gao, H. C. Ong, H. V. Lee, J. C. Juan, W. H. Chen and K. T. Lee, *Renewable Sustainable Energy Rev.*, 2019, **112**, 834–852.
7 H. S. Roh, I. H. Eum, D. W. Jeong, B. E. Yi, J. G. Na and C. H. Ko, *Catal. Today*, 2011, **164**, 457–460.
8 P. Kumar, S. R. Yenumala, S. K. Maity and D. Shee, *Appl. Catal., A*, 2014, **471**, 28–38.
9 F. Hameed Kamil, A. Salmiaton, R. Mohamad Hafriz Raja Shahruzzaman, R. Omar, A. Ghassan Alsultsan, H. K. Faten, A. Salmiaton, R. M. H. R. Shahruzzaman, R. Omar and A. G. Alsultsan, *Bull. Chem. React. Eng. Catal.*, 2017, **12**, 81–88.
10 G. Abdulkareem-Alsultan, N. Asikin-Mijan, L. K. Obeas, R. Yunus, S. Z. Razali, A. Islam and Y. Hin Taufiq-Yap, *Chem. Eng. J.*, 2022, **429**, 132206.
11 N. Arun, R. V. Sharma and A. K. Dalai, *Renewable Sustainable Energy Rev.*, 2015, **48**, 240–255.

12 S. Kouider Elouahed, N. Asikin-Mijan, A. Alsultan, O. Kaddour, M. R. Yusop, H. Mimoun, S. Samidin, N. Mansir and Y. H. Taufiq-Yap, *Energy Convers. Manag.*, 2024, **303**, 118185.
13 T.-Y. Y. Abdulkareem-Alsultan, G. Asikin-Mijan, N. Lee, H. V. G. Abdulkareem-Alsultan, N. Asikin-Mijan, H. V. Lee and Y. H. Taufiq-Yap, in Innovations in Sustainable Energy and Cleaner Environment. *Green Energy and Technology*, ed. R. A. Gupta, A. De, S. Aggarwal, A. Kushari, Springer Singapore, 2020, pp. 489–504.
14 N. Asikin-Mijan, H. V. Lee, J. C. Juan, A. R. Noorsaadah, H. C. Ong, S. M. Razali and Y. H. Taufiq-Yap, *Appl. Catal., A*, 2018, **552**, 38–48.
15 N. Asikin-Mijan, H. V. Lee, Y. H. Taufiq-Yap, G. Abdulkrem-Alsultan, M. S. Mastuli and H. C. Ong, *Energy Convers. Manag.*, 2017, **141**, 325–338.
16 N. Mansir, H. M. Sidek, S. H. Teo, N.-A. Mijan, A. G. Alsultan, C. H. Ng, M. R. Shamsuddin and Y. H. Taufiq-Yap, *Bioresour. Technol. Rep.*, 2022, **17**, 100988.
17 E. Abd-Alkuder Salman, K. Abaid Samawi, M. Fawzi Nassar, G. Abdulkareem-Alsultan and E. Abdulmalek, *J. Electroanal. Chem.*, 2023, **945**, 117629.
18 L. Hermida, A. Z. Abdullah and A. R. Mohamed, *Renewable Sustainable Energy Rev.*, 2015, **42**, 1223–1233.
19 M. Ameen, M. T. Azizan, S. Yusup, A. Ramli and M. Yasir, *Renewable Sustainable Energy Rev.*, 2017, **80**, 1072–1088.
20 M. M. X. Lum, K. H. Ng, S. Y. Lai, A. R. Mohamed, A. G. Alsultan, Y. H. Taufiq-Yap, M. K. Koh, M. A. Mohamed, D. V. N. Vo, M. Subramaniam, K. S. Mulya and N. Imanuella, *Process Saf. Environ. Prot.*, 2023, **176**, 580–604.
21 A. Zheng, Z. Huang, G. Wei, K. Zhao, L. Jiang, Z. Zhao, Y. Tian and H. Li, *Iscience*, 2020, **23**, 100814.
22 S. Z. Razali, R. Yunus, D. Kania, S. A. Rashid, L. H. Ngee, G. Abdulkareem-Alsultan and B. M. Jan, *J. Mater. Res. Technol.*, 2022, **21**, 2891–2905.
23 S. Janampelli and S. Darbha, *Catal. Today*, 2018, **309**, 219–226.
24 C. Detoni, F. Bertella, M. M. V. M. Souza, S. B. C. Pergher and D. A. G. Aranda, *Appl. Clay Sci.*, 2014, **95**, 388–395.
25 L. N. Silva, I. C. P. Fortes, F. P. De Sousa and V. M. D. Pasa, *Fuel*, 2016, **164**, 329–338.
26 N. Asikin-Mijan, J. C. Juan, Y. H. Taufiq-Yap, H. C. Ong, Y. C. Lin, G. AbdulKareem-Alsultan and H. V. Lee, *Catal. Commun.*, 2023, **182**, 106741.
27 K. Abaid Samawi, E. Abd-Alkuder Salman, B. Abd-Alsatar Alshekhly, M. Fawzi Nassar, M. Yousefzadeh Borzehandani, G. Abdulkareem-Alsultan, M. Alif Mohammad Latif and E. Abdulmalek, *Comput. Theor. Chem.*, 2022, **1212**, 113725.
28 A. Abdulkareem Ghassan, N.-A. Mijan and Y. Hin Taufiq-Yap, in *Nanorods and Nanocomposites*, 2020.
29 S. Oh, J. H. Lee, I.-G. Choi and J. W. Choi, *Renewable Energy*, 2020, **149**, 1–10.
30 K. A. Rogers and Y. Zheng, *ChemSusChem*, 2016, **9**, 1750–1772.
31 K. A. Samawi, S. J. Abdulrazzaq, M. Zorah, M. Al-Bahrani, H. A. M. A. Mahmoud, G. Abdulkareem-Alsultan, A. G. Taki and M. F. Nassar, *J. Solid State Chem.*, 2024, **334**, 124690.
32 G. Abdulkareem-Alsultan, N. Asikin-Mijan and Y. H. Taufiq-Yap, *Key Eng. Mater.*, 2016, **707**, 175–181.
33 S. T. Lim, S. Sethupathi, A. G. Alsultan and Y. Munusamy, *Energy Fuels*, 2021, **35**, 16212–16221.
34 N. Hongloi, P. Prapainainar, A. Seubsai, K. Sudsakorn and C. Prapainainar, *Energy*, 2019, **182**, 306–320.
35 K. B. Baharudin, Y. H. Taufiq-Yap, J. Hunns, M. Isaacs, K. Wilson and D. Derawi, *Microporous Mesoporous Mater.*, 2019, **276**, 13–22.
36 N. Asikin-Mijan, H. Mohd Sidek, A. G. AlSultan, N. A. Azman, N. A. Adzahar and H. C. Ong, *Catalysts*, 2021, **11**, 1470.
37 R. S. R. M. Hafriz, I. Nor Shafizah, A. Salmiaton, N. A. Arifin, R. Yunus, Y. H. Taufiq Yap and S. Abd Halim, *Comparative study of transition metal-doped calcined Malaysian dolomite catalysts for WCO deoxygenation reaction*, King Saud University, 2020, vol. 13.
38 F. Batool, T. A. Kurniawan, A. Mohyuddin, M. H. D. Othman, I. Ali, G. Abdulkareem-Alsultan, A. Anouzla, H. H. Goh, D. Zhang, F. Aziz and K. Wayne Chew, *Chem. Eng. Sci.*, 2024, **293**, 120057.
39 M. Safa Gamal, N. Asikin-Mijan, M. Arumugam, U. Rashid and Y. H. Taufiq-Yap, *J. Anal. Appl. Pyrolysis*, 2019, **144**, 104690.
40 A. G. Alsultan, N. Asikin-Mijan, L. K. Obeas, A. Islam, N. Mansir, S. H. Teo, S. Z. Razali, M. F. Nassar, S. Mohamad and Y. H. Taufiq-Yap, *Catalysts*, 2022, **12**, 566.
41 N. A. Abdul Razak, N.-A. Mijan, Y. H. Taufiq-Yap and D. Derawi, *J. Cleaner Prod.*, 2022, **366**, 132971.
42 M. H. Wondi, R. Shamsudin, R. Yunus, G. A. Alsultan and A. H. Iswardi, *J. Food Process Eng.*, 2020, **43**, e13426.
43 I. Shah, R. Adnan, A. G. Alsultan and Y. H. Taufiq-Yap, *J. Dispers. Sci. Technol.*, 2020, **0**, 1–16.
44 A. Shamil Albazzaz, *J. Energy Environ. Chem. Eng.*, 2018, **3**, 40.
45 A. M. Robinson, J. E. Hensley and J. Will Medlin, *ACS Catal.*, 2016, **6**, 5026–5043.
46 T. Nordgreen, T. Liliedahl and K. Sjöström, *Fuel*, 2006, **85**, 689–694.
47 A. Afiqah-Idrus, G. Abdulkareem-Alsultan, N. Asikin-Mijan, M. Fawzi Nassar, L. Voon, S. Hwa Teo, T. Agustiono Kurniawan, N. Athirah Adzahar, M. Surahim, S. Zulaika Razali, A. Islam, R. Yunus, N. Alomari and Y. Hin Taufiq-Yap, *Energy Convers. Manage.: X*, 2024, **23**, 100589.
48 R. E. Nugraha, A. R. Y. Sunarti, H. Tehubijuluw and Z. Mumtazah, *J. Kim. Ris.*, 2022, **7**, 81–93.
49 S. Li and J. Gong, *Chem. Soc. Rev.*, 2014, **43**, 7245–7256.
50 K. A. Samawi, B. A. Mohammed, E. A. A. Salman, H. A. M. A. Mahmoud, A. Z. Sameen, S. M. Mohealdeen, G. Abdulkareem-Alsultan and M. F. Nassar, *Phys. Chem. Chem. Phys.*, 2024, **26**, 9284–9294.
51 *European Commission, EUR-Lex - 52019DC0640 - EN - EUR-Lex*, **https://eur-lex.europa.eu/legal-content/EN/TXT/?uri=COM%3A2019%3A640%3AFIN%0Ahttps://eur-lex.europa.eu/legal-content/EN/TXT/?qid=1596443911913&uri=CELEX:52019DC0640#document2%0Ahttps://eur-lex.europa.eu/legal-content/IT/ALL/?uri=CELEX:52019DC0640%0Ahttps:**, (accessed 20 January 2024).

52 K. A. Samawi, E. A. A. Salman, H. A. Hasan, H. A. M. A. Mahmoud, S. M. Mohealdeen, G. Abdulkareem-Alsultan, E. Abdulmalek and M. F. Nassar, *Mol. Syst. Des. Eng.*, 2024, **9**, 464–476.
53 S. T. Lim, S. Sethupathi, A. G. Alsultan, L. K. Leong and Y. H. Taufiq-Yap, *Key Eng. Mater.*, 2020, **853 KEM**, 228–234.
54 *Paris Agreement, The Paris Agreement | UNFCCC*, **https://unfccc.int/process-and-meetings/the-paris-agreement**, (accessed 20 January 2024).
55 N. Asikin, H. V. Lee, G. A. Alsultan and T. Yap, *Mater. Sci. Forum*, 2016, **840**, 353–358.
56 N. Asikin, H. V. Lee, G. A. Alsultan and T. Yap, *Synthesis and characterization of silica-alumina supported Ca and Ni catalyst for deoxygenation of vegetable oil into diesel*, 2016.
57 G. Ceballos, P. R. Ehrlich, A. D. Barnosky, A. García, R. M. Pringle and T. M. Palmer, *Sci. Adv.*, 2015, **1**, e1400253.
58 P. M. Cox, R. A. Betts, C. D. Jones, S. A. Spall and I. J. Totterdell, *Nature*, 2000, **408**, 184–187.
59 R. E. Gullison, P. C. Frumhoff, J. G. Canadell, C. B. Field, D. C. Nepstad, K. Hayhoe, R. Avissar, L. M. Curran, P. Friedlingstein and C. D. Jones, *Science*, 2007, **316**, 985–986.
60 H. Chang, G. Abdulkareem-Alsultan, Y. H. Taufiq-Yap, S. Mohd Izham and S. Sivasangar, *Fuel*, 2024, **355**, 129459.
61 E. J. Dlugokencky, L. P. Steele, P. M. Lang and K. A. Masarie, *J. Geophys. Res.*, 2022, **99**, 17021–17043.
62 A. P. Schurer, M. E. Mann, E. Hawkins, S. F. B. Tett and G. C. Hegerl, *Nat. Clim. Change*, 2017, **7**, 563–567.
63 H. A. Alrazen, S. M. Aminossadati, H. A. Mahmood, M. M. Hasan, G. Abdulkreem-Alsultan and M. Konarova, *Energy*, 2023, **282**, 128754.
64 M. X. Y. Ravindran, N. Asikin-Mijan, H. C. Ong, D. Derawi, M. R. Yusof, M. S. Mastuli, H. V. Lee, W. N. A. S. Wan Mahmood, M. S. Razali, G. Abdulkareem Al-Sultan and Y. H. Taufiq-Yap, *J. Anal. Appl. Pyrolysis*, 2022, **168**, 105772.
65 N. A. Adzahar, N. Asikin-Mijan, M. I. Saiman, G. A. Alsultan, M. S. Mastuli, M. R. Shamsuddin and Y. H. Taufiq-Yap, *RSC Adv.*, 2022, **12**, 16903–16917.
66 I. E. Agency, *World energy outlook*, OECD/IEA Paris, 2009.
67 L. K. Obeas, A. Khalid Ghalib, G. A. Kareem-Alsultan, N. A. Mijan and R. Yunus, *Orient. J. Chem.*, 2021, **37**, 256–268.
68 K. Davron, T. A. Kurniawan, B. Akbarbek, E. Rasulbek, N. Shavkat, B. Zebo, F. Batool and G. AbdulKareem-Alsultan, *J. Taiwan Inst. Chem. Eng.*, 2024, **166**, 105481.
69 H. Wang, Z. Lei, X. Zhang, B. Zhou and J. Peng, *Energy Convers. Manag.*, 2019, **198**, 111799.
70 N. Asikin-Mijan, D. Derawi, N. Salih, J. Salimon, G. A. Alsultan, M. S. Mastuli and M. X. Y. Ravindran, *Innov. Thermochem. Technol. Biofuel Process.*, 2022, 197–219.
71 B. Pillot, M. Muselli, P. Poggi and J. B. Dias, *Energy Policy*, 2019, **127**, 113–124.
72 S. H. Teo, C. H. Ng, A. Islam, G. Abdulkareem-Alsultan, C. G. Joseph, J. Janaun, Y. H. Taufiq-Yap, S. Khandaker, G. J. Islam, H. Znad and M. R. Awual, *J. Cleaner Prod.*, 2022, **332**, 130039.
73 K. L. Yu, B. S. Zainal, H. Mohamed, P. J. Ker, H. C. Ong, H. B. Zaman, G. Abdulkareem-Alsultan and Y. H. Taufiq-Yap, *Int. J. Hydrogen Energy*, 2025, **104**, 240–251.
74 *U.S. Energy Information Administration, Biomass explained - U.S. Energy Information Administration*, **https://www.eia.gov/energyexplained/biomass/**, (accessed 5 April 2024).
75 *U. S. Department of Energy, 5 Everyday Products Made from Biomass: A Few May Surprise You | Department of Energy*, **https://www.energy.gov/eere/articles/5-everyday-products-made-biomass-few-may-surprise-you**, (accessed 5 April 2024).
76 W. Dizayee, M. M. Hamarashid, M. Zorah, H. A. M. A. Mahmoud, M. Al-Bahrani, A. G. Taki, G. Abdulkareem-Alsultan and M. F. Nassar, *J. Alloys Compd.*, 2024, **1004**, 175825.
77 E. Emmanouilidou, A. Lazaridou, S. Mitkidou and N. C. Kokkinos, *J. Mol. Struct.*, 2024, **1306**, 137870.
78 Z. B. Megawati, A. Damayanti, R. D. A. Putri, B. Triwibowo, H. Prasetiawan, S. P. K. Aji and A. Prawisnu, *Mater. Today Proc.*, 2022, **63**, S373–S378.
79 M. Sadeghi and M. H. Husseini, *J. Appl. Chem. Res.*, 2013, **7**, 39–49.
80 I. Abrantes, A. F. Ferreira, A. Silva and M. Costa, *J. Cleaner Prod.*, 2021, **313**, 127937.
81 T. A. Kurniawan, M. Riaz, A. Mohyuddin, A. Haider, S. Ali, G. Abdulkareem-Alsultan, M. H. D. Othman, H. H. Goh, A. Anouzla, H. E. Al-Hazmi, F. Aziz, Y. Wibisono, T. D. Kusworo, S. A. A. Alkhadher and M. M. H. Khan, *Inorganic membrane: a game changer for gas separation and purification*, Springer International Publishing, 2024, vol. 78.
82 T. A. Kurniawan, S. Khan, A. Mohyuddin, A. Haider, T. M. T. Lei, M. H. D. Othman, H. H. Goh, D. Zhang, A. Anouzla, F. Aziz, M. Mahmoud, I. Ali, S. Haddout, G. AbdulKareem-Alsultan and S. A. A. Alkhadher, *Chem. Pap.*, 2024, **78**, 6843–6871.
83 J. Holladay, Z. Abdullah and J. Heyne, U.S. Dep. Energy - Off. Energy Effic. Renew. Energy, 2020, September, Report No. DOE/EE-2041.
84 International Energy Agency, Aviation - IEA, **https://www.iea.org/energy-system/transport/aviation**, (accessed 17 January 2024).
85 IATA, IATA - Air Passenger Numbers to Recover in 2024, **https://www.iata.org/en/pressroom/2022-releases/2022-03-01-01/**.
86 F. N. Maadh, E. Abdulmalek, M. F. Ismail, S. A. A. Ahmad and G. Abdulkreem-Alsultan, *High Energy Chem.*, 2024, **58**, 16–58.
87 A. Islam, S. H. Teo, M. T. Islam, A. H. Mondal, H. Mahmud, S. Ahmed, M. Ibrahim, Y. H. Taufiq-Yap, M. L. Hossain, M. C. Sheikh, A. I. Rasee, A. I. Rehan, R. M. Waliullah, M. E. Awual, M. M. Hasan, M. S. Hossain, K. T. Kubra, M. S. Salman, M. N. Hasan and M. R. Awual, *Renewable Sustainable Energy Rev.*, 2025, **208**, 115033.
88 C. Gutiérrez-Antonio, F. I. Gómez-Castro and S. Hernández, *Chem. Eng. Trans.*, 2018, **69**, 319–324.
89 A. R. Abu Talib, Y. S. M. Altarazi, J. Yu, E. Gires, M. Fahmi Abdul Ghafir, A. Tahmasebi, T. Yusaf, A. G. Alsultan and R. Yunus, *Fuel*, 2024, **378**, 132860.
90 M. Y. Albalushi, G. Abdulkreem-Alsultan, N. Asikin-Mijan, M. I. bin Saiman, Y. P. Tan and Y. H. Taufiq-Yap, *Catalysts*, 2022, **12**, 1537.

91 L. Zhang, T. L. Butler and B. Yang, *Green Energy to Sustainability: Strategies for Global Industries*, 2020, 85–110.
92 A. G. Alsultan, N. Asikin-Mijan, L. K. Obeas, A. Isalam, N. Mansir, M. F. Nassar, S. Z. Razali, R. Yunus and Y. H. Taufiq-Yap, *Biofuel and biorefinery technologies,* IntechOpen Rijeka, Croatia, 2023.
93 *ICAO, Carbon offsetting and reduction scheme for international aviation (CORSIA)*, **https://info.carbon-clear.com/hubfs/Factsheets/CORSIA/CORSIA_Factsheet_EN.pdf?submissionGuid=c319185f-35af-4e9a-b10a-8875f97a53c2**, (accessed 2 April 2024).
94 H. Chang, H. V. Lee, Y. H. Taufiq-Yap, G. Abdulkareem-Alsultan and S. Seenivasagam, *Renewable Energy*, 2025, **238**, 121882.
95 IATA, *Int. Air Transp. Assoc.*, 2021, 1–3.
96 IATA, *IATA Fact sheet*, 2023, 1–3.
97 F. Alshaeer, M. Zorah, H. M. Mahmoud, L. Abdalgadir, A. G. Taki, B. A. Mohammed, G. Abdulkareem-Alsultan and M. F. Nassar, *J. Alloys Compd.*, 2023, **1011**, 178247.
98 A. ASTM, DoiOrg/101520/D7566-19.
99 B. S. Zainal, K. L. Yu, H. C. Ong, H. Mohamed, P. J. Ker, G. Abdulkreem-Alsultan, Y. H. Taufiq-Yap and T. I. Mahlia, *Process Saf. Environ. Prot.*, 2024, **192**, 424–436.
100 N. A. Adzahar, G. AbdulKareem-Alsultan, N. A. Mijan, M. S. Mastuli, H. V. Lee and Y. H. Taufiq-Yap, *Energy*, 2025, **314**, 133957.
101 G. Omer-Alsultan, A. A. Alsahlani, G. Mohamed-Alsultan, G. Abdulkareem-Alsultan, M. F. Nassar, T. A. Kurniawan and Y. H. Taufiq-Yap, *Towards zero emission: exploring innovations in wind turbine design for sustainable energy a comprehensive review*, Springer, London, 2024.
102 S. Kramer, G. Andac, J. Heyne, J. Ellsworth, P. Herzig and K. C. Lewis, *Front. Energy Res.*, 2022, **9**, 782823.
103 T. A. Kurniawan, M. Ali, A. Mohyuddin, A. Haider, M. H. D. Othman, A. Anouzla, H. H. Goh, D. Zhang, W. Dai, F. Aziz, M. I. Khan, I. Ali, M. Mahmoud, S. A. A. Alkhadher and G. A. Alsultan, *Process Saf. Environ. Prot.*, 2025, **193**, 643–664.
104 S. Samidin, A. Anuar, G. Abdulkareem-Alsultan, N. Asikin-Mijan, W. N. R. W. Isahak, L. H. Voon, S. Y. Lai, M. Surahim, A. Salmiaton, M. R. Shamsuddin and Y. H. Taufiq-Yap, *Chem. Pap.*, 2025, **79**, 481–496.
105 S. Samidin, W. N. R. W. Isahak, K. N. Ahmad, N. A. Mijan, M. R. Yusop, A. Samsuri, G. Abdulkareem-Alsultan and M. A. Yarmo, *Fuel*, 2024, **373**, 132370.
106 N. A. Mohamad Aziz, Y. K. Ling, H. Mohamed, B. S. Zainal, H. B. Zaman and A. G. Alsultan, *IOP Conf. Ser. Earth Environ. Sci.*, 2024, **1372**, 012032, DOI: **10.1088/1755-1315/1372/1/012032**.
107 S. De Jong, K. Antonissen, R. Hoefnagels, L. Lonza, M. Wang, A. Faaij and M. Junginger, *Biotechnol. Biofuels*, 2017, **10**, 1–18.
108 N. Azri, R. Irmawati, U. I. Nda-Umar, M. I. Saiman, Y. H. Taufiq-Yap and G. Abdulkareem-Alsultan, *Pertanika J. Sci. Technol.*, 2024, **32**, 1141–1159.
109 G. Abdulkareem-alsultan, H. Voon, N. Asikin-mijan, S. Samidin and N. Athirah, *Techno-Economic, Environmental, Policy Status and Perspectives on Sustainable Resource Conversion Into Transportation Fuels*, Elsevier, 2nd edn, 2024.
110 G. Liu, B. Yan and G. Chen, *Renewable Sustainable Energy Rev.*, 2013, **25**, 59–70.
111 G. Abdulkareem-alsultan, N. Asikin-mijan, M. Fawzi, S. Samidin, N. Athirah and L. Hwei, *Hydrogen Production From Methanol Reforming Processes*, Elsevier, 2nd edn, 2024.
112 H. Wei, W. Liu, X. Chen, Q. Yang, J. Li and H. Chen, *Fuel*, 2019, **254**, 115599.
113 G. Abdulkareem-Alsultan, N. Asikin-Mijan, M. F. Nassar, S. Samidin, N. A. Adzahar, L. H. Voon, T. A. Kurniawan and Y. H. Taufiq-Yap, *Biodiesel Blend With Different Alcohol Emission Evaluation*, Elsevier, 2nd edn, 2024.
114 G. A. Alsultan, N. Asikin-Mijan, H. V. Lee, A. S. Albazzaz and Y. H. Taufiq-Yap, *Energy Convers. Manag.*, 2017, **151**, 311–323.
115 R. S. R. M. Hafriz, S. H. Habib, N. A. Raof, M. Y. Ong, C. C. Seah, S. Z. Razali, R. Yunus, N. M. Razali and A. Salmiaton, *Energy Convers. Manage.: X*, 2024, **24**, 100749.
116 C. S. Smoljan, J. M. Crawford and M. A. Carreon, *Catal. Commun.*, 2020, **143**, 106046.
117 D. Septriana, M. M. Azis and J. Wintoko, *ASEAN J. Chem. Eng.*, 2023, **23**, 128–141.
118 R. S. R. M. Hafriz, S. H. Habib, N. A. Raof, S. Z. Razali, R. Yunus, N. M. Razali and A. Salmiaton, *J. Taiwan Inst. Chem. Eng.*, 2024, **165**, 105700.
119 C. C. Tung and N. Jo-Han, *Am.-Eurasian J. Sustain. Agric.*, 2014, 69–75.
120 T. G. Kreutz, E. D. Larson, G. Liu and R. H. Williams, in *25th annual international Pittsburgh coal conference*, International Pittsburgh Coal Conference Pittsburgh, Pennsylvania, 2008, vol. 29.
121 D. Leckel, *Energy Fuels*, 2009, **23**, 2342–2358.
122 R. Luque, A. R. de la Osa, J. M. Campelo, A. A. Romero, J. L. Valverde and P. Sanchez, *Energy Environ. Sci.*, 2012, **5**, 5186–5202.
123 S. L. Soled, E. Iglesia, R. A. Fiato, J. E. Baumgartner, H. Vroman and S. Miseo, *Top. Catal.*, 2003, **26**, 101–109.
124 M. Vannice and R. Garten, *J. Catal.*, 1979, **56**, 236–248.
125 A. P. Steynberg, M. E. Dry, B. H. Davis and B. B. Breman, in *Fischer-Tropsch Technology*, ed. A. Steynberg and C. Dry, Elsevier, 2004, vol. 152, pp. 64–195.
126 C. H. Zhang, Y. Yang, B. T. Teng, T. Z. Li, H. Y. Zheng, H. W. Xiang and Y. W. Li, *J. Catal.*, 2006, **237**, 405–415.
127 J. Li, X. Cheng, C. Zhang, W. Dong, Y. Yang and Y. Li, *Catal. Lett.*, 2016, **146**, 2574–2584.
128 D. Xu, W. Li, H. Duan, Q. Ge and H. Xu, *Catal. Lett.*, 2005, **102**, 229–235.
129 M. F. Shahriar and A. Khanal, *Fuel*, 2022, **325**, 124905.
130 A. Ringsred, S. van Dyk and J. J. Saddler, *Appl. Energy*, 2021, **287**, 116587.
131 T. Hanaoka, T. Miyazawa, K. Shimura and S. Hirata, *Fuel Process. Technol.*, 2015, **129**, 139–146.
132 B.-Y. Yu and C.-C. Tsai, *Chem. Eng. Res. Des.*, 2020, **159**, 47–65.

133 X. Xue, X. Hui, P. Singh and C.-J. Sung, *Fuel*, 2017, **210**, 343–351.
134 M. J. A. Romero, A. Pizzi, G. Toscano, G. Busca, B. Bosio and E. Arato, *Waste Manage.*, 2016, **47**, 62–68.
135 M. Žula, M. Grilc and B. Likozar, *Chem. Eng. J.*, 2022, **444**, 136564.
136 M. S. Sowe, A. R. Lestari, E. Novitasari, M. Masruri and S. M. Ulfa, *Bull. Chem. React. Eng. Catal.*, 2022, **17**, 135–145.
137 Y. Wu, X. Liu, J. Zhang, Y. Zhang, X. Li, H. Xia and F. Wang, *Ind. Eng. Chem. Res.*, 2022, **61**, 12338–12348.
138 S. Shao, X. Hu, W. Dong, X. Li, H. Zhang, R. Xiao and Y. Cai, *J. Cleaner Prod.*, 2021, **282**, 124331.
139 A. Çakan, B. Kiren and N. Ayas, *Mol. Catal.*, 2023, **546**, 113219.
140 A. A. Ayandiran, P. E. Boahene, S. Nanda, A. K. Dalai and Y. Hu, *Mol. Catal.*, 2022, **523**, 111358.
141 M. Makcharoen, A. Kaewchada, N. Akkarawatkhoosith and A. Jaree, *Energy Convers. Manage.: X*, 2021, **12**, 100125.
142 S. Khan, K. M. Qureshi, A. N. Kay Lup, M. F. A. Patah and W. M. A. Wan Daud, *Biomass Bioenergy*, 2022, **164**, 106563.
143 C. Papadopoulos, E. Kordouli, L. Sygellou, K. Bourikas, C. Kordulis and A. Lycourghiotis, *Fuel Process. Technol.*, 2021, **217**, 106820.
144 H. Pan, X. Zhou, S. Xie, Z. Du, G. Li, C. Zhang, Y. Luo and X. Zhang, *Biomass Bioenergy*, 2022, **165**, 106592.
145 M. Azkaar, Z. Vajglova, P. Mäki-Arvela, A. Aho, N. Kumar, H. Palonen, K. Eränen, M. Peurla, L. A. Kulikov and A. L. Maximov, *Fuel*, 2020, **278**, 118193.
146 T. Li, J. Cheng, R. Huang, J. Zhou and K. Cen, *Bioresour. Technol.*, 2015, **197**, 289–294.
147 X. Wu, P. Jiang, F. Jin, J. Liu, Y. Zhang, L. Zhu, T. Xia, K. Shao, T. Wang and Q. Li, *Fuel*, 2017, **188**, 205–211.
148 G. J. Bishop and B. Elvers, *Handbook of Fuels: Energy Sources for Transportation*, 2021, pp. 503–527.
149 P. Bartocci, R. Tschentscher, Y. Yan, H. Yang, G. Bidini and F. Fantozzi, *Biofuel Prod. Technol. Crit. Anal. Sustain.*, 2020, 1–36.
150 A. G. Romero-Izquierdo, F. I. Gómez-Castro, C. Gutiérrez-Antonio, S. Hernández and M. Errico, *Chem. Eng. Process.*, 2021, **160**, 108270.
151 S. M. Yui, in *Catalytic Hydroprocessing of Petroleum and Distillates*, CRC Press, 2020, pp. 236–252.
152 E. Zikhonjwa, *Hydrogenation of coconut oil into Biofuel (bio-jet fuel and high-value low molecule hydrocarbons)*, Doctoral dissertation, Durban University of Technology, 2021.
153 D. T. Sarve, S. K. Singh and J. D. Ekhe, *Inorg. Chem. Commun.*, 2022, **139**, 109397.
154 S. Chuklina, A. Zhukova, Y. Fionov, M. Kadyko, A. Fionov, D. Zhukov, A. Il'icheva, L. Podzorova and I. Mikhalenko, *ChemistrySelect*, 2022, **7**, e202203031.
155 S. Sahebdelfar, P. M. Bijani and F. Yaripour, *Fuel*, 2022, **310**, 122443.
156 T. K. Phung, L. P. Hernández, A. Lagazzo and G. Busca, *Appl. Catal., A*, 2015, **493**, 77–89.
157 K. Shimura, S. Yoshida, H. Oikawa and T. Fujitani, *Catalysts*, 2023, **13**, 1303.
158 A. de Reviere, D. Gunst, M. Sabbe and A. Verberckmoes, *J. Ind. Eng. Chem.*, 2020, **89**, 257–272.
159 Y. Nakagawa, M. Yabushita and K. Tomishige, *RSC Sustainability*, 2023, **1**, 814–837.
160 Y. Shi, A. S. Weller, A. J. Blacker and P. W. Dyer, *Catal. Commun.*, 2022, **164**, 106421.
161 Y. Kim, H. B. Im, U. H. Jung, J. C. Park, M. H. Youn, H.-D. Jeong, D.-W. Lee, G. B. Rhim, D. H. Chun and K. B. Lee, *Fuel*, 2019, **256**, 115957.
162 L. Attanatho, S. Lao-ubol, A. Suemanotham, N. Prasongthum, P. Khowattana, T. Laosombut, N. Duangwongsa, S. Larpkiattaworn and Y. Thanmongkhon, *SN Appl. Sci.*, 2020, **2**, 1–12.
163 P. Panpian, T. T. V. Tran, S. Kongparakul, L. Attanatho, Y. Thanmongkhon, P. Wang, G. Guan, N. Chanlek, Y. Pooarporn and C. Samart, *Fuel*, 2021, **287**, 119831.
164 J. Gulbinski, L. Ren, V. Vattipalli, H. Chen, J. Delaney, P. Bai, P. Dauenhauer, M. Tsapatsis, O. A. Abdelrahman and W. Fan, *Ind. Eng. Chem. Res.*, 2020, **59**, 22049–22056.
165 F. Jin, Y. Yan and G. Wu, *Catal. Today*, 2020, **355**, 148–161.
166 Z. Buniazet, A. Cabiac, S. Maury, D. Bianchi and S. Loridant, *Appl. Catal., B*, 2019, **243**, 594–603.
167 A. Milbrandt, C. Kinchin and R. McCormick, *Feasibility of producing and using biomass-based diesel and jet fuel in the United States*, National Renewable Energy Lab.(NREL), Golden, CO (United States), 2013.
168 A. Ahmad, F. Banat and H. Taher, *Environ. Technol. Innov.*, 2020, **20**, 101138.
169 A. Iram, D. Cekmecelioglu and A. Demirci, *Processes*, 2020, **9**, 38.
170 J. Baeyens, H. Zhang, J. Nie, L. Appels, R. Dewil, R. Ansart and Y. Deng, *Renewable Sustainable Energy Rev.*, 2020, **131**, 110023.
171 M. Bomgardner, *Chem. Eng. News*, 2012, **90**, 8.
172 R. Davis, M. J. Biddy, E. Tan, L. Tao and S. B. Jones, *Biological conversion of sugars to hydrocarbons technology pathway*, Pacific Northwest National Lab.(PNNL), Richland, WA (United States), 2013.
173 R. K. Mawhood, E. Gazis, R. Hoefnagels, S. De Jong and R. Slade, Technological and commercial maturity of aviation biofuels: Emerging options to produce jet from lignocellulosic biomass, in *14th International Conference on Sustainable Engineering Technologies*, 2015.
174 J. C. McAuliffe, A. T. Nielsen, C. M. Peres, D. V. Vaviline and D. H. Wells, *US Pat.*, 8975051, 2015.
175 B. Kim, S. Lee, D. Jeong, J. Yang, M.-K. Oh and J. Lee, *PLoS One*, 2014, **9**, e105322.
176 A. N. Phan and T. M. Phan, *Fuel*, 2008, **87**, 3490–3496.
177 H. Chen, M. Ding, Y. Li, H. Xu, Y. Li and Z. Wei, *J. Traffic Transp. Eng.*, 2020, **7**, 791–807.
178 P. Obando-Pacheco, A. J. Justicia-Grande, I. Rivero-Calle, C. Rodríguez-Tenreiro, P. Sly, O. Ramilo, A. Mejías, E. Baraldi, N. G. Papadopoulos and H. Nair, *J. Infect. Dis.*, 2018, **217**, 1356–1364.
179 D. Kim, M. Hanifzadeh and A. Kumar, *Environ. Prog. Sustainable Energy*, 2018, **37**, 7–19.

180 R. Sotelo-Boyás, Y. Liu and T. Minowa, *Ind. Eng. Chem. Res.*, 2011, **50**, 2791–2799.
181 Y. Sugami, E. Minami and S. Saka, *Fuel*, 2016, **166**, 376–381.
182 C. A. Scaldaferri and V. M. D. Pasa, *Fuel*, 2019, **245**, 458–466.
183 M. Herskowitz, M. V. Landau, Y. Reizner and D. Berger, *Fuel*, 2013, **111**, 157–164.
184 T. Kurniawan, A. Setiawan, N. A. Putri, A. Irawan, A. B. D. Nandiyanto and Y. Bindar, *Biomass Convers. Biorefin.*, 2023, **13**, 6847–6858.
185 A. Zikri and M. Aznury, in *IOP conference series: materials science and engineering*, IOP Publishing, 2020, vol. 823, p. 12026.
186 N. Srihanun, P. Dujjanutat, P. Muanruksa and P. Kaewkannetra, *Catalysts*, 2020, **10**, 241.
187 M. Ruangudomsakul, N. Osakoo, J. Wittayakun, C. Keawkumay, T. Butburee, S. Youngjan, K. Faungnawakij, Y. Poo-arporn, P. Kidkhunthod and P. Khemthong, *Mol. Catal.*, 2022, **523**, 111422.
188 M. M. Gui, K. T. Ã. Lee and S. Bhatia, *Energy*, 2008, **33**, 1646–1653.
189 R. R. Watson and F. De Meester, *Handbook of cholesterol*, Wageningen Academic Publishers, 2016.
190 A. M. N. Renzaho, J. K. Kamara and M. Toole, *Renewable Sustainable Energy Rev.*, 2017, **78**, 503–516.
191 M. Khanna, W. Wang, T. W. Hudiburg and E. H. Delucia, *Nat. Commun.*, 2017, **8**, 1–9.
192 D. F. Correa, H. L. Beyer, H. P. Possingham, S. R. Thomas-Hall and P. M. Schenk, *Renewable Sustainable Energy Rev.*, 2017, **74**, 1131–1146.
193 D. J. Garcia and F. You, *J. Cleaner Prod.*, 2018, **182**, 313–330.
194 W. Gerbens-Leenes and A. Y. Hoekstra, *Energy Environ. Sci.*, 2011, **4**, 2658–2668.
195 M. Munir, M. Saeed, M. Ahmad, A. Waseem, M. Alsaady, S. Asif, A. Ahmed, M. Shariq Khan, A. Bokhari, M. Mubashir, L. Fatt Chuah and P. Loke Show, *Fuel*, 2023, **332**, 126265.
196 M. Munir, M. Ahmad, M. Mubashir, S. Asif, A. Waseem, A. Mukhtar, S. Saqib, H. Siti Halimatul Munawaroh, M. K. Lam, K. Shiong Khoo, A. Bokhari and P. Loke Show, *Bioresour. Technol.*, 2021, **328**, 124859.
197 H. Bibi, M. Ahmad, A. I. Osman, A. A. Alsahli, M. Munir, A. H. Al-Muhtaseb, D. W. Rooney and S. Sultana, *GCB Bioenergy*, 2024, **16**, 1–25.
198 B. Chaudhry, M. Ahmad, M. Munir, M. Fawzy Ramadan, M. Munir, C. Ussemane Mussagy, S. Faisal, T. M. M. Abdellatief and A. Mustafa, *Sustain. Energy Technol. Assess.*, 2024, **65**, 103781.
199 J. Heller, *Physic nut, Jatropha curcas L.*, Bioversity International, 1996, vol. 1.
200 G. Corro, N. Tellez, E. Ayala and A. Marinez-Ayala, *Fuel*, 2010, **89**, 2815–2821.
201 Y. Y. Tye, K. T. Lee, W. N. W. Abdullah and C. P. Leh, *Renewable Sustainable Energy Rev.*, 2016, **60**, 155–172.
202 X.-H. Yu, R. Rawat and J. Shanklin, *BMC Plant Biol.*, 2011, **11**, 1–10.
203 C. H. Bindhu, J. R. C. Reddy, B. Rao, T. Ravinder, P. P. Chakrabarti, M. S. L. Karuna and R. B. N. Prasad, *J. Am. Oil Chem. Soc.*, 2012, **89**, 891–896.
204 MPOC, Malaysian Palm Oil Industry Has A Long-Term Plan To Address EU Regulation, **https://mpoc.org.my/malaysian-palm-oil-industry-has-a-long-term-plan-to-address-eu-regulation/**, (accessed 5 April 2024).
205 S. Aznam Shah, *Malaysia increases green fuel mix to B20*, **https://themalaysianreserve.com/2020/02/21/malaysia-increases-green-fuel-mix-to-b20/**, (accessed 5 April 2024).
206 Y. Basiron and Y. Foong-Kheong, *J. Oil Palm, Environ. Heal.*, 2013, **4**, 69–77, DOI: **10.5366/jope.2013.07**.
207 F. Y. Ng, F. K. Yew, Y. Basiron and K. Sundram, *J. Oil Palm, Environ. Heal.*, 2012, **2**, 1–7, DOI: **10.5366/jope.2011.01**.
208 A. L. S. Murta, M. A. V. De Freitas, C. G. Ferreira and M. M. D. C. L. Peixoto, *Renewable Energy*, 2021, **164**, 521–530.
209 Y. Subramaniam and T. A. Masron, *Energy Convers. Manage.: X*, 2021, **10**, 100064.
210 *Supply Chain, How oil palm is grown - Golden Agri-Resources*, **https://goldenagri.com.sg/oil-palm-grown/**, (accessed 5 April 2024).
211 C. Y. May, M. A. Ngan, C. K. Yoo, R. A. Majid, A. Y. K. Chung, H. L. L. Nang, C. S. Foon, Y. C. Liang, P. C. Wei and N. M. Han, *Palm Oil Dev.*, 2005, **23**, 3–7.
212 N. S. Sulaiman, M. D. Sintang, S. Mantihal, H. M. Zaini, E. Munsu, H. Mamat, S. Kanagaratnam, M. H. A. Jahurul and W. Pindi, *Heliyon*, 2022, **8**, e11041.
213 S. Mekhilef, S. Siga and R. Saidur, *Renewable Sustainable Energy Rev.*, 2011, **15**, 1937–1949.
214 M. H. M. Yasin, R. Mamat, G. Najafi, O. M. Ali, A. F. Yusop and M. H. Ali, *Renewable Sustainable Energy Rev.*, 2017, **79**, 1034–1049.
215 K. T. Lee, C. Ofori-Boateng, K. T. Lee and C. Ofori-Boateng, *Sustainability of Biofuel Production from Oil Palm Biomass*, 2013, pp. 107–146.
216 G. K. A. Parveez, E. Hishamuddin, S. K. Loh, M. Ong-Abdullah, K. M. Salleh, M. Bidin, S. Sundram, Z. A. A. Hasan and Z. Idris, *J. Oil Palm Res.*, 2020, **32**, 159–190.
217 A. R. González, Y. J. O. Asencios, E. M. Assaf and J. M. Assaf, *Appl. Surf. Sci.*, 2013, **280**, 876–887.
218 A. N. K. Lup, F. Abnisa, W. M. A. W. Daud and M. K. Aroua, *Appl. Catal., A*, 2017, **541**, 87–106.
219 M. Peroni, I. Lee, X. Huang, E. Baráth, O. Y. Gutiérrez and J. A. Lercher, *ACS Catal.*, 2017, **7**, 6331–6341.
220 P. Arora, E. L. Grennfelt, L. Olsson and D. Creaser, *Chem. Eng. J.*, 2019, **364**, 376–389.
221 S. M. Kim, M. E. Lee, J.-W. Choi, D. J. Suh and Y.-W. Suh, *Catal. Commun.*, 2011, **16**, 108–113.
222 M. Elkelawy, H. A.-E. Bastawissi, A. M. Radwan, M. T. Ismail and M. El-Sheekh, in *Handbook of algal biofuels*, Elsevier, 2022, pp. 331–361.
223 S. Maroa and F. Inambao, *J. Energy South. Africa*, 2019, **30**, 1–13.
224 L. Jeczmionek and K. Porzycka-Semczuk, *Fuel*, 2014, **128**, 296–301.
225 C. González, P. Marín, F. V. Díez and S. Ordóñez, *Ind. Eng. Chem. Res.*, 2016, **55**, 2319–2327.

226 S. R. Yenumala, S. K. Maity and D. Shee, *Catal. Sci. Technol.*, 2016, **6**, 3156–3165.
227 L. Qu, X. Jiang, Z. Zhang, X. Zhang, G. Song, H. Wang, Y. Yuan and Y. Chang, *Green Chem.*, 2021, **23**, 9348–9376.
228 S. Khan, A. N. Kay Lup, K. M. Qureshi, F. Abnisa, W. M. A. Wan Daud and M. F. A. Patah, *J. Anal. Appl. Pyrolysis*, 2019, **140**, 1–24.
229 R. W. Gosselink, S. A. W. Hollak, S. W. Chang, J. Van Haveren, K. P. De Jong, J. H. Bitter and D. S. Van Es, *ChemSusChem*, 2013, **6**, 1576–1594.
230 S. De, B. Saha and R. Luque, *Bioresour. Technol.*, 2015, **178**, 108–118.
231 B. P. Pattanaik and R. D. Misra, *Renewable Sustainable Energy Rev.*, 2017, **73**, 545–557.
232 US Energy, DOE Explains. Catalysts | Department of Energy, **https://www.energy.gov/science/doe-explainscatalysts**, (accessed 5 April 2024).
233 J. J. Berzelius, *Lehrbuch der chemie*, Arnold, 1856.
234 V. Fourmond, N. Plumeré and C. Léger, *Nat. Rev. Chem.*, 2021, **5**, 348–360.
235 P. Kalita, B. Basumatary, P. Saikia, B. Das and S. Basumatary, *Energy Nexus*, 2022, **6**, 100087.
236 P. S. Sreeprasanth, R. Srivastava, D. Srinivas and P. Ratnasamy, *Appl. Catal., A*, 2006, **314**, 148–159.
237 R. O. Araujo, V. O. Santos, F. C. P. Ribeiro, J. da, S. Chaar, A. M. Pereira, N. P. S. Falcão and L. K. C. de Souza, *Energy Convers. Manag.*, 2021, **228**, 113636.
238 N. Degirmenbasi, N. Boz and D. M. Kalyon, *Appl. Catal., B*, 2014, **150**, 147–156.
239 Y. Shitao, X. Cao, S. Wu, Q. Chen, L. Li and H. Li, *Ind. Crops Prod.*, 2020, **150**, 112362.
240 O. Ejeromedoghene, *Mater. Today Proc.*, 2021, **47**, 1580–1583.
241 J. I. Orege, A. O. Adeyemo, O. F. Adeyinka, O. B. Omitola, A. Usman and E. I. Adeyeye, *Orient. J. Chem.*, 2020, **36**, 106.
242 A. Guldhe, P. Singh, F. A. Ansari, B. Singh and F. Bux, *Fuel*, 2017, **187**, 180–188.
243 O. Ogunkunle, O. O. Oniya and A. O. Adebayo, *Energy Policy Res.*, 2017, **4**, 21–28.
244 S. Chozhavendhan, M. V. P. Singh, B. Fransila, R. P. Kumar and G. K. Devi, *Curr. Res. Green Sustain. Chem.*, 2020, **1**, 1–6.
245 A. K. Endalew, Y. Kiros and R. Zanzi, *Energy*, 2011, **36**, 2693–2700.
246 U. Habib, F. Ahmad, M. Awais, N. Naz, M. Aslam, M. Urooj, A. Moqeem, H. Tahseen, A. Waqar and M. Sajid, *J. Chem. Environ.*, 2023, **2**, 14–53.
247 N. S. Lani, N. Ngadi, N. Y. Yahya and R. A. Rahman, *J. Cleaner Prod.*, 2017, **146**, 116–124.
248 Z. Huang, Z. Zhao, C. Zhang, J. Lu, H. Liu, N. Luo, J. Zhang and F. Wang, *Nat. Catal.*, 2020, **3**, 170–178.
249 P. Li, B. Niu, H. Pan, Y. Zhang and D. Long, *J. Cleaner Prod.*, 2023, **384**, 135653.
250 K. B. Tan, Y. Qiu, Y. Li, B. Chen, L. Xia, D. Cai, S. Ali, J. Huang and G. Zhan, *Mol. Catal.*, 2024, **565**, 114361.
251 E. S. K. Why, H. C. Ong, H. V. Lee, W. H. Chen, N. Asikin-Mijan, M. Varman and W. J. Loh, *Energy*, 2022, **239**, 122017.
252 E. S. K. Why, H. C. Ong, H. V. Lee, W. H. Chen, N. Asikin-Mijan and M. Varman, *Energy Convers. Manag.*, 2021, **243**, 114311.
253 Y. Zheng, J. Wang, D. Li, C. Liu, Y. Lu, X. Lin and Z. Zheng, *Int. J. Hydrogen Energy*, 2021, **46**, 27922–27940.
254 S. Janampelli and S. Darbha, *Catal. Commun.*, 2019, **125**, 70–76.
255 D. Y. Murzin, M. E. Martínez-Klimov, P. Mäki-Arvela, Z. Vajglova, M. Alda-Onggar, I. Angervo, N. Kumar, K. Eränen, M. Peurla, M. H. Calimli, J. Muller, A. Shchukarev and I. L. Simakova, *Energy Fuels*, 2021, **35**, 17755–17768.
256 S. Chen, W. Wang, X. Li, P. Yan, W. Han, T. Sheng, T. Deng, W. Zhu and H. Wang, *J. Energy Chem.*, 2022, **66**, 576–586.
257 H. Baek, K. Kashimura, T. Fujii, S. Tsubaki, Y. Wada, S. Fujikawa, T. Sato, Y. Uozumi and Y. M. A. Yamada, *ACS Catal.*, 2020, **10**, 2148–2156.
258 T. Bangjang, A. Kaewchada and A. Jaree, *Can. J. Chem. Eng.*, 2021, **99**, 435–446.
259 A. Ali and C. Zhao, *Chin. J. Catal.*, 2020, **41**, 1174–1185.
260 L. Yang and M. A. Carreon, *ACS Appl. Mater. Interfaces*, 2017, **9**, 31993–32000.
261 Y. Liu, X. Yang, H. Liu, Y. Ye and Z. Wei, *Appl. Catal., B*, 2017, **218**, 679–689.
262 S. Lei, S. Qin, B. Li and C. Zhao, *J. Catal.*, 2021, **400**, 244–254.
263 S. Xie, C. Jia, A. Prakash, M. I. Palafox, J. Pfaendtner and H. Lin, *ACS Catal.*, 2019, **9**, 3753–3763.
264 H. Liu, J. Han, Q. Huang, H. Shen, L. Lei, Z. Huang, Z. Zhang, Z. K. Zhao and F. Wang, *Ind. Eng. Chem. Res.*, 2020, **59**, 17440–17450.
265 C. C. Tran, D. Akmach and S. Kaliaguine, *Green Chem.*, 2020, **22**, 6424–6436.
266 X. Cao, J. Zhao, F. Long, X. Zhang, J. Xu and J. Jiang, *Appl. Catal., B*, 2022, **305**, 121068.
267 L. Zhou, W. Lin, K. Liu, Z. Wang, Q. Liu, H. Cheng, C. Zhang, M. Arai and F. Zhao, *Catal. Sci. Technol.*, 2020, **10**, 222–230.
268 F. Paquin, J. Rivnay, A. Salleo, N. Stingelin and C. Silva, *J. Mater. Chem. C*, 2015, **3**, 10715–10722.
269 T. Burimsitthigul, B. Yoosuk, C. Ngamcharussrivichai and P. Prasassarakich, *Renewable Energy*, 2021, **163**, 1648–1659.
270 J. Zhang, C. Zhao, C. Li, S. Li, C.-W. Tsang and C. Liang, *Catal. Sci. Technol.*, 2020, **10**, 2948–2960.
271 E. Puello-Polo, Y. Pájaro and E. Márquez, *Catalysts*, 2020, **10**, 894.
272 F. Wang, W. Zhang, J. Jiang, J. Xu, Q. Zhai, L. Wei, F. Long, C. Liu, P. Liu, W. Tan and D. He, *Chem. Eng. J.*, 2020, **382**, 122464.
273 J. Wang, X. Chen, X. Chen, C. Zhao, Y. Ling and C. Liang, *Sustainable Energy Fuels*, 2022, **6**, 3025–3034.
274 L. Skuhrovcová, H. de Paz Carmona, Z. Tišler, E. Svobodová, M. Michálková, K. Strejcová, R. Velvarská and U. Akhmetzyanova, *Mol. Catal.*, 2023, **537**, 112930.
275 N. Kaewtrakulchai, A. Smuthkochorn, K. Manatura, G. Panomsuwan, M. Fuji and A. Eiad-Ua, *Materials*, 2022, **15**, 6584.

276 M. F. Wagenhofer, E. Baráth, O. Y. Gutiérrez and J. A. Lercher, *ACS Catal.*, 2017, **7**, 1068–1076.
277 S. Thongkumkoon, W. Kiatkittipong, U. W. Hartley, N. Laosiripojana and P. Daorattanachai, *Renewable Energy*, 2019, **140**, 111–123.
278 M. Peronia, G. Mancino, E. Baráth, O. Y. Gutiérrez and J. A. Lercher, *Appl. Catal., B*, 2016, **180**, 301–311.
279 M. Ruangudomsakul, N. Osakoo, C. Keawkumay, C. Kongmanklang, T. Butburee, S. Kiatphuengporn, K. Faungnawakij, N. Chanlek, J. Wittayakun and P. Khemthong, *Catal. Today*, 2021, **367**, 153–164.
280 S. Phimsen, W. Kiatkittipong, H. Yamada, T. Tagawa, K. Kiatkittipong, N. Laosiripojana and S. Assabumrungrat, *Energy Convers. Manag.*, 2017, **151**, 324–333.
281 X. Chen, X. Chen, C. Li and C. Liang, *Sustainable Energy Fuels*, 2020, **4**, 2370–2379.
282 S. Kawi, Y. Kathiraser, J. Ni, U. Oemar, Z. Li and E. T. Saw, *ChemSusChem*, 2015, **8**, 3556–3575.
283 N. Gao, J. Salisu, C. Quan and P. Williams, *Renewable Sustainable Energy Rev.*, 2021, **145**, 111023.
284 Z. Zhang, J. Cheng, Y. Zhu, H. Guo and W. Yang, *Fuel*, 2020, **269**, 117465.
285 S.-U. Lee, E. S. Kim, T.-W. Kim, J.-R. Kim, K.-E. Jeong, S. Lee and C.-U. Kim, *J. Ind. Eng. Chem.*, 2020, **83**, 366–374.
286 Q. Tan, Y. Cao and J. Li, *Renewable Energy*, 2020, **150**, 370–381.
287 Y. Zhu, Z. Zhang, J. Cheng, H. Guo and W. Yang, *Int. J. Hydrogen Energy*, 2021, **46**, 3898–3908.
288 P. Chintakanan, T. Vitidsant, P. Reubroycharoen, P. Kuchonthara, T. Kida and N. Hinchiranan, *Fuel*, 2021, **293**, 120472.
289 A. Zitouni, R. Bachir, W. Bendedouche and S. Bedrane, *Fuel*, 2021, **297**, 120783.
290 J. Cheng, Y. Shao, H. Guo, Z. Zhang, Y. Mao, L. Qian, K. Xin and W. Yang, *Fuel*, 2022, **318**, 123679.
291 A. Ramesh, K. Shanthi and M.-T. Nguyen-Le, *Mol. Catal.*, 2022, **518**, 112113.
292 W. Hunsiri, N. Chaihad, C. Ngamcharussrivichai, D. N. Tungasmita, P. Reubroycharoen and N. Hinchiranan, *Fuel Process. Technol.*, 2023, **248**, 107825.
293 M. S. Kuttiyathil, K. Sivaramakrishnan, L. Ali, T. Shittu, M. Z. Iqbal, A. Khaleel and M. Altarawneh, *Bioresour. Technol. Rep.*, 2023, **22**, 101437.
294 M. S. Gamal, N. Asikin-Mijan, W. N. A. W. Khalit, M. Arumugam, S. M. Izham and Y. H. Taufiq-Yap, *Fuel Process. Technol.*, 2020, **208**, 106519.
295 J. de Barros Dias Moreira, D. Bastos de Rezende and V. Márcia Duarte Pasa, *Fuel*, 2020, **269**, 117253.
296 V. K. Soni, S. Dhara, R. Krishnapriya, G. Choudhary, P. R. Sharma and R. K. Sharma, *Fuel*, 2020, **266**, 117065.
297 M. Y. Choo, L. E. Oi, T. C. Ling, E. P. Ng, Y. C. Lin, G. Centi and J. C. Juan, *J. Anal. Appl. Pyrolysis*, 2020, **147**, 104797.
298 J. A. Melo, M. S. de Sá, A. Moral, F. Bimbela, L. M. Gandía and A. Wisniewski Jr, *Nanomaterials*, 2021, **11**, 1659.
299 M. Safa-Gamal, N. Asikin-Mijan, M. Arumugam, W. N. A. W. Khalit, I. Nur Azreena, F. S. Hafez and Y. H. Taufiq-Yap, *J. Anal. Appl. Pyrolysis*, 2021, **160**, 105334.
300 C. Muangsuwan, W. Kriprasertkul, S. Ratchahat, C. G. Liu, P. Posoknistakul, N. Laosiripojana and C. Sakdaronnarong, *ACS Omega*, 2021, **6**, 2999–3016.
301 N. Asikin-Mijan, G. AbdulKareem-Alsultan, M. S. Mastuli, A. Salmiaton, M. Azuwa Mohamed, H. V. Lee, Y. H. H. Taufiq-yap, A. G. Alsultan, A. G. Alsultan, A. G. Alsultan, N. A. Mijan, G. A. Alsultan, M. S. Mastuli, A. Ali, M. A. Mohamed, H. V. Voon, Y. H. H. Taufiq-yap, E. S. Chan, I. P. Jain, A. Rownaghi, M. Anwar, K. Wilson and A. Lee, *Fuel*, 2022, **325**, 124917.
302 M. Saidi and A. Zhandnezhad, *J. Environ. Manage.*, 2023, **326**, 116761.
303 A. Athirah, N. Othman and M. N. M. Jaafar, *Malays. J. Catal.*, 2023, **7**, 1–5.
304 P. S. Shinde, P. S. Suryawanshi, K. K. Patil, V. M. Belekar, S. A. Sankpal, S. D. Delekar and S. A. Jadhav, *J. Compos. Sci.*, 2021, **5**, 75.
305 J. Huang, A. Jones, T. D. Waite, Y. Chen, X. Huang, K. M. Rosso, A. Kappler, M. Mansor, P. G. Tratnyek and H. Zhang, *Chem. Rev.*, 2021, **121**, 8161–8233.
306 H. Wang, K. H. L. Zhang, J. P. Hofmann and F. E. Oropeza, *J. Mater. Chem. A*, 2021, **9**, 19465–19488.
307 W. H. Lee, M. H. Han, Y.-J. Ko, B. K. Min, K. H. Chae and H.-S. Oh, *Nat. Commun.*, 2022, **13**, 605.
308 H. N. Bhatti, Z. Iram, M. Iqbal, J. Nisar and M. I. Khan, *Mater. Res. Express*, 2020, **7**, 15802.
309 S. Xia, K. Hu, C. Lei and J. Jin, *Org. Lett.*, 2020, **22**, 1385–1389.
310 Z. Li, X. Wang, S. Xia and J. Jin, *Org. Lett.*, 2019, **21**, 4259–4265.
311 D. Wang and Z. Li, *Res. Chem. Intermed.*, 2017, **43**, 5169–5186.
312 G. Chen, Y. Zhu, H. M. Chen, Z. Hu, S. Hung, N. Ma, J. Dai, H. Lin, C. Chen and W. Zhou, *Adv. Mater.*, 2019, **31**, 1900883.
313 F. N. I. Sari, S. Abdillah and J.-M. Ting, *Chem. Eng. J.*, 2021, **416**, 129165.
314 M. Minella, G. Marchetti, E. De Laurentiis, M. Malandrino, V. Maurino, C. Minero, D. Vione and K. Hanna, *Appl. Catal., B*, 2014, **154**, 102–109.
315 A. Safarzadeh-Amiri, J. R. Bolton and S. R. Cater, *J. Adv. Oxid. Technol.*, 1996, **1**, 18–26.
316 X. Yu, J. Chen and T. Ren, *RSC Adv.*, 2014, **4**, 46427–46436.
317 Y. Zhai, X. Ren, Y. Sun, D. Li, B. Wang and S. F. Liu, *Appl. Catal., B*, 2023, **323**, 122091.
318 F.-P. Wu, L.-L. Qiu, Y.-P. Zhao, Z.-P. Fu, J. Xiao, J. Li, F.-J. Liu, J. Liang and J.-P. Cao, *Fuel Process. Technol.*, 2023, **252**, 107977.
319 R. Deplazes, C. A. Teles, C. Ciotonea, A. Sfeir, N. Canilho, F. Richard and S. Royer, *Catal. Today*, 2024, **430**, 114514.
320 W. Widayat, D. Andhika Putra and I. Nursafitri, *Mater. Today Proc.*, 2019, **13**, 97–102.
321 Z. Zhang, J. Ye, D. Tan, Z. Feng, J. Luo, Y. Tan and Y. Huang, *Fuel*, 2021, **290**, 120039.
322 Z. Zhang, J. Li, J. Tian, Y. Zhong, Z. Zou, R. Dong, S. Gao, W. Xu and D. Tan, *Fuel Process. Technol.*, 2022, **230**, 107213.

323 Z. Zhang, J. Tian, J. Li, C. Cao, S. Wang, J. Lv, W. Zheng and D. Tan, *Fuel Process. Technol.*, 2022, **233**, 107317.
324 E. C. S. Santos, T. C. Dos Santos, R. B. Guimarães, L. Ishida, R. S. Freitas and C. M. Ronconi, *RSC Adv.*, 2015, **5**, 48031–48038.
325 J. Dantas, E. Leal, D. R. Cornejo, R. H. G. A. Kiminami and A. C. F. M. Costa, *Arab. J. Chem.*, 2020, **13**, 3026–3042.
326 K. Liu, R. Wang and M. Yu, *Renewable Energy*, 2018, **127**, 531–538.
327 L. Zhou, W. Lin, K. Liu, Z. Wang, Q. Liu, H. Cheng, C. Zhang, M. Arai and F. Zhao, *Catal. Sci. Technol.*, 2020, **10**, 222–230.
328 A. I. Cotar, A. M. Grumezescu, K.-S. Huang, G. Voicu, C. M. Chifiriuc and R. Radulescu, *Biointerface Res. Appl. Chem.*, 2013, **3**(2), 559–565.
329 W. Xie and J. Li, *Renewable Sustainable Energy Rev.*, 2023, **171**, 113017.
330 L. Bai, A. Tajikfar, S. Tamjidi, R. Foroutan and H. Esmaeili, *Renewable Energy*, 2021, **170**, 426–437.
331 A. Ara, R. Khattak, M. S. Khan, B. Begum, S. Khan and C. Han, *Catalysts*, 2022, **12**, 1–19.
332 D. Ho, X. Sun and S. Sun, *Acc. Chem. Res.*, 2011, **44**, 875–882.
333 J. Wallyn, N. Anton, D. Mertz, S. Begin-Colin, F. Perton, C. A. Serra, F. Franconi, L. Lemaire, M. Chiper and H. Libouban, *ACS Appl. Mater. Interfaces*, 2018, **11**, 403–416.
334 G. S. Aguilar-Moreno, E. Navarro-Cerón, A. Velázquez-Hernández, G. Hernández-Eugenio, M. Á. Aguilar-Méndez and T. Espinosa-Solares, *Renewable Energy*, 2020, **147**, 204–213.
335 X. Song, C. Ren, Q. Zhao and B. Su, *Chem. Eng. J.*, 2020, **381**, 122586.
336 A. Gallo-Cordova, J. Lemus, F. J. Palomares, M. P. Morales and E. Mazarío, *Sci. Total Environ.*, 2020, **711**, 134644.
337 A. Wang, P. Sudarsanam, Y. Xu, H. Zhang, H. Li and S. Yang, *Green Chem.*, 2020, **22**, 2977–3012.
338 Z.-H. Zhang and R. Balasubramanian, *Appl. Energy*, 2015, **146**, 270–278.
339 N. M. Ribeiro, A. C. Pinto, C. M. Quintella, G. O. Da Rocha, L. S. G. Teixeira, L. L. N. Guarieiro, M. do Carmo Rangel, M. C. C. Veloso, M. J. C. Rezende and R. Serpa da Cruz, *Energy Fuels*, 2007, **21**, 2433–2445.
340 W. Z. Tawfik, M. Esmat and S. I. El-Dek, *Appl. Nanosci.*, 2017, **7**, 863–870.
341 A. Fadli, A. Adnan and A. S. Addabsi, in *IOP Conference Series: Materials Science and Engineering*, IOP Publishing, 2019, vol. 622, p. 12013.
342 H. Chen, X. Zhang, J. Zhang and Q. Wang, *Catal. Sci. Technol.*, 2018, **8**, 1126–1133.
343 N. A. A. Razak, N.-A. Mijan, K. B. Baharuddin, Y. H. Taufiq-Yap and D. Derawi, *Biomass Bioenergy*, 2024, **186**, 107269.
344 R. Kaewmeesri, J. Nonkumwong, W. Kiatkittipong, N. Laosiripojana and K. Faungnawakij, *J. Environ. Chem. Eng.*, 2021, **9**, 105128.
345 H. Zhang, H. Lin and Y. Zheng, *Appl. Catal., B*, 2014, **160–161**, 415–422.
346 J. G. Dickinson and P. E. Savage, *J. Mol. Catal. A: Chem.*, 2014, **388**, 56–65.
347 Y. H. Kim, P. H. Hor, X. L. Dong, F. Zhou and Z. X. Zhao, *Solid State Commun.*, 2013, **156**, 85–89.
348 C. H. Bartholomew, *Appl. Catal., A*, 2001, **212**, 17–60.
349 Z. Hao, Q. Zhu, Z. Jiang, B. Hou and H. Li, *Fuel Process. Technol.*, 2009, **90**, 113–121.
350 S. Echeandia, B. Pawelec, V. L. Barrio, P. L. Arias, J. F. Cambra, C. V. Loricera and J. L. G. Fierro, *Fuel*, 2014, **117**, 1061–1073.
351 A. Ausavasukhi, Y. Huang, A. T. To, T. Sooknoi and D. E. Resasco, *J. Catal.*, 2012, **290**, 90–100.
352 M. S. Zanuttini, M. A. Peralta and C. A. Querini, *Ind. Eng. Chem. Res.*, 2015, **54**, 4929–4939.
353 R. Singh, N. Chakinala, K. Mohanty and A. G. Chakinala, *J. Environ. Chem. Eng.*, 2023, **11**, 111518.
354 W. Lonchay, G. Bagnato and A. Sanna, *Bioresour. Technol.*, 2022, **361**, 127727.
355 G. F. Froment, *Catal. Rev.*, 2008, **50**, 1–18.
356 B. Zhao, J. Zou, C. Chen, Q. He, Q. Tang, L. Liu and J. Dong, *Chem. Eng. J.*, 2023, **478**, 147396.
357 N. D. Charisiou, K. Polychronopoulou, N. Dimitratos, M. A. Goula, K. N. Papageridis, V. Sebastian, G. I. Siakavelas and D. Motta, The effect of noble metal (M: Ir, Pt, Pd) on M/Ce_2O_3-γ-Al_2O_3 catalysts for hydrogen production *via* the steam reforming of glycerol, *Catalysts*, 2020, **10**, 790.
358 V. Gunasekaran, H. Gurusamy, G. Ravi and Y. Rathinam, *Renewable Energy*, 2024, 120130.
359 A. Kunamalla and S. K. Maity, *Fuel*, 2023, **332**, 125977.
360 S. Eser, R. Venkataraman and O. Altin, *Ind. Eng. Chem. Res.*, 2006, **45**, 8956–8962.
361 S. Eser, R. Venkataraman and O. Altin, *Ind. Eng. Chem. Res.*, 2006, **45**, 8946–8955.
362 M. A. A. Aziz, A. A. Jalil, S. Wongsakulphasatch and D.-V. N. Vo, *Catal. Sci. Technol.*, 2020, **10**, 35–45.
363 Z. Zhang, X. Zhang, L. Zhang, Y. Wang, X. Li, S. Zhang, Q. Liu, T. Wei, G. Gao and X. Hu, *Energy Convers. Manag.*, 2020, **205**, 112301.
364 D. Xu, J. Lin, R. Ma, L. Fang, S. Sun and J. Luo, *Renewable Energy*, 2022, **184**, 124–133.
365 F. Lin, M. Xu, K. K. Ramasamy, Z. Li, J. L. Klinger, J. A. Schaidle and H. Wang, *ACS Catal.*, 2022, **12**, 13555–13599.
366 D. Gao, C. Schweitzer, H. T. Hwang and A. Varma, *Ind. Eng. Chem. Res.*, 2014, **53**, 18658–18667.
367 A. N. Kay Lup, F. Abnisa, W. M. A. Wan Daud and M. K. Aroua, *J. Ind. Eng. Chem.*, 2017, **56**, 1–34.
368 P. M. Mortensen, H. W. P. de Carvalho, J.-D. Grunwaldt, P. A. Jensen and A. D. Jensen, *J. Catal.*, 2015, **328**, 208–215.
369 K. Li, R. Wang and J. Chen, *Energy Fuels*, 2011, **25**, 854–863.
370 N. Asikin-Mijan, H. V. Lee, J. C. Juan, A. R. Noorsaadah, G. Abdulkareem-Alsultan, M. Arumugam and Y. H. Taufiq-Yap, *J. Anal. Appl. Pyrolysis*, 2016, **120**, 110–120.
371 H. Tani, T. Hasegawa, M. Shimouchi, K. Asami and K. Fujimoto, *Catal. Today*, 2011, **164**, 410–414.
372 D. Purchase, G. Abbasi, L. Bisschop, D. Chatterjee, C. Ekberg, M. Ermolin, P. Fedotov, H. Garelick,

K. Isimekhai and N. G. Kandile, *Pure Appl. Chem.*, 2020, **92**, 1733–1767.
373 I. Sádaba, M. L. Granados, A. Riisager and E. Taarning, *Green Chem.*, 2015, **17**, 4133–4145.
374 L. Santamaría Arana, S. A. Korili and A. Gil Bravo, *Chem. Eng. J.*, 2023, **455**, 140551.
375 I. Arends and R. A. Sheldon, *Appl. Catal., A*, 2001, **212**, 175–187.
376 S. G. Wettstein, J. Q. Bond, D. M. Alonso, H. N. Pham, A. K. Datye and J. A. Dumesic, *Appl. Catal., B*, 2012, **117**, 321–329.
377 C. Zhao, S. Kasakov, J. He and J. A. Lercher, *J. Catal.*, 2012, **296**, 12–23.
378 X. Liu, Z. Li, B. Zhang and M. Hu, *Fuel*, 2017, **204**, 144–151.
379 J. Yan, H. Zhang, Z. Yang and Y. Li, *J. Environ. Chem. Eng.*, 2025, **13**, 114968.
380 M. Rabaev, M. V. Landau, R. Vidruk-Nehemya, A. Goldbourt and M. Herskowitz, *J. Catal.*, 2015, **332**, 164–176.
381 S. Bezergianni, A. Dimitriadis, A. Kalogianni and P. A. Pilavachi, *Bioresour. Technol.*, 2010, **101**, 6651–6656.
382 M. Anand and A. K. Sinha, *Bioresour. Technol.*, 2012, **126**, 148–155.
383 F. Pinto, F. T. Varela, M. Gonçalves, R. N. André, P. Costa and B. Mendes, *Fuel*, 2014, **116**, 84–93.
384 P. Šimáček, D. Kubička, G. Šebor and M. Pospíšil, *Fuel*, 2010, **89**, 611–615.
385 O. V. Kikhtyanin, A. E. Rubanov, A. B. Ayupov and G. V. Echevsky, *Fuel*, 2010, **89**, 3085–3092.
386 J. Hancsók, M. Krár, S. Magyar, L. Boda, A. Holló and D. Kalló, *Microporous Mesoporous Mater.*, 2007, **101**, 148–152.
387 S. Bezergianni and A. Dimitriadis, *Fuel*, 2013, **103**, 579–584.
388 A. Srifa, K. Faungnawakij, V. Itthibenchapong, N. Viriya-Empikul, T. Charinpanitkul and S. Assabumrungrat, *Bioresour. Technol.*, 2014, **158**, 81–90.
389 A. Sonthalia and N. Kumar, *J. Energy Inst.*, 2019, **92**, 1–17.
390 S. D. A. Sharuddin, F. Abnisa, W. M. A. W. Daud and M. K. Aroua, *Energy Convers. Manag.*, 2016, **115**, 308–326.
391 A. Srifa, K. Faungnawakij, V. Itthibenchapong and S. Assabumrungrat, *Chem. Eng. J.*, 2014, **278**, 1–10.
392 S. T. Mohammed, S. A. Gheni, D. Y. Aqar, K. I. Hamad, S. M. R. Ahmed, M. A. Mahmood, G. H. Abdullah and M. K. Ali, *Process Saf. Environ. Prot.*, 2022, **159**, 489–499.
393 Z. Ding, T. Zhao, Q. Zhu, S. Liao, L. Ning, Y. Bi and H. Chen, *Biomass Bioenergy*, 2020, **143**, 105879.
394 V. Itthibenchapong, A. Srifa, R. Kaewmeesri, P. Kidkhunthod and K. Faungnawakij, *Energy Convers. Manage.*, 2017, **134**, 188–196.
395 T. Ramezani, S. M. Sadrameli, A. Bayat and A. H. S. Dehaghani, *Fuel Process. Technol.*, 2022, **238**, 107514.
396 N. A. A. Razak, Y. H. Taufiq-Yap and D. Derawi, *J. Anal. Appl. Pyrolysis*, 2024, 106369.
397 F. W. Mezaal, I. Zainol, N. M. Abbass, N. Rahim and A. A. Majhool, *J. Green Eng.*, 2020, **10**, 376–398.
398 G. Abdulkareem-Alsultan, N. Asikin-Mijan, N. Mansir, H. V. Lee, Z. Zainal, A. Islam and Y. H. Taufiq-Yap, *J. Anal. Appl. Pyrolysis*, 2019, **137**, 171–184.
399 O. N. Syazwani, S. H. Teo, A. Islam and Y. H. Taufiq-Yap, *Process Saf. Environ. Prot.*, 2017, **105**, 303–315.
400 T. Morgan, D. Grubb, E. Santillan-Jimenez and M. Crocker, *Top. Catal.*, 2010, **53**, 820–829.
401 V. Balasundram, N. Ibrahim, R. M. Kasmani, M. K. A. Hamid, R. Isha, H. Hasbullah and R. R. Ali, *Energy Procedia*, 2017, **142**, 801–808.
402 N. Asikin-Mijan, H. V. Lee, T. S. Marliza and Y. H. Taufiq-Yap, *J. Anal. Appl. Pyrolysis*, 2018, **129**, 221–230.
403 P. Mäki-Arvela, I. Kubickova, M. Snåre, K. Eränen and D. Y. Murzin, *Energy Fuels*, 2007, **21**, 30–41.
404 M. Snåre, I. Kubičková, P. Mäki-Arvela, K. Eränen and D. Y. Murzin, *Ind. Eng. Chem. Res.*, 2006, **45**, 5708–5715.
405 K. C. Kwon, H. Mayfield, T. Marolla, B. Nichols and M. Mashburn, *Renewable Energy*, 2011, **36**, 907–915.
406 P. Mäki-Arvela, B. Rozmysłowicz, S. Lestari, O. Simakova, K. Eränen, T. Salmi and D. Y. Murzin, *Energy Fuels*, 2011, **25**, 2815–2825.
407 P.-B. Chen, J.-W. Yang, Z.-X. Rao, Q. Wang, H.-T. Tang, Y.-M. Pan and Y. Liang, *J. Colloid Interface Sci.*, 2023, **652**, 866–877.
408 L. Boda, G. Onyestyák, H. Solt, F. Lónyi, J. Valyon and A. Thernesz, *Appl. Catal., A*, 2010, **374**, 158–169.
409 M. R. De Brimont, C. Dupont, A. Daudin, C. Geantet and P. Raybaud, *J. Catal.*, 2012, **286**, 153–164.
410 I. Kubičková, M. Snåre, K. Eränen, P. Mäki-Arvela and D. Y. Murzin, *Catal. Today*, 2005, **106**, 197–200.
411 I. H. Choi, K. R. Hwang, J. S. Han, K. H. Lee, J. S. Yun and J. S. Lee, *Fuel*, 2015, **158**, 98–104.
412 S. Lestari, P. Mäki-Arvela, K. Eränen, J. Beltramini, G. Q. Max Lu and D. Y. Murzin, *Catal. Lett.*, 2010, **134**, 250–257.
413 I. Simakova, O. Simakova, P. Mäki-Arvela and D. Y. Murzin, *Catal. Today*, 2010, **150**, 28–31.
414 T. Morgan, E. Santillan-Jimenez, A. E. Harman-Ware, Y. Ji, D. Grubb and M. Crocker, *Chem. Eng. J.*, 2012, **189–190**, 346–355.
415 H. Heriyanto, S. Murti, S. Is Heriyanti, I. Sholehah and A. Rahmawati, *MATEC Web Conf.*, 2018, **156**, 3032.
416 F. T. Yani, H. Husin, Darmadi, S. Muhammad, F. Abnisa, Nurhazanah, F. Nasution and Erdiwansyah, *J. Cleaner Prod.*, 2022, **354**, 131704.
417 H. Tang, Q. Dai, Y. Cao, J. Li, X. Wei, K. Jibran and S. Wang, *Biomass Bioenergy*, 2023, **177**, 106927.
418 K. Li, F. Zhou, X. Liu, H. Ma, J. Deng, G. Xu and Y. Zhang, *Catal. Sci. Technol.*, 2020, **10**, 1151–1160.
419 S. Xing, P. Lv, C. Zhao, M. Li, L. Yang, Z. Wang, Y. Chen and S. Liu, *Fuel Process. Technol.*, 2018, **179**, 324–333.
420 Z. Cai, Y. Wang, Y. Cao, P. Yu, Y. Ding, Y. Ma, Y. Zheng, K. Huang and L. Jiang, *Fuel*, 2023, **337**, 127175.
421 K. Malins, *Fuel*, 2021, **285**, 119129.
422 L. Chen, K. Huang, Q. Xie, S. Mun Lam, J. Chung Sin, T. Su, H. Jiab and Z. Qin, *Catal. Sci. Technol.*, 2021, **11**, 1602.
423 G. Lawer-Yolar, B. Dawson-Andoh and E. Atta-Obeng, *Sustainable Chem.*, 2021, **2**, 206–221.
424 R. K. Saluja, V. Kumar and R. Sham, *Renewable Sustainable Energy Rev.*, 2016, **62**, 866–881.
425 J. Yang, Z. Xin, Q. (Sophia) He, K. Corscadden and H. Niu, *Fuel*, 2019, **237**, 916–936.

426 R. Mawhood, E. Gazis, S. de Jong, R. Hoefnagels and R. Slade, *Biofuels, Bioprod. Biorefin.*, 2016, **10**, 462–484.
427 M. A. Rumizen, *Front. Energy Res.*, 2021, **9**, 1–8.
428 E. Halim, C. Lee, W. Wang, J. Lin and Y. Lin, *Int. J. Energy Res.*, 2022, **46**, 1059–1076.
429 M. Zanata, S. Tri Wulan Amelia, M. R. Mumtazy, F. Kurniawansyah and A. Roesyadi, in *Materials Science Forum*, Trans Tech Publ, 2019, vol. 964, pp. 193–198.
430 L. M. Orozco, D. A. Echeverri, L. Sánchez and L. A. Rios, *Chem. Eng. J.*, 2017, **322**, 149–156.
431 A. I. Tsiotsias, S. Hafeez, N. D. Charisiou, S. M. Al-Salem, G. Manos, A. Constantinou, S. AlKhoori, V. Sebastian, S. J. Hinder, M. A. Baker, K. Polychronopoulou and M. A. Goula, *Renewable Energy*, 2023, **206**, 582–596.
432 I. Aziz, L. Adhani, M. I. Maulana, M. Ali Marwono, A. A. Dwiatmoko and S. Nurbayti, *J. Kim. Val.*, 2022, **8**, 240–250.